

**Combining local and non-local correlations
from methods to real materials**

Dissertation

zur Erlangung des Doktorgrades

an der Fakultät für Mathematik, Informatik und Naturwissenschaften

Fachbereich Physik

der Universität Hamburg

vorgelegt von

Arthur Huber

Hamburg 2018

Gutachter der Dissertation: Prof. Dr. Alexander Lichtenstein
PD. Dr. Alexander Chudnovskiy

Zusammensetzung der Prüfungskommission: Prof. Dr. Alexander Lichtenstein
Prof. Dr. Michael Potthoff
Prof. Dr. Daniela Pfannkuche
Prof. Dr. Nils Huse
PD Dr. Elena Vedmedenko

Vorsitzende der Prüfungskommission: Prof. Dr. Daniela Pfannkuche

Datum der Disputation: 07.03.2019

Vorsitzender Fach-Promotionsausschusses PHYSIK: Prof. Dr. Michael Potthoff

Leiter des Fachbereichs PHYSIK: Prof. Dr. Wolfgang Hansen

Dekan der Fakultät MIN: Prof. Dr. Heinrich Graener

Zusammenfassung

Die Arbeit, die in dieser Dissertation vorgestellt wird, illustriert die Untersuchung von kollektiven Ladungsanregungen und die Vereinigung von lokalen und nicht lokalen Korrelationen in stark korrelierten Materialien und Gitter Systemen. Dabei wurde moderne zeitkontinuierliche Quantum-Monte-Carlo Algorithmen und Störungstheorie um die dynamische Molekularfeldtheorie herum verwendet.

Die verwendeten numerischen Modelle wurden auf realistische Materialien angewandt, um kollektive Ladungsanregungen in den dotierten Mott Isolatoren C_2H und C_2F zu untersuchen.

Darüber hinaus wurde eine effektive bosonische Wirkung für die Ladungsfreiheitsgrade für das erweiterte Hubbard Modell hergeleitet. Es wurde gezeigt das Ladungsanregungen mit einer einfachen Theorie, welche ähnlich zur RPA Theorie beschrieben werden können.

Abschliessend wurde Frequenzverdoppelung in Graphen mittels Brechung der Inversionssymmetrie untersucht. Dieser Effekt kann als sensitives Werkzeug genutzt werden um Valley Polarization erzeugt durch polarisierendes Licht zu untersuchen.

Abstract

The work presented in this thesis illustrates the applicability of collective charge excitations and how to combine local and non-local correlations of strongly correlated materials and lattice systems by using modern continuous time quantum Monte Carlo algorithms and perturbation expansions around dynamical mean field theory.

The used numerical models were applied to realistic materials, to discuss collective charge excitations in the highly doped Mott Insulator materials C_2H and C_2F .

Furthermore, effective bosonic action for the charge degrees of freedom for the extended Hubbard model was derived and it was showed that charge excitations can be described by a simple RPA-like theory.

Subsequently, second-harmonic generation in graphene by breaking of inversion symmetry was probed. It can be used as a sensitive tool to measure the valley polarization e.g. by polarized light.

CONTENTS

I. Preface	3
II. Theoretical framework	8
III. From local to non-local correlations: the Dual Boson perspective	15
IV. Effective Ising model for correlated systems with charge ordering	34
A. Introduction	37
B. Bosonic action for electronic charge	40
C. Regime of strong charge fluctuations	43
D. Extended Hubbard model upon doping	48
E. Effective Ising model	49
F. Conclusion	53
G. Appendix A: Bosonic action for the extended Hubbard model	54
H. Appendix B: Vertex approximation	61
V. Plasmons In Doped Mott Insulators	64
A. Introduction	66
B. Calculation	69
C. Analysis of the Results	72
VI. Probing of valley polarization in Graphene via optical second-harmonic generation	77
VII. General conclusions and perspectives	87
Appendix	90
A: List of publications and authors contributions	90
Bibliography	93
References	93

I. PREFACE

Description of electronic systems with strong Coulomb correlations is one of the most interesting topics in modern condensed matter physics. Even though there are plenty of available methods which are rich enough and contain interesting physics, the task is still theoretically challenging. In the case where one can assume that the electron-electron interaction is local and that long-range inter-site interactions are fully screened or may be ignored the underlying physics is well described by the Hubbard model. The Hubbard model describes the physics of the competition of electron localization and itinerancy. It is one of the simplest models which can describe this competition and therefore used to describe correlation effects in lattices [1]. It is also believed that the single-band Hubbard model in two dimensions with the local on-site interaction can be used to explain the general physics of high-temperature superconductivity of cuprates [2].

Dynamical mean-field theory (DMFT) [1, 3], which is a well-established approximation for strongly correlated system, provides an approximate solution of Hubbard model by mapping it to a local quantum impurity model. In the limit of infinite dimensions this approximation becomes exact [1, 3]. DMFT is a very powerful method and captures the formation of Hubbard bands [4, 5] as well as the Mott transition [6, 7].

There are also cases where the non-local Coulomb interaction is not negligible [8] and this provides motivation to look at the ex-

tended Hubbard model, where charge-ordering effects and screening of the local interactions due to the non-local Coulomb interaction are included in addition to the Hubbard model physics. The extended Hubbard model describes the screening of local Coulomb interactions by the non-local Coulomb repulsion. The investigation of charge-ordering transition and the screening effect in the extended Hubbard model have been done in numerous theoretical studies [9–12].

To treat screening by non-local interactions one has to deal with the extended dynamical mean-field theory (EDMFT) [9, 13–15], which was introduced to include bosonic degrees of freedom, such as charge or spin fluctuations, into DMFT. Within the EDMFT framework, a description of fermionic and bosonic correlations on an equal footing was started [9, 16]. Although DMFT and EDMFT are by construction similar, the reduction of correlation effects to their local part is more efficient for fermions than for bosons. Furthermore, it was realized that the EDMFT approach was not fully successful due to strongly non-local nature of collective excitations, therefore it was necessary to extend EDMFT to treat non-local correlations. One of the first examples beyond EDMFT is EDMFT+GW approach [9], where EDMFT served as a starting point and all spatial contributions are added by GW. In EDMFT+GW one has to be aware of double counting which is related to the fact that all local contributions have already been accounted at EDMFT level.

More sophisticated approaches that treat non-local effects diagrammatically in terms of lattice and impurity quantities include DFA [17], 1PI [18] and DMF²RG [19]. These methods demonstrate an extension of DMFT by including two-particle vertex corrections for the diagrams. Nevertheless, these approaches cannot describe collective degrees of freedom coming up from non-local in-

teractions. The recent TRILEX [20] approach, which is not based on the mean-field solution, was introduced to treat diagrammatically both fermionic and bosonic excitations. In this method, the authors approximate an exact Hedin [21] form of lattice self-energy and polarization operator by including full impurity fermion-boson vertex correction in the diagrams. In all these approaches EDMFT served as a starting point for theories that include spatial correlations. TRILEX, as well as EDMFT+GW, have their drawbacks. For example, EDMFT+GW depends on a decoupling scheme of the Coulomb interaction and the results differs strongly. Both theories are not sufficient to satisfy conservation laws such as charge conservation.

Beside the route of constructing one can also use the proper dynamical mean-field extension in terms of lattice Green's functions and introduce so-called dual fermions (DF) [22] and the dual bosons (DB) [23, 24] and then do diagrammatic perturbation theory with new dual degrees of freedom. Nonetheless, the local impurity model still serves as the starting point of the perturbation expansion and (E)DMFT is reproduced in DF(DB) respectively as the non-interacting dual problem. Still, there are major advantages e.g. the self-energy and polarization operator in DF and DB are free from double counting problems by construction. There is no overlap between the impurity contribution to the self-energy and polarization operator and local parts of dual diagrams since the impurity model deals with purely local Green's functions only and the dual theory is constructed from purely non-local building blocks.

The focus of this work lies on some particular cases of the DB approach, in which one uses the dual way of excluding non-locality from diagrams and constructs correct EDMFT extensions with the three point and four point vertex as well as without vertex corrections. As

well as applications for realistic materials.

II. THEORETICAL FRAMEWORK

In this Chapter we will give a brief overview over the most important concepts which will be used in this thesis. The extended Hubbard model serves as the canonical example of a strongly correlated systems where non-local effects play a crucial role. In momentum space, its action is given by the following relation

$$S = - \sum_{\mathbf{k}\nu\sigma} c_{\mathbf{k}\nu\sigma}^* [i\nu + \mu - \varepsilon_{\mathbf{k}}] c_{\mathbf{k}\nu\sigma} + \frac{1}{2} \sum_{\mathbf{q}\omega} U_{\mathbf{q}} \rho_{\mathbf{q}\omega}^* \rho_{\mathbf{q}\omega}. \quad (1)$$

Here we are interested only in the charge fluctuations, so in the following we suppress the spin labels on Grassmann variables $c_{\mathbf{q}\nu}^*$ ($c_{\mathbf{q}\nu}$) corresponding to creation (annihilation) of an electron with momentum \mathbf{k} and fermionic Matsubara frequency ν . The interaction $U_{\mathbf{q}} = U + V_{\mathbf{q}}$ consists of the on-site and nearest-neighbour interactions respectively. The charge fluctuations are given by the complex bosonic variable $\rho_{\omega} = n_{\omega} - \langle n \rangle \delta_{\omega}$, where $n_{\omega} = \sum_{\nu\sigma} c_{\nu}^* c_{\nu+\omega}$ counts the number of electrons and ω is a bosonic Matsubara frequency. The chemical potential μ is chosen in such a way that the average number of electrons per site is one (half-filling). Finally, $\varepsilon_{\mathbf{k}}$ is the Fourier transform of the hopping integral t between neighboring sites.

In EDMFT, the lattice action [\(75\)](#) is split up into a set of single-site

local impurity actions S_{imp} and a non-local remaining part S_{rem}

$$S = \sum_j S_{\text{imp}}^{(j)} + S_{\text{rem}}, \quad (2)$$

which are given by the following explicit relations

$$S_{\text{imp}} = - \sum_{\nu} c_{\nu}^* [i\nu + \mu - \Delta_{\nu}] c_{\nu} + \frac{1}{2} \sum_{\omega} \mathcal{U}_{\omega} \rho_{\omega}^* \rho_{\omega}, \quad (3)$$

$$S_{\text{rem}} = - \sum_{\mathbf{k}\nu} c_{\mathbf{k}\nu}^* [\Delta_{\nu} - \varepsilon_{\mathbf{k}}] c_{\mathbf{k}\nu} + \frac{1}{2} \sum_{\mathbf{q}\omega} (U_{\mathbf{q}} - \mathcal{U}_{\omega}) \rho_{\mathbf{q}\omega}^* \rho_{\mathbf{q}\omega}. \quad (4)$$

All theories which are an extension of EDMFT we call here EDMFT++. Importantly, a solution of every EDMFT++ theory can be exactly written in terms of EDMFT Green's functions and renormalized interactions as follows

$$G_{\mathbf{k}\nu}^{-1} = G_0^{-1} - \Sigma_{\mathbf{k}\nu} = G_{\text{E}}^{-1} - \tilde{\Sigma}_{\mathbf{k}\nu}, \quad (5)$$

$$W_{\mathbf{q}\omega}^{-1} = W_0^{-1} - \Pi_{\mathbf{q}\omega} = W_{\text{E}}^{-1} - \tilde{\Pi}_{\mathbf{q}\omega}, \quad (6)$$

where $\Sigma_{\mathbf{k}\nu}$ and $\Pi_{\mathbf{q}\omega}$ are the exact, unknown in general, self-energy and polarization operator of the model respectively, and

$\bar{\Sigma}_{\mathbf{k}\nu} = \Sigma_{\mathbf{k}\nu} - \Sigma_{\text{imp}}$ and $\bar{\Pi}_{\mathbf{q}\omega} = \Pi_{\mathbf{q}\omega} - \Pi_{\text{imp}}$ are the corrections to the dynamical mean-field solution. With EDMFT as a starting point, the goal of EDMFT++ theories is to approximate these corrections. As pointed out above, $\bar{\Sigma}_{\mathbf{k}\nu}$ and $\bar{\Pi}_{\mathbf{q}\omega}$ should be introduced without double counting with an effective local impurity problem, but still can give a local contributions to the lattice self-energy and polarization operator.

Now we introduce the so called DB approach which uses EDMFT as a starting point and can be seen as an EDMFT++ theory. The DB theory can be viewed as a perturbation expansion around EDMFT.

The dual transformations of the non-local part of the action S_{rem} can be made in the same way as in previous works on DB approach. In order to define the three-point vertex in the TRILEX way, here we introduce a different rescaling of the dual bosonic fields.

The partition function of our problem is given by

$$Z = \int D[c^*, c] e^{-S} \quad (7)$$

where the action S is given by (23). Performing the Hubbard–Stratonovich transformations one can introduce the new *dual* variables f^*, f, ϕ

$$\begin{aligned} e^{\sum_{\mathbf{k}\nu\sigma} c_{\mathbf{k}\nu\sigma}^* [\Delta_{\nu\sigma} - \varepsilon_{\mathbf{k}}] c_{\mathbf{k}\nu\sigma}} &= D_f \times \\ &\int D[f^*, f] e^{-\sum_{\mathbf{k}\nu\sigma} \{f_{\mathbf{k}\nu\sigma}^* [\Delta_{\nu\sigma} - \varepsilon_{\mathbf{k}}]^{-1} f_{\mathbf{k}\nu\sigma} + c_{\nu\sigma}^* f_{\nu\sigma} + f_{\nu\sigma}^* c_{\nu\sigma}\}}, \\ e^{\frac{1}{2} \sum_{\mathbf{q}\omega} \rho_{\mathbf{q}\omega}^* [\Lambda_{\omega} - V_{\mathbf{q}}] \rho_{\mathbf{q}\omega}} &= D_b \times \\ &\int D[\phi] e^{-\frac{1}{2} \sum_{\mathbf{q}\omega} \{\phi_{\mathbf{q}\omega}^* [\Lambda_{\omega} - V_{\mathbf{q}}]^{-1} \phi_{\mathbf{q}\omega} + \rho_{\omega}^* \phi_{\omega} + \phi_{\omega}^* \rho_{\omega}\}}. \end{aligned} \quad (8)$$

Terms $D_f = \det[\Delta_{\nu\sigma} - \varepsilon_{\mathbf{k}}]$ and $D_b^{-1} = \sqrt{\det[\Lambda_{\omega} - V_{\mathbf{q}}]}$ can be neglected, because they do not contribute to expectation values. Rescaling the fermionic fields $f_{\mathbf{k}\nu\sigma}$ as $f_{\mathbf{k}\nu\sigma} g_{\nu\sigma}^{-1}$, the bosonic fields $\phi_{\mathbf{q}\omega}$ as $\phi_{\mathbf{q}\omega} \alpha_{\omega}^{-1}$, where $\alpha_{\omega} = (1 + \mathcal{U}_{\omega} \chi_{\omega})$, and integrating out the original degrees of freedom c^* and c we arrive at the dual action

$$\tilde{S} = - \sum_{\mathbf{k}\nu} f_{\mathbf{k}\nu}^* \tilde{G}_0^{-1} f_{\mathbf{k}\nu} - \frac{1}{2} \sum_{\mathbf{q}\omega} \phi_{\mathbf{q}\omega}^* \tilde{W}_0^{-1} \phi_{\mathbf{q}\omega} + \tilde{V}. \quad (9)$$

with the bare dual propagators

$$\tilde{G}_0 = [g_\nu^{-1} + \Delta_\nu - \varepsilon_{\mathbf{k}}]^{-1} - g_\nu = G_E - g_\nu, \quad (10)$$

$$\tilde{W}_0 = \alpha_\omega^{-1} [[U_{\mathbf{q}} - \mathcal{U}_\omega]^{-1} - \chi_\omega]^{-1} \alpha_\omega^{-1} = W_E - \mathcal{W}_\omega, \quad (11)$$

and the dual interaction term \tilde{V} . The explicit form of the dual interaction can be obtained by expanding the c^* and c dependent part of partition function in an infinite row and integrating out these degrees of freedom as follows

$$\begin{aligned} & \int e^{-\sum_{\nu\omega} \{c_\nu^* g_\nu^{-1} f_\nu + f_\nu^* g_\nu^{-1} c_\nu + \rho_\omega^* \alpha_\omega^{-1} \phi_\omega + \phi_\omega^* \alpha_\omega^{-1} \rho_\omega\}} \\ & e^{-S_{\text{imp}}[c^*, c]} D[c^*, c] = f_{\nu_1}^* f_{\nu_2} \langle c_{\nu_1} c_{\nu_2}^* \rangle g_{\nu_1}^{-1} g_{\nu_2}^{-1} \\ & + \frac{1}{2} \phi_{\omega_1}^* \phi_{\omega_2} \langle \rho_{\omega_1} \rho_{\omega_2}^* \rangle \alpha_{\omega_1}^{-1} \alpha_{\omega_2}^{-1} \\ & - f_{\nu_1}^* f_{\nu_2} \phi_{\omega_3}^* \langle c_{\nu_1} c_{\nu_2}^* \rho_{\omega_3} \rangle g_{\nu_1}^{-1} g_{\nu_2}^{-1} \alpha_{\omega_3}^{-1} \\ & + \frac{1}{4} f_{\nu_1}^* f_{\nu_2}^* f_{\nu_3} f_{\nu_4} \langle c_{\nu_1} c_{\nu_2} c_{\nu_3}^* c_{\nu_4}^* \rangle g_{\nu_1}^{-1} g_{\nu_2}^{-1} g_{\nu_3}^{-1} g_{\nu_4}^{-1} + \dots \\ & = -f_\nu^* g_\nu^{-1} f_\nu - \frac{1}{2} \phi_\omega^* \alpha_\omega^{-1} \chi_\omega \alpha_\omega^{-1} \phi_\omega \\ & - f_{\nu_1}^* f_{\nu_2} \phi_{\omega_3}^* \langle c_{\nu_1} c_{\nu_2}^* \rho_{\omega_3} \rangle g_{\nu_1}^{-1} g_{\nu_2}^{-1} \alpha_{\omega_3}^{-1} \\ & + \frac{1}{4} f_{\nu_1}^* f_{\nu_2}^* f_{\nu_3} f_{\nu_4} \langle c_{\nu_1} c_{\nu_2} c_{\nu_3}^* c_{\nu_4}^* \rangle g_{\nu_1}^{-1} g_{\nu_2}^{-1} g_{\nu_3}^{-1} g_{\nu_4}^{-1} + \dots \\ & = e^{-\{f_\nu^* g_\nu^{-1} f_\nu + \frac{1}{2} \phi_\omega^* \alpha_\omega^{-1} \chi_\omega \alpha_\omega^{-1} \phi_\omega + \tilde{V}\}}. \end{aligned} \quad (12)$$

Therefore dual interaction has the form of infinite expansion on the full vertices of the local impurity problem

$$\begin{aligned} \tilde{V} &= f_{\nu_1}^* f_{\nu_2} \phi_{\omega_3}^* \langle c_{\nu_1} c_{\nu_2}^* \rho_{\omega_3} \rangle g_{\nu_1}^{-1} g_{\nu_2}^{-1} \alpha_{\omega_3}^{-1} - \\ & \frac{1}{4} f_{\nu_1}^* f_{\nu_2}^* f_{\nu_3} f_{\nu_4} g_{\nu_1}^{-1} g_{\nu_2}^{-1} g_{\nu_3}^{-1} g_{\nu_4}^{-1} \{ \langle c_{\nu_1} c_{\nu_2} c_{\nu_3}^* c_{\nu_4}^* \rangle - \\ & \langle c_{\nu_1} c_{\nu_4}^* \rangle \langle c_{\nu_2} c_{\nu_3}^* \rangle + \langle c_{\nu_1} c_{\nu_3}^* \rangle \langle c_{\nu_2} c_{\nu_4}^* \rangle \} + \dots \end{aligned} \quad (13)$$

Here we define the three- and four-point vertex functions as ($\gamma_{\nu\omega}$ is the shorthand notation for the $\gamma_{\nu\omega}^{2,1}$)

$$\gamma_{\nu\omega} = g_{\nu}^{-1} g_{\nu+\omega}^{-1} \alpha_{\omega}^{-1} \langle c_{\nu} c_{\nu+\omega}^* \rho_{\omega} \rangle, \quad (14)$$

$$\gamma_{\nu\nu'\omega}^{4,0} = g_{\nu}^{-1} g_{\nu'}^{-1} g_{\nu'-\omega}^{-1} g_{\nu+\omega}^{-1} \left[\langle c_{\nu} c_{\nu'} c_{\nu'-\omega}^* c_{\nu+\omega}^* \rangle - g_{\nu} g_{\nu'} (\delta_{\omega} - \delta_{\nu', \nu+\omega}) \right], \quad (15)$$

with the simple connection between them

$$\gamma_{\nu\omega} = \alpha_{\omega}^{-1} \sum_{\nu'} [1 - \gamma_{\nu\nu'\omega}^{4,0} g_{\nu'} g_{\nu'-\omega}]. \quad (16)$$

In the weakly-interacting limit, namely $U \rightarrow 0$, the renormalization factor α_{ω} goes to unity and the four-point vertex $\gamma^{4,0}$ is zero, as detailed in the previous works [23–25] on the DB approach. Then, the three-point vertex can be reduced to its bare form $\gamma_0 = 1$.

Then, the two first terms in \tilde{V} are given by

$$\tilde{V} = \gamma_{\nu\omega} f_{\nu}^* f_{\nu+\omega} \phi_{\omega}^* + \frac{1}{4} \gamma_{\nu\nu'\omega}^{4,0} f_{\nu}^* f_{\nu'}^* f_{\nu+\omega} f_{\nu'-\omega}. \quad (17)$$

The dual Green's function $\tilde{G}_{\mathbf{k}\nu} = -\langle f_{\mathbf{k}\nu} f_{\mathbf{k}\nu}^* \rangle$ and renormalized dual interaction $\tilde{W}_{\mathbf{q}\omega} = -\langle \phi_{\mathbf{q}\omega} \phi_{\mathbf{q}\omega}^* \rangle$, as well as dual self-energy $\tilde{\Sigma}_{\mathbf{k}\nu}$ and polarization operator $\tilde{\Pi}_{\mathbf{q}\omega}$, can be obtained diagrammatically [23–25]. These dual quantities have usual connection

$$\tilde{G}_{\mathbf{k}\nu}^{-1} = \tilde{G}_0^{-1} - \tilde{\Sigma}_{\mathbf{k}\nu}, \quad (18)$$

$$\tilde{W}_{\mathbf{q}\omega}^{-1} = \tilde{W}_0^{-1} - \tilde{\Pi}_{\mathbf{q}\omega}. \quad (19)$$

Finally, lattice Green's function $G_{\mathbf{k}\nu}$ and susceptibility $X_{\mathbf{q}\omega}$ can

be expressed in terms of dual propagators via exact relations

$$G_{\mathbf{k}\nu} = - [\varepsilon_{\mathbf{k}} - \Delta_{\nu}]^{-1} + [\varepsilon_{\mathbf{k}} - \Delta_{\nu}]^{-1} g_{\nu}^{-1} \tilde{G}_{\mathbf{k}\nu} g_{\nu}^{-1} [\varepsilon_{\mathbf{k}} - \Delta_{\nu}]^{-1}, \quad (20)$$

$$X_{\mathbf{q}\omega} = - [U_{\mathbf{q}} - \mathcal{U}_{\omega}]^{-1} + [U_{\mathbf{q}} - \mathcal{U}_{\omega}]^{-1} \alpha_{\omega}^{-1} \tilde{W}_{\mathbf{q}\omega} \alpha_{\omega}^{-1} [U_{\mathbf{q}} - \mathcal{U}_{\omega}]^{-1}. \quad (21)$$

One can also rewrite the last relation and obtain the relation for the full dual renormalized interaction

$$\alpha_{\omega}^{-1} \tilde{W}_{\mathbf{q}\omega} \alpha_{\omega}^{-1} = [U_{\mathbf{q}} - \mathcal{U}_{\omega}] + [U_{\mathbf{q}} - \mathcal{U}_{\omega}] X_{\mathbf{q}\omega} [U_{\mathbf{q}} - \mathcal{U}_{\omega}], \quad (22)$$

to show that the dual propagator $\tilde{W}_{\mathbf{q}\omega}$ is evidently a renormalized interaction in the non-local part of the action, where the impurity interaction is excluded on the level of the bare interaction. It is worth mentioning, that for the case of $\Lambda_{\omega} = 0$, which corresponds to the DMFT theory as a basis, the renormalized interaction is exactly that of the usual V -decoupling.

III. FROM LOCAL TO NON-LOCAL CORRELATIONS: THE DUAL BOSON PERSPECTIVE

Development of first-principles electronic structure methods for correlated materials including high- T_c cuprates, iron pnictides as well as heavy-fermion compounds presents a great challenge for computational material science. In the last decade one of the main breakthroughs is related to a new theoretical approach which combined the accuracy of realistic GW-scheme with advanced local many body (extended) dynamical mean-field theory ((E)DMFT+GW). Avoiding double-counting is crucial for every diagrammatic approach that treats non-local correlations beyond the dynamical mean-field level ((E)DMFT++ theory). Until now, the general issue of double-counting remained unsolved.

The goal of this work was to combine local and non-local correlations, by deriving it from a higher principle and using reasonable and controllable approximations. Furthermore, a condition was that the approximation could be used for real material applications, meaning it should not be too heavy computationally. Here we used the dual boson approximation as a starting point, which can be derived by using a special form of a Hubbard-Stratonovich transformation.

We employed the dual boson approach and simplified it to an EDMFT+GW like approximation, but with the advantage to have a methodical derivation, a controllable limit (for small local Coulomb interaction) and without having to take care of double-counting of

diagrams by construction. This approximation is called dual boson GW (DB–GW). Existing approximations for the treatment of local and non-local correlation effects and its physics were done before, for example in the above mentioned the EDMFT+GW approximation. The idea of the EDMFT+GW approximation is to combine the purely local self-energy and polarization function of EDMFT with the spatially non-local contributions from GW approach.

In the previous studies phase diagrams in the on-site Coulomb interaction U and the nearest-neighbor Coulomb Interaction V , as well as retarded interactions and local spectral functions, have been calculated for the extended Hubbard model and the GW-EDMFT approach [9, 11, 12, 15, 26].

It was found that the charge-ordering line $V_c(U)$ in the U/V phase diagram for the transition from Fermi liquid to charge-ordering, that EDMFT overestimates the local interaction while the EDMFT+GW approach in the V -decoupling underestimates the local interaction or rather overestimates the non-local interaction V in comparison to the naive mean-field estimation $V_c = U/z$ [12]. Where here z is the number of nearest neighbors. In contrast to the V -decoupling scheme of the EDMFT+GW approximation there is also the so called UV –decoupling scheme where the local and non-local interactions are treated on equal footing [26]. GW+EDMFT in the UV -decoupling scheme reproduces the GW phase boundary for small local interactions and slightly differs for larger U , when one reaches the Mott insulator phase [27]. Nonetheless, the dual boson approximation is very successful [28]. It is still an important topic to find a suitable and computationally lightweight approximation which combines local and non-local correlations and describes collective bosonic excitations for real materials.

**From local to non-local correlations: the Dual Boson
perspective**

Reprinted with permissions from

E. A. Stepanov, A. Huber, E. G. C. P. van Loon, A. I. Lichtenstein,
M. I. Katsnelson
Phys. Rev. B **94**, 205110 (2016).

©2016 by the American Physical Society

The reference numbering used in this reprinted article is only valid
within this specific article.

From local to nonlocal correlations: The Dual Boson perspective

E. A. Stepanov,¹ A. Huber,² E. G. C. P. van Loon,¹ A. I. Lichtenstein,² and M. I. Katsnelson¹

¹*Radboud University, Institute for Molecules and Materials, NL-6525AJ Nijmegen, The Netherlands*

²*Institute of Theoretical Physics, University of Hamburg, D-20355 Hamburg, Germany*

(Received 26 April 2016; revised manuscript received 12 July 2016; published 7 November 2016)

Extended dynamical mean-field theory (EDMFT) is insufficient to describe nonlocal effects in strongly correlated systems, since corrections to the mean-field solution are generally large. We present an efficient scheme for the construction of diagrammatic extensions of EDMFT that avoids the usual double-counting problem by using an exact change of variables (the Dual Boson formalism) to distinguish the correlations included in the dynamical mean-field solution and those beyond. With a computational efficiency comparable to the EDMFT + GW approach, our scheme significantly improves on the charge order transition phase boundary in the extended Hubbard model.

DOI: [10.1103/PhysRevB.94.205110](https://doi.org/10.1103/PhysRevB.94.205110)

I. INTRODUCTION

The description of strongly correlated electronic systems is still one of the most challenging problems in condensed matter physics, despite a lot of efforts and plenty of suggested theories. One of the most popular approaches is the dynamical mean-field theory (DMFT) [1–4], which provides an approximate solution of the (multiband) Hubbard model by mapping it to a local impurity problem. Although DMFT neglects nonlocal correlation effects, it is able to capture important properties of the system such as the formation of Hubbard bands [5,6] and the Mott transition [7,8]. Later, an extended dynamical mean-field theory (EDMFT) [9–12] was introduced to include collective (bosonic) degrees of freedom, such as charge or spin fluctuations, into DMFT. Unfortunately, these collective excitations have a strongly nonlocal nature, so a dynamical mean-field approach is insufficient and it was necessary to develop some extensions, we will call them EDMFT++, to treat nonlocal correlations.

The quantities of physical interest in EDMFT++ are the electronic self-energy $\Sigma_{\mathbf{k}\nu}$ and polarization operator $\Pi_{\mathbf{q}\omega}$. The main idea of the dynamical mean-field approach is that all local correlations are already accounted for in the effective local impurity problem which results in the self-consistency conditions on the local part of lattice Green's function and susceptibility. The mean-field ideology implies that in the EDMFT approach, the local self-energy and polarization operator are given by those of the impurity model. To go beyond, one needs to determine the corrections $\tilde{\Sigma}_{\mathbf{k}\nu}$ and $\tilde{\Pi}_{\mathbf{q}\omega}$ to the electronic self-energy and polarization operator that describe nonlocal excitations.

However, as soon as one goes beyond the dynamical mean-field level, the *nonlocal* corrections also change the *local* parts of $\Sigma_{\mathbf{k}\nu}$ and $\Pi_{\mathbf{q}\omega}$. Indeed, the self-consistency condition on the local part of the lattice Green's function $G_{\mathbf{k}\nu}$ is not able to fix the local part of the self-energy $\Sigma_{\mathbf{k}\nu}$ at the same time. Thus, the exact local part of full self-energy is no longer determined within the effective impurity problem and has contributions both from the dynamical mean-field solution and from the nonlocal corrections. The same holds true for the polarization operator and the self-consistency condition on the local part of renormalized interaction. Therefore, great care should be taken to avoid double-counting of correla-

tion effects when merging EDMFT with a diagrammatic approach.

The EDMFT + GW approach [13–19] combines GW diagrams [20–22] for the self-energy and polarization operator with EDMFT. In an attempt to avoid double-counting, all local contributions of the GW diagrams are subtracted and only the *purely nonlocal* part of $\tilde{\Sigma}_{\mathbf{k}\nu}$ and $\tilde{\Pi}_{\mathbf{q}\omega}$ is used to describe nonlocal correlations. Exclusion of the impurity contributions from the diagrams introduced beyond EDMFT is necessary for a correct construction of the theory. However, the EDMFT + GW way of treating the double-counting problem is not unique and is the subject of hot discussions.

More complicated approaches invented to describe nonlocal effects with the impurity problem as a starting point are D Γ A [23], 1PI [24] and DMF²RG [25]. These extensions of DMFT include two-particle vertex corrections in their diagrams. However, D Γ A and 1PI methods cannot describe the collective degrees of freedom arising from nonlocal interactions that are of interest here, and the DMF²RG approach has not yet been applied to this problem. On the other hand, the recent TRILEX [26,27] approach was introduced to treat diagrammatically both fermionic and bosonic excitations. In this method the exact Hedin form [20] of the lattice self-energy and polarization operator are approximated by including the full impurity fermion-boson vertex in the diagrams.

Instead of trying to construct the proper dynamical mean-field extension in terms of lattice Green's functions, one can take a different route and introduce so-called dual fermions (DF) [28] and Dual Bosons (DB) [29–31] and then deal with new *dual* degrees of freedom. In these methods the local impurity model still serves as the starting point of a perturbation expansion, so (E)DMFT is reproduced as the noninteracting dual problem. It is important to point out that the self-energy and polarization operator in DF and DB are free from double-counting problems by construction: There is no overlap between the impurity contribution to the self-energy and polarization operator and local parts of dual diagrams since the impurity model deals with *purely local* Green's functions only and the dual theory is constructed from *purely nonlocal* building blocks. The impurity contribution has been excluded already on the level of the bare dual Green's function and interaction. Contrary to the existing methods, the DB approach does allow one

to describe strongly nonlocal collective excitations such as plasmons [32].

The self-energy and polarization operator in self-consistent DB are built up as a ladder consisting of full fermion-fermion and fermion-boson vertices obtained from the local impurity problem. For computational applications, particularly those aimed at realistic multiorbital systems, it can be convenient to use simpler approximations that do not require the computational complexity of the full two-particle vertex. To that end, we construct EDMFT++ schemes that do not require the full two-particle vertex, that exclude double-counting using the dual theory, and that contain the most essential parts of the nonlocal physics. We illustrate this by means of the charge-order transition in the extended Hubbard model.

II. EDMFT++ THEORIES

The extended Hubbard model serves as the canonical example of a strongly correlated system where nonlocal effects play a crucial role. In momentum space, its action is given by the following relation:

$$S = - \sum_{\mathbf{k}\nu\sigma} c_{\mathbf{k}\nu\sigma}^* [i\nu + \mu - \varepsilon_{\mathbf{k}}] c_{\mathbf{k}\nu\sigma} + \frac{1}{2} \sum_{\mathbf{q}\omega} U_{\mathbf{q}} \rho_{\mathbf{q}\omega}^* \rho_{\mathbf{q}\omega}. \quad (1)$$

Here we are interested only in the charge fluctuations, so in the following we suppress the spin labels on Grassmann variables $c_{\mathbf{q}\nu}^*$ ($c_{\mathbf{q}\nu}$) corresponding to creation (annihilation) of an electron with momentum \mathbf{k} and fermionic Matsubara frequency ν . The interaction $U_{\mathbf{q}} = U + V_{\mathbf{q}}$ consists of the on-site U and nonlocal interaction $V_{\mathbf{q}}$, respectively. Here we consider $V_{\mathbf{q}}$ as a nearest-neighbor interaction for simplicity. The charge fluctuations are given by the complex bosonic variable $\rho_{\omega} = n_{\omega} - \langle n \rangle \delta_{\omega}$, where $n_{\omega} = \sum_{\nu\sigma} c_{\nu}^* c_{\nu+\omega}$ counts the number of electrons and ω is a bosonic Matsubara frequency. The chemical potential μ is chosen in such a way that the average number of electrons per site is one (half-filling). Finally, $\varepsilon_{\mathbf{k}}$ is the Fourier transform of the hopping integral t between neighboring sites.

First of all, since we are interested in the EDMFT++ theories, let us briefly recall the main statements of the extended dynamical mean-field theory. In EDMFT, the lattice action (1) is split up into a set of single-site local impurity actions S_{imp} and a nonlocal remaining part S_{rem} ,

$$S = \sum_j S_{\text{imp}}^{(j)} + S_{\text{rem}}, \quad (2)$$

which are given by the following explicit relations:

$$S_{\text{imp}} = - \sum_{\nu} c_{\nu}^* [i\nu + \mu - \Delta_{\nu}] c_{\nu} + \frac{1}{2} \sum_{\omega} \mathcal{U}_{\omega} \rho_{\omega}^* \rho_{\omega}, \quad (3)$$

$$S_{\text{rem}} = - \sum_{\mathbf{k}\nu} c_{\mathbf{k}\nu}^* [\Delta_{\nu} - \varepsilon_{\mathbf{k}}] c_{\mathbf{k}\nu} + \frac{1}{2} \sum_{\mathbf{q}\omega} (U_{\mathbf{q}} - \mathcal{U}_{\omega}) \rho_{\mathbf{q}\omega}^* \rho_{\mathbf{q}\omega}. \quad (4)$$

Since the impurity model is solved exactly, our goal is to move most of the correlation effects into the impurity, so that the remainder is only weakly correlated. For this reason, two hybridization functions Δ_{ν} and Λ_{ω} are introduced to describe the interplay between the impurity and external fermionic and bosonic baths, respectively. These functions are determined self-consistently for an optimal description of local correlation effects. The local bare interaction of the impurity model is then equal to $\mathcal{U}_{\omega} = U + \Lambda_{\omega}$. The impurity problem can be solved using, e.g., continuous-time quantum Monte Carlo solvers [33,34], and one can obtain the local impurity Green's function g_{ν} , susceptibility χ_{ω} and renormalized interaction \mathcal{W}_{ω} as

$$g_{\nu} = - \langle c_{\nu} c_{\nu}^* \rangle_{\text{imp}}, \quad (5)$$

$$\chi_{\omega} = - \langle \rho_{\omega} \rho_{\omega}^* \rangle_{\text{imp}}, \quad (6)$$

$$\mathcal{W}_{\omega} = \mathcal{U}_{\omega} + \mathcal{U}_{\omega} \chi_{\omega} \mathcal{U}_{\omega}, \quad (7)$$

where the average is taken with respect to the impurity action (3). One can also introduce the local impurity self-energy Σ_{imp} and polarization operator Π_{imp} ,

$$\Sigma_{\text{imp}} = i\nu + \mu - \Delta_{\nu} - g_{\nu}^{-1}, \quad (8)$$

$$\Pi_{\text{imp}}^{-1} = \chi_{\omega}^{-1} + \mathcal{U}_{\omega}, \quad (9)$$

that are used as the basis for the EDMFT Green's function G_{E} and renormalized interaction W_{E} defined as

$$G_{\text{E}}^{-1} = G_0^{-1} - \Sigma_{\text{imp}} = g_{\nu}^{-1} - (\varepsilon_{\mathbf{k}} - \Delta_{\nu}), \quad (10)$$

$$W_{\text{E}}^{-1} = W_0^{-1} - \Pi_{\text{imp}} = U_{\mathbf{q}}^{-1} - (\chi_{\omega}^{-1} + \mathcal{U}_{\omega})^{-1}. \quad (11)$$

Here $G_0 = (i\nu + \mu - \varepsilon_{\mathbf{k}})^{-1}$ is the bare lattice Green's function and W_0 is the bare interaction, which is equal to $U_{\mathbf{q}}$, or $V_{\mathbf{q}}$ in the case of $UV-$, or $V-$ decoupling, respectively [15,16].

Importantly, a solution of every EDMFT++ theory can be exactly written in terms of EDMFT Green's functions and renormalized interactions as follows:

$$G_{\mathbf{k}\nu}^{-1} = G_0^{-1} - \Sigma_{\mathbf{k}\nu} = G_{\text{E}}^{-1} - \tilde{\Sigma}_{\mathbf{k}\nu}, \quad (12)$$

$$W_{\mathbf{q}\omega}^{-1} = W_0^{-1} - \Pi_{\mathbf{q}\omega} = W_{\text{E}}^{-1} - \tilde{\Pi}_{\mathbf{q}\omega}, \quad (13)$$

where $\Sigma_{\mathbf{k}\nu}$ and $\Pi_{\mathbf{q}\omega}$ are the exact, unknown in general, self-energy and polarization operator of the model, respectively, and $\tilde{\Sigma}_{\mathbf{k}\nu} = \Sigma_{\mathbf{k}\nu} - \Sigma_{\text{imp}}$ and $\tilde{\Pi}_{\mathbf{q}\omega} = \Pi_{\mathbf{q}\omega} - \Pi_{\text{imp}}$ are the corrections to the dynamical mean-field solution. With EDMFT as a starting point, the goal of EDMFT++ theories is to approximate these corrections. As pointed out above, $\tilde{\Sigma}_{\mathbf{k}\nu}$ and $\tilde{\Pi}_{\mathbf{q}\omega}$ should be introduced without double-counting with an effective local impurity problem, but still can give a local contribution to the lattice self-energy and polarization operator.

There is, in fact, a numerically exact way to obtain the nonlocal self-energy using the so-called bold diagrammatic Monte Carlo method [35]. However, this method is very expensive for realistic calculations, so we will be focused on less expensive diagrammatic methods.

A. (E)DMFT + GW approach

Historically, the EDMFT + GW approach [13–17] introduced the first approximations for $\bar{\Sigma}_{\mathbf{k}v}$ and $\bar{\Pi}_{\mathbf{q}\omega}$. Here, the self-energy and polarization operator diagrams from the GW approximation [20–22] are added to the dynamical mean-field solution to treat nonlocal correlations,

$$\Sigma_{\mathbf{k}v}^{\text{GW}} = - \sum_{\mathbf{q}, \omega} G_{\mathbf{k}+\mathbf{q}, v+\omega} W_{\mathbf{q}\omega}, \quad (14)$$

$$\Pi_{\mathbf{q}\omega}^{\text{GW}} = 2 \sum_{\mathbf{k}, v} G_{\mathbf{k}+\mathbf{q}, v+\omega} G_{\mathbf{k}v}, \quad (15)$$

where the coefficient “2” in Eq. (15) accounts for the spin degeneracy. To avoid double-counting between the impurity correlations and the GW correlations, only the nonlocal part of Eqs. (14) and (15) is used, i.e., $\bar{\Sigma}_{\mathbf{k}v}^{\text{GW}} = \Sigma_{\mathbf{k}v}^{\text{GW}} - \Sigma_{\text{loc}}^{\text{GW}}$ and $\bar{\Pi}_{\mathbf{q}\omega}^{\text{GW}} = \Pi_{\mathbf{q}\omega}^{\text{GW}} - \Pi_{\text{loc}}^{\text{GW}}$. Since the local interaction U has already been accounted for in the impurity problem, the bare nonlocal interaction in Eq. (14) can be taken in the form of V -decoupling ($W_0 = V_{\mathbf{q}}$), which leads to a simple separation of local and nonlocal contributions to the self-energy $\bar{\Sigma}_{\mathbf{k}v}$. Unfortunately, this form of renormalized interaction overestimates nonlocal interactions [15,16]. Alternatively, the form of UV -decoupling ($W_0 = U_{\mathbf{q}}$) is more consistent with standard perturbation theory for the full Coulomb interaction, but leads to the problems with separation of local and nonlocal parts of the diagrams. For example, it accounts only for the large local contribution \mathcal{W}_ω instead of the small full local four-point vertex function $\gamma^{4,0}$ as shown in Appendix B. Therefore, the form of the renormalized interaction and the way to avoid the double-counting in general is a topic of hot discussions nowadays [36].

Note that hereinafter the name V - or UV -decoupling in the EDMFT++ theories implies only the form of interaction W_0 used in the self-energy diagrams beyond the dynamical-field level. Since the aim of the paper is to compare the existing schemes of exclusion of the double-counting, the form of the self-energy diagrams in these both cases remains the same. Our notations can differ from those introduced in the previous works on EDMFT++ theories by the presence of additional diagrams in the different versions of decoupling schemes (see, for example, Ref. [16]).

It should be noted, that there is another clear way to avoid the double-counting problem, namely simply ignoring nonlocal interactions in the dynamical mean-field part of the action and including them in the nonlocal corrections only. The impurity model then corresponds to DMFT, i.e., $\mathcal{U}_\omega = U$. Then, the nonlocal renormalized interaction in Eq. (14) can be taken in the form of V -decoupling as $W_0 = V_{\mathbf{q}}$, and the local part of this self-energy diagram is automatically zero. Although the DMFT + GW approach is free from double-counting by construction, it is less advanced than EDMFT+GW, since it ignores screening of the local interaction by nonlocal processes.

B. Local vertex corrections beyond the EDMFT

The exact self-energy and polarization operator of the lattice problem (1) are given by the following

relations [20]:

$$\Sigma_{\mathbf{k}v} = - \sum_{\mathbf{q}\omega} G_{\mathbf{k}+\mathbf{q}, v+\omega} W_{\mathbf{q}\omega} \Gamma_{v\omega}^{\mathbf{k}\mathbf{q}} = \text{diagram}, \quad (16)$$

$$\Pi_{\mathbf{q}\omega} = 2 \sum_{\mathbf{k}v} G_{\mathbf{k}+\mathbf{q}, v+\omega} G_{\mathbf{k}v} \Gamma_{v\omega}^{\mathbf{k}\mathbf{q}} = \text{diagram}, \quad (17)$$

where $\Gamma_{v\omega}^{\mathbf{k}\mathbf{q}}$ is the exact three-point Hedin vertex. Unfortunately, the full three-point vertex of the considered problem is unknown, and the self-energy and polarization operator can be found only approximately. The most important correlation effects beyond EDMFT and the GW diagrams are expected in the frequency dependence of the fermion-boson vertex [26,30]. For this reason, the recent TRILEX [26,27] approach with application to the Hubbard model was introduced. In this approach the exact Hedin vertex is approximated by the full local three-point vertex of impurity problem, which results in

$$\Sigma_{\mathbf{k}v}^{\text{TRILEX}} = - \sum_{\mathbf{q}\omega} G_{\mathbf{k}+\mathbf{q}, v+\omega} W_{\mathbf{q}\omega} \gamma_{v\omega}, \quad (18)$$

$$\Pi_{\mathbf{q}\omega}^{\text{TRILEX}} = 2 \sum_{\mathbf{k}v} G_{\mathbf{k}+\mathbf{q}, v+\omega} G_{\mathbf{k}v} \gamma_{v\omega}, \quad (19)$$

where $\gamma_{v\omega}$ is the full three-point vertex of the impurity problem determined below [see Eq. (33)]. Thus, the local parts of the self-energy and polarization operator are identically equal to the local impurity quantities Σ_{imp} and Π_{imp} , respectively. Moreover, it is possible to split $\Sigma_{\mathbf{k}v}^{\text{TRILEX}}$ and $\Pi_{\mathbf{q}\omega}^{\text{TRILEX}}$ into the local impurity part and nonlocal contribution as it was shown in Ref. [27],

$$\Sigma_{\mathbf{k}v}^{\text{TRILEX}} = \Sigma_{\text{imp}} + \bar{\Sigma}_{\mathbf{k}v}^{\text{TRILEX}}, \quad (20)$$

$$\Pi_{\mathbf{q}\omega}^{\text{TRILEX}} = \Pi_{\text{imp}} + \bar{\Pi}_{\mathbf{q}\omega}^{\text{TRILEX}}, \quad (21)$$

where

$$\bar{\Sigma}_{\mathbf{k}v}^{\text{TRILEX}} = - \sum_{\mathbf{q}\omega} \bar{G}_{\mathbf{k}+\mathbf{q}, v+\omega}^{\text{TRILEX}} \bar{W}_{\mathbf{q}\omega}^{\text{TRILEX}} \gamma_{v\omega}, \quad (22)$$

$$\bar{\Pi}_{\mathbf{q}\omega}^{\text{TRILEX}} = 2 \sum_{\mathbf{k}v} \bar{G}_{\mathbf{k}+\mathbf{q}, v+\omega}^{\text{TRILEX}} \bar{G}_{\mathbf{k}v}^{\text{TRILEX}} \gamma_{v\omega}, \quad (23)$$

and $\bar{G}_{\mathbf{k}v}^{\text{TRILEX}} = G_{\mathbf{k}v} - g_v$, $\bar{W}_{\mathbf{q}\omega}^{\text{TRILEX}} = W_{\mathbf{q}\omega} - \mathcal{W}_\omega$ are nonlocal parts of the full lattice Green's function and renormalized interaction, respectively. Therefore, the TRILEX approach is nothing more than an (E)DMFT+GW approximation with the same exclusion of double-counting, where the GW diagrams are additionally dressed with the local three-point vertex from one side. In this case, the lattice Green's function and renormalized interaction are given by the same Dyson Eqs. (12) and (13) with $\bar{\Sigma}_{\mathbf{k}v}^{\text{TRILEX}}$ and $\bar{\Pi}_{\mathbf{q}\omega}^{\text{TRILEX}}$ introduced beyond the dynamical mean-field level.

The main advantage of the TRILEX approach compared to existing diagrammatic methods is a computational efficiency due to the use of only the three-point vertex $\gamma_{v\omega}$ to treat nonlocal correlations. Nevertheless, even with this vertex function one can approximate the exact Hedin form of the self-energy and polarization function in a better way.

It is of course true, that if the self-energy and polarization operator in the exact form of Eqs. (16) and (17) do not

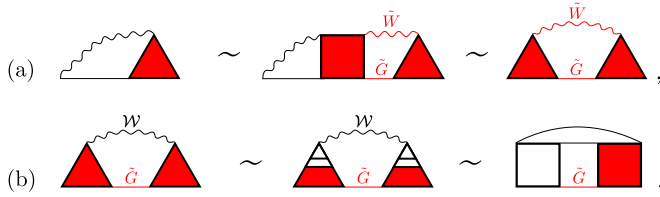


FIG. 1. Hedin form of the self-energy diagram in case of (a) at least one nonlocal Green's function \tilde{G} and nonlocal renormalized interaction \tilde{W} , and (b) only local renormalized interactions \mathcal{W} . Straight and wave lines correspond to the Green's function and renormalized interaction.

contain any nonlocal propagators, then these quantities are given by the impurity Σ_{imp} and Π_{imp} , respectively. Therefore, the improvements concern only the contributions $\tilde{\Sigma}_{\mathbf{k}\nu}^{\text{TRILEX}}$ and $\tilde{\Pi}_{\mathbf{q}\omega}^{\text{TRILEX}}$, written in terms of nonlocal propagators and local impurity vertex functions. As it was mentioned above, the self-consistency condition on the local parts of the Green's function and renormalized interaction cannot also fix the local parts of $\Sigma_{\mathbf{k}\nu}$ and $\Pi_{\mathbf{q}\omega}$ at the same time. Therefore, additional local contributions to the self-energy and polarization operator, hidden in the nonlocal structure of the exact three-point vertex, can appear from the diagrams introduced beyond the dynamical mean-field level. For example, the Hedin vertex with the same lattice indices at all three external points can contain nonlocal parts,

$$\Gamma_{\nu\omega}^{\mathbf{k}\mathbf{q}} = \begin{array}{c} i \\ \triangle \\ i \end{array} \sim \begin{array}{c} G \\ i \quad j \\ G \end{array} \begin{array}{c} W \\ \text{---} \\ i \end{array} \quad (24)$$

Therefore, these contributions are not provided by the local impurity problem and should be taken into account.

It is worth mentioning, that the Hedin form of the self-energy and polarization operator is exact for the theories with only one type of propagators. As soon as one includes the vertex functions of the impurity problem in the diagrams, all propagators become effectively separated into two different types. Now, since the correction to the dynamical mean-field level is introduced in terms of only one (nonlocal) type of lines and all local lines are gathered in the local vertices, the Hedin form does not provide the exact result for the self-energy and polarization as shown in Refs. [37,38].

In order to discuss this in more detail, let us take a closer look at the Hedin diagram (16) for the self-energy. Above we discussed the case of only local propagators. Now let us assume, that the Hedin vertex contains at least one nonlocal Green's function $\tilde{G}_{\mathbf{k}\nu}$ and renormalized interaction $\tilde{W}_{\mathbf{q}\omega}$. Then, the self-energy diagram can be reduced to the form of two renormalized three-point vertices with the nonlocal propagators in between as shown in Fig. 1(a). It may also happen that one particular contribution to the lattice self-energy does not contain the nonlocal renormalized interaction at all. This case is shown in Fig. 1(b). The last case without a nonlocal Green's function is not considered here due to appearance of higher-order vertex functions of the impurity problem in the diagrams. The same procedure can be used for the polarization operator. Then, if we restrict ourselves only to the lowest order vertex function $\gamma_{\nu\omega}$, the self-energy

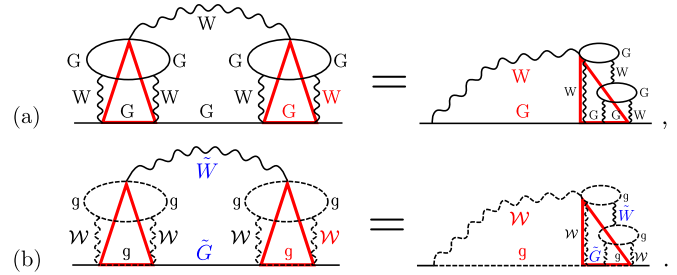


FIG. 2. Structure of the vertex corrections in theories consisted of (a) one and (b) two types of propagators. Solid straight and wave lines correspond to the Green's function and renormalized interaction of one type and the dashed lines to those of the second type, respectively.

and polarization operator introduced beyond the dynamical mean-field level are

$$\tilde{\Sigma}^{(2)} = \begin{array}{c} \tilde{W} \\ \triangle \\ \tilde{G} \end{array}, \quad (25)$$

$$\tilde{\Pi}^{(2)} = \begin{array}{c} \tilde{G} \\ \triangleleft \quad \triangleright \\ \tilde{G} \end{array}, \quad (26)$$

where, according to the above discussions, the three-point vertices appear at both sides of the GW diagrams, as was already discussed in Ref. [13]. Moreover, the specified form of the diagrams for the self-energy and polarization operator allows one to resum more diagrams than with the use of the TRILEX form.

The illustration of the importance of having the three-point vertex functions on both sides is also shown in Fig. 2. The top row corresponds to a theory constructed from only one type of Green's function. Then, the fermion-boson vertices are composed of the same propagators as the remainder of the diagram, and it is always possible to "move" all vertex correction to the right side of the diagram and obtain the Hedin form for the self-energy [20]. On the other hand, if the vertex functions are constructed from propagators (for example, g_ν and \mathcal{W}_ω obtained from the impurity problem) that differ from the Green's function G and renormalized interaction W , it is no longer possible to obtain the Hedin form for this diagram. More clearly, the Hedin form is hidden inside of the impurity vertices. "Moving" the left part of the diagram to the right, as in the bottom row of Fig. 2, gives a diagram with the same Hedin structure, but with different propagators.

So, if one prefers to work with the bare lattice propagators and to use the Hedin form of self-energy, then it would be consistent to approximate the exact Hedin vertex using the same bare lattice quantities without inclusion of any other types of propagators. If, instead, a combination of Green's functions and impurity vertices coming from different models is used, the renormalized vertices should be included at both ends of the GW diagram for the self-energy and polarization operator.

In order to take the above corrections into account and to compare the double-counting exclusion schemes, one can introduce the EDMFT + GW γ approach in the same way as

EDMFT+GW by including the local impurity vertex $\gamma_{v\omega}$ in the GW diagrams as

$$\Sigma_{\mathbf{k}\nu}^{\text{GW}\gamma} = - \sum_{\mathbf{q},\omega} \gamma_{v\omega} G_{\mathbf{k}+\mathbf{q},v+\omega} W_{\mathbf{q}\omega} \gamma_{v+\omega,-\omega}, \quad (27)$$

$$\Pi_{\mathbf{q}\omega}^{\text{GW}\gamma} = 2 \sum_{\mathbf{k},\nu} \gamma_{v\omega} G_{\mathbf{k}+\mathbf{q},v+\omega} G_{\mathbf{k}\nu} \gamma_{v+\omega,-\omega}. \quad (28)$$

Similarly to the EDMFT+GW case, only the nonlocal parts $\tilde{\Sigma}_{\mathbf{k}\nu}^{\text{GW}\gamma}$ and $\tilde{\Pi}_{\mathbf{q}\omega}^{\text{GW}\gamma}$ of the self-energy (27) and the polarization operator (28) are used beyond the EDMFT. Then, the lattice quantities are given by the same equations (12) and (13).

III. DUAL BOSON APPROACH

A different way of accounting for nonlocal correlations beyond EDMFT is given by the Dual Boson approach [29,31]. The nonlocal part S_{rem} of the lattice action (1) can be rewritten in terms of new *dual* variables f^*, f, ϕ by performing a Hubbard-Stratonovich transformation, which leads to the dual action,

$$\tilde{S} = - \sum_{\mathbf{k}\nu} f_{\mathbf{k}\nu}^* \tilde{G}_0^{-1} f_{\mathbf{k}\nu} - \frac{1}{2} \sum_{\mathbf{q}\omega} \phi_{\mathbf{q}\omega}^* \tilde{W}_0^{-1} \phi_{\mathbf{q}\omega} + \tilde{V}, \quad (29)$$

with the bare dual propagators,

$$\tilde{G}_0 = G_E - g_\nu, \quad (30)$$

$$\tilde{W}_0 = W_E - \mathcal{W}_\omega, \quad (31)$$

and the full dual interaction \tilde{V} that includes the impurity vertex functions $\gamma^{n,m}$ with n fermion and m boson lines to all orders in n and m , as detailed in Appendix A. The first two terms in \tilde{V} are given by the following relation:

$$\tilde{V} = \gamma_{v,\omega}^{2,1} f_v^* f_{v+\omega} \phi_\omega^* + \frac{1}{4} \gamma_{v,v',\omega}^{4,0} f_v^* f_{v'}^* f_{v+\omega} f_{v'-\omega}. \quad (32)$$

We define the three-point vertex $\gamma_{v\omega}^{2,1}$ in the same way as it is done in the TRILEX [26,27] approach:

$$\gamma_{v\omega}^{2,1} = g_\nu^{-1} g_{v+\omega}^{-1} \alpha_\omega^{-1} \langle c_\nu c_{v+\omega}^* \rho_\omega \rangle, \quad (33)$$

where $\alpha_\omega = \mathcal{W}_\omega / \mathcal{U}_\omega = (1 + \mathcal{U}_\omega \chi_\omega)$ is the local renormalization factor. It is important to realize that this factor only affects the transformations from lattice to dual quantities and vice versa. Therefore, it does not change the final results written in terms of the initial lattice degrees of freedom. In order to shorten notations, hereinafter we call the three-point vertex $\gamma_{v\omega}$. The four-point vertex function $\gamma_{vv',\omega}^{4,0}$ can be determined similarly to the previous papers on the Dual Boson formalism [29,31],

$$\gamma_{vv',\omega}^{4,0} = g_\nu^{-1} g_{v'}^{-1} g_{v'-\omega}^{-1} g_{v+\omega}^{-1} [\langle c_\nu c_{v'} c_{v'-\omega}^* c_{v+\omega}^* \rangle - g_\nu g_{v'} (\delta_\omega - \delta_{v',v+\omega})]. \quad (34)$$

Then, the dual Green's function $\tilde{G}_{\mathbf{k}\nu} = -\langle f_{\mathbf{k}\nu} f_{\mathbf{k}\nu}^* \rangle$ and renormalized dual interaction $\tilde{W}_{\mathbf{q}\omega} = -\langle \phi_{\mathbf{q}\omega} \phi_{\mathbf{q}\omega}^* \rangle$, as well as dual self-energy $\tilde{\Sigma}_{\mathbf{k}\nu}$ and polarization operator $\tilde{\Pi}_{\mathbf{q}\omega}$, can be obtained diagrammatically [29–31]. These dual quantities have the

usual connection,

$$\tilde{G}_{\mathbf{k}\nu}^{-1} = \tilde{G}_0^{-1} - \tilde{\Sigma}_{\mathbf{k}\nu}, \quad (35)$$

$$\tilde{W}_{\mathbf{q}\omega}^{-1} = \tilde{W}_0^{-1} - \tilde{\Pi}_{\mathbf{q}\omega}. \quad (36)$$

To close the circle, the Green's function $G_{\mathbf{k}\nu}$ and renormalized interaction $W_{\mathbf{q}\omega}$ of the original model can be exactly expressed in terms of dual quantities via the similar Dyson Eqs. (12) and (13) as follows:

$$G_{\mathbf{k}\nu}^{-1} = G_E^{-1} - \tilde{\Sigma}_{\mathbf{k}\nu}, \quad (37)$$

$$W_{\mathbf{q}\omega}^{-1} = W_E^{-1} - \tilde{\Pi}_{\mathbf{q}\omega}, \quad (38)$$

where the self-energy and polarization operator introduced beyond EDMFT are

$$\tilde{\Sigma}_{\mathbf{k}\nu} = \frac{\tilde{\Sigma}_{\mathbf{k}\nu}}{1 + g_\nu \tilde{\Sigma}_{\mathbf{k}\nu}}, \quad (39)$$

$$\tilde{\Pi}_{\mathbf{q}\omega} = \frac{\tilde{\Pi}_{\mathbf{q}\omega}}{1 + \mathcal{W}_\omega \tilde{\Pi}_{\mathbf{q}\omega}}. \quad (40)$$

It should be noted that the bare dual Green's function (30) and renormalized interaction (31) are strongly nonlocal due to the EDMFT self-consistency conditions,

$$\sum_{\mathbf{k}} G_E = g_\nu, \quad (41)$$

$$\sum_{\mathbf{q}} W_E = \mathcal{W}_\omega. \quad (42)$$

Therefore, the dual theory is free from the double-counting problem by construction, and the local impurity contribution is excluded from the diagrams on the level of the bare propagators (30) and (31). The DB relations up to this point are exact and derived without any approximations.

It is worth mentioning, that the noninteracting dual theory ($\tilde{V} = 0$) is equivalent to EDMFT. However, even in the weakly interacting limit of the original model, $U \rightarrow 0$, the fermion-boson vertex $\gamma^{2,1}$ is nonzero and equal to unity, as shown in Appendix A and previous works on the DB approach. Thus, the Dual Boson formalism explicitly shows that corrections to EDMFT are not negligible. Therefore, the dynamical mean-field level is insufficient for describing nonlocal bosonic excitations, because the interactions between the nonlocal fermionic and bosonic degrees of freedom are always relevant.

A. Dual diagrams for the self-energy and polarization operator

The impurity vertices $\gamma^{n,m}$ are computationally expensive to calculate for large n and m . Practical DB calculations are usually restricted to $\gamma^{4,0}$ and $\gamma^{2,1}$, since that is sufficient to satisfy conservation laws and since processes involving higher-order vertices can be suppressed with the appropriate self-consistency condition [31].

As it was shown above, the dual theory can be rewritten in terms of lattice quantities [see Eqs. (37) and (38)], where the dual diagrams are constructed in terms of only one type of bare propagators, i.e., the nonlocal part of EDMFT Green's function

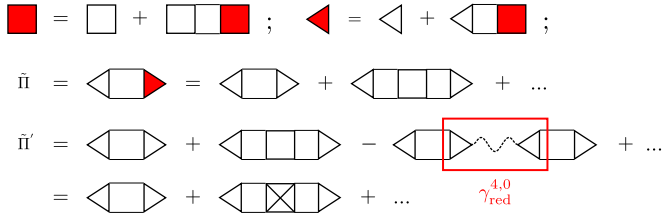


FIG. 3. Structure of the vertex corrections in different theories in case of one (top line) and two (bottom line) types of propagators. Solid straight and wave lines correspond to the Green's function and renormalized interaction of one type and the dashed lines to those of the second type, respectively.

and renormalized interaction given by Eqs. (30) and (31). Local parts of the bare EDMFT propagators, namely g_ν and \mathcal{W}_ω , are of the second type and hidden in the full local vertex functions of the impurity problem, which serve as the bare interaction vertices in dual space. Then, with the same logic presented in Sec. II B, the DB self-energy and polarization operator in the ladder approximation are given by

$$\tilde{\Sigma} = \text{diagram with two red triangles} + \text{diagram with two white squares and a red square}, \quad (43)$$

$$\tilde{\Pi} = \text{diagram with a white triangle and a red triangle}, \quad (44)$$

where the renormalized vertex functions are taken in the ladder approximation (see Fig. 3, top line). Note that here the splitting of propagators into the two parts is nominal and matters only for the dual theory when all diagrams are written in terms of only one nonlocal type of bare propagator. In general, the initial lattice theory works only with one type of Green's function and renormalized interaction, namely the bare EDMFT propagators, that for the local case we call impurity g_ν or \mathcal{W}_ω and for nonlocal dual \tilde{G}_0 or \tilde{W}_0 . Since the dual theory gives the correction to the lattice quantities, the dual contributions $\tilde{\Sigma}_{\mathbf{k}\nu}$ and $\tilde{\Pi}_{\mathbf{q}\omega}$ introduced beyond EDMFT should be irreducible with respect both to the impurity and the dual propagators.

Let us turn to a more detailed explanation. As was shown in Eqs. (37) and (38), the lattice self-energy and polarization operator introduced beyond EDMFT are not given by the dual $\tilde{\Sigma}_{\mathbf{k}\nu}$ and $\tilde{\Pi}_{\mathbf{q}\omega}$ and have the form of Eqs. (39) and (40). Note that the denominators in the expressions for $\tilde{\Sigma}_{\mathbf{k}\nu}$ and $\tilde{\Pi}_{\mathbf{q}\omega}$ have a very important physical meaning. The DB theory works with the *full* vertex functions of the impurity problem, that obviously contain one-particle reducible contributions. Therefore, the denominators in Eqs. (39) and (40) exclude these one-particle reducible contributions from the diagrams for the self-energy and polarization operator in order to avoid the double-counting in the Dyson Eqs. (37) and (38). Similar discussions were presented in Ref. [24] with regards to the DF approach.

To show this more explicitly, let us consider the following example. The dual polarization operator in the form of the full two-particle ladder can be written in a matrix form as (see the

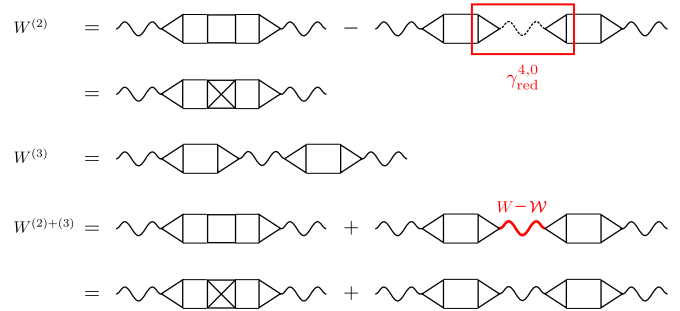


FIG. 4. Diagrammatic representation of the second- and the third-order contribution to the renormalized interaction.

second line of Fig. 3 for the diagrammatic representation)

$$\tilde{\Pi}_{\mathbf{k}\omega} = \frac{\gamma \tilde{G} \tilde{G} \gamma}{1 + [\gamma]^{-1} \gamma^{4,0} \tilde{G} \tilde{G} \gamma}, \quad (45)$$

where $\gamma^{4,0}$ is the full local four-point vertex of the impurity problem. Using these relations, Eq. (38) can be rewritten as (see the third line of Fig. 3)

$$\tilde{\Pi}_{\mathbf{q}\omega} = \frac{\gamma \tilde{G} \tilde{G} \gamma}{1 + [\gamma]^{-1} (\gamma^{4,0} + \gamma \mathcal{W}_\omega \gamma) \tilde{G} \tilde{G} \gamma}. \quad (46)$$

Here

$$\begin{aligned} \gamma_{\text{irr}}^{4,0} &= \gamma^{4,0} + \gamma \mathcal{W}_\omega \gamma, \\ \boxtimes &= \square - \text{diagram with dashed lines} \end{aligned} \quad (47)$$

is identically the irreducible part $\gamma_{\text{irr}}^{4,0}$ of the full four-fermionic vertex function of the impurity problem with respect to the renormalized interaction \mathcal{W}_ω . Then the polarization operator $\tilde{\Pi}$ introduced beyond EDMFT is nothing more than the normal dual polarization operator $\tilde{\Pi}$ taken in the form of the full dual ladder, but with irreducible four-point vertices $\gamma_{\text{irr}}^{4,0}$ instead of the full vertices $\gamma^{4,0}$ of the impurity problem. Therefore, the exact relation (40) automatically corrects the structure of the polarization operator, which is irreducible with respect to the dual renormalized interaction, to be also irreducible with respect to the impurity interaction \mathcal{W}_ω .

Let us then compare the second- and the third-order term of diagrammatic expansion of Eq. (38) shown in Fig. 4,

$$W_{\mathbf{q}\omega}^{(2)} = W_{\mathbf{q}\omega}^E \tilde{\Pi}_{\mathbf{q}\omega} W_{\mathbf{q}\omega}^E, \quad (48)$$

$$W_{\mathbf{q}\omega}^{(3)} = W_{\mathbf{q}\omega}^E \tilde{\Pi}_{\mathbf{q}\omega} W_{\mathbf{q}\omega}^E \tilde{\Pi}_{\mathbf{q}\omega} W_{\mathbf{q}\omega}^E. \quad (49)$$

After the substitution of the second term of $\tilde{\Pi}$ to Eq. (48) and of the first term of $\tilde{\Pi}$ to Eq. (49) we get

$$W_{\mathbf{q}\omega}^{(2)} = -W_E \gamma G G \gamma_{\text{irr}}^{4,0} G G \gamma W_E, \quad (50)$$

$$\begin{aligned} W_{\mathbf{q}\omega}^{(3)} &= W_E \gamma G G \gamma \mathcal{W}_\omega \gamma G G \gamma W_E \\ &+ W_E \gamma G G \gamma (W_E - \mathcal{W}_\omega) \gamma G G \gamma W_{\mathbf{q}\omega}^E, \end{aligned} \quad (51)$$

$$\begin{aligned} W_{\mathbf{q}\omega}^{(2)+(3)} &= -W_E \gamma G G \gamma_{\text{irr}}^{4,0} G G \gamma W_E \\ &+ W_E \gamma G G \gamma W_E \gamma G G \gamma W_{\mathbf{q}\omega}^E. \end{aligned} \quad (52)$$

Then one can see that the first term in Eq. (51) exactly gives the reducible contribution to the full four-point vertex function that was excluded from Eq. (50) by the denominator of $\tilde{\Pi}$. If one neglects this denominator, it will immediately lead to the double-counting in Dyson Eq. (52).

The same holds for the self-energy, where all contributions, coming from the denominator, give corrections to the six-point vertices $\gamma^{6,0}$ and $\gamma^{2,2}$ and remove the reducible contributions with respect to the local impurity Green's function g_v . Previous DB studies did not account for the six- and higher-point vertices, because they are negligibly small in both the large and small U limits [31]. Therefore, from one point of view, if the ladder approximation for the dual self-energy does not contain these six-point vertices, then the denominator in Eq. (39) should be neglected, because otherwise it will cancel the reducible terms in Dyson Eq. (37) with respect to the impurity g_v . On the other hand, one of the advantages of the DB formalism is the fact that all dual diagrams are written in terms of full impurity vertices instead of irreducible ones. Therefore, in the strong interaction limit, where the formal diagrammatic expansion cannot be performed, the full high-order vertices are small, which is not the case for the irreducible ones. Thus, writing the dual diagrams in terms of full vertices, it allows us to exclude the terms with the six-point vertices from the self-energy. Then, the presence of the denominator in Eq. (39) helps to include irreducible contributions of the high-order vertices when their full contributions are negligibly small.

B. DB – GW approach

With the four-fermion vertex $\gamma^{4,0}$, the Dual Boson approach can obviously include more correlation effects than EDMFT + GW, at a significant computational cost. However, it is also possible to construct a EDMFT++ approach from DB that does not require the full two-particle vertex. Taking $\gamma^{4,0} = 0$, the fermion-boson vertex $\gamma_{v\omega}$ can be approximated as unity, as was discussed above, and the expressions for the dual $\tilde{\Sigma}_{\mathbf{k}v}$ and $\tilde{\Pi}_{\mathbf{q}\omega}$ operator are

$$\tilde{\Sigma}_{\mathbf{k}v}^{\text{DB-GW}} = - \sum_{\mathbf{q}\omega} \tilde{G}_{\mathbf{k}+\mathbf{q},v+\omega} \tilde{W}_{\mathbf{q}\omega}, \quad (53)$$

$$\tilde{\Pi}_{\mathbf{q}\omega}^{\text{DB-GW}} = 2 \sum_{\mathbf{k}v} \tilde{G}_{\mathbf{k}+\mathbf{q},v+\omega} \tilde{G}_{\mathbf{k}v}. \quad (54)$$

We call this the DB – GW approximation. According to the above discussions, in this simplest case the denominator in Eqs. (39) and (40) should be excluded, since we are interested in the contribution of only lower-order vertex functions, so we should take

$$\tilde{\Sigma}_{\mathbf{k}v} = \tilde{\Sigma}_{\mathbf{k}v}^{\text{DB-GW}}, \quad (55)$$

$$\tilde{\Pi}_{\mathbf{q}\omega} = \tilde{\Pi}_{\mathbf{q}\omega}^{\text{DB-GW}}, \quad (56)$$

without the denominators presented in Eqs. (39) and (40). Thus we see that the EDMFT + GW and DB – GW approaches start with the same form of the self-energy and polarization operator diagrams and with similar propagators based on the same EDMFT quantities G_E and W_E . The difference between the two approaches lies in the way double-counting is excluded from these diagrams, which for the DB – GW case is shown

in Eqs. (30) and (31). This results in different self-energies $\tilde{\Sigma}_{\mathbf{k}v}$, and polarization operators $\tilde{\Pi}_{\mathbf{q}\omega}$ that are used to treat nonlocal effects beyond the EDMFT in these two different cases. Since the local and nonlocal correlation effects are intertwined in a complicated way, it is more efficient to exclude double-counting already on the level of the bare EDMFT Green's function and bare interaction in the dual formalism, rather than to remove the local contribution of the full diagram. This happens naturally in the exact dual Hubbard-Stratonovich transformation.

It is worth mentioning that the dual renormalized interaction $\tilde{W}_{\mathbf{q}\omega}$ does not depend on the form of decoupling. As it is shown in Eq. (A16), both UV - and V -decoupling forms lead to the same result $U_{\mathbf{q}} - \mathcal{U}_{\omega} = V_{\mathbf{q}} - \Lambda_{\omega}$ for the interaction accounted beyond the dynamical mean-field level in the DB theory. It is then easy to see that the DMFT+GW theory in a V -decoupling form excludes the impurity interaction in a proper way, since the dual renormalized interaction (A16) in the case $\Lambda_{\omega} = 0$ has exactly the form of V -decoupling. Due to the problems arising in the EDMFT+GW approach in the UV -decoupling form mentioned in Appendix B we take the renormalized interaction for the EDMFT + GW(γ) theories in the form of V -decoupling for the later comparison with DB results.

C. Local vertex corrections in DB method

To add vertex corrections to the DB – GW approach, one can take the second-order diagrams for the dual self-energy $\tilde{\Sigma}^{\text{GW}\gamma} = \tilde{\Sigma}_{\mathbf{k}v}^{(2)}$ (25) and polarization operator $\tilde{\Pi}^{\text{GW}\gamma} = \tilde{\Pi}_{\mathbf{q}\omega}^{(2)}$ (26), which are dressed with the full local impurity fermion-boson vertices $\gamma_{v\omega}$ as

$$\tilde{\Sigma}_{\mathbf{k}v}^{\text{GW}\gamma} = - \sum_{\mathbf{q}\omega} \gamma_{v\omega} \tilde{G}_{\mathbf{k}+\mathbf{q},v+\omega} \tilde{W}_{\mathbf{q}\omega} \gamma_{v+\omega,-\omega}, \quad (57)$$

$$\tilde{\Pi}_{\mathbf{q}\omega}^{\text{GW}\gamma} = 2 \sum_{\mathbf{k}v} \gamma_{v\omega} \tilde{G}_{\mathbf{k}+\mathbf{q},v+\omega} \tilde{G}_{\mathbf{k}v} \gamma_{v+\omega,-\omega}. \quad (58)$$

Similarly to the DB – GW approach we neglect the denominator in Eqs. (39) and (40) and repeat all calculations in the same way.

The four approaches are summarized in Fig. 5, showing the self-energy and polarization operator diagram, where square brackets $[\dots]_{\text{loc}}$ denote the exclusion of the local part. The computational recipes for all the EDMFT++ theories is shown in Fig. 6.

IV. NUMERICAL RESULTS

To test the EDMFT++ schemes, we study the charge-order transition in the square lattice Hubbard model, a popular testing ground for extensions of EDMFT [16,17,30]. Here we show calculations where first Δ_v and Λ_{ω} are determined self-consistently on the EDMFT level for all schemes. Then, the nonlocal correlation effects are included. Having the same impurity problem as the starting point for all approaches allows us to compare clearly the effect from the extensions only. We use $t = 1/4$, $\beta = 50$, and a 32×32 lattice. The resulting phase boundary between the charge-ordered phase (CO) and the Fermi liquid (FL), determined in the same way as in Ref. [30], is shown in Fig. 7. The checkerboard CO phase is characterized

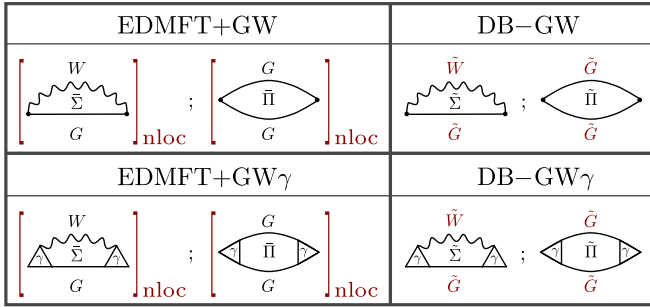


FIG. 5. Self-energy and polarization operator for EDMFT++ approaches. The square brackets $[\dots]_{\text{nloc}}$ denote exclusion of the local part. DMFT + GW is not listed here, it has the same diagrams as EDMFT + GW and only differs in their choice of \mathcal{U}_ω .

by a divergent charge susceptibility at the wave vector $\mathbf{q} = (\pi, \pi)$. The phase boundary may therefore be located by looking for zeros of the inversed susceptibility $X_{\omega=0, \mathbf{q}=(\pi, \pi)}^{-1}$. Note that the renormalized interaction $W_{\mathbf{q}\omega}$ in DMFT + GW, EDMFT + GW, and EDMFT + GW γ approaches is taken in the form of the V -decoupling as discussed above.

Since ordering is unfavorable for the interaction energy for $V < U/4$, the true phase boundary is expected to be above the $V = U/4$ line. Indeed, the full DB result is above this line [30]. In all other EDMFT++ approximations with fewer correlation effects, the phase transition occurs at smaller V . The DB – GW γ approximation performs best in this respect, and is close to the DB phase boundary for all values of U . The two approximations that include local vertex corrections via $\gamma_{\nu\omega}$ perform better than their counterparts without, and both DB-based approaches outperform their EDMFT + GW counterpart.

At $U = 0$, we expect the random phase approximation (RPA) to give a reasonable prediction for the phase boundary. The RPA limit is recovered by all shown EDMFT++ approaches, but already at relatively small $U = 0.5$, strong differences between the methods become clear.

In the opposite limit of large U , EDMFT itself starts to give an accurate phase boundary, since it accounts for all local effects and those are most important at large U . Both DB-based approaches converge to EDMFT at $U = 2.5$, whereas both EDMFT + GW approaches give a phase boundary at the same, slightly smaller V .

We even observe that DMFT + GW performs better than EDMFT + GW, although it is simpler. Although DMFT + GW contains fewer correlation effects than EDMFT + GW, it is free from double-counting by construction. This clearly shows the huge role that double-counting can play. On the other hand, comparison of DMFT + GW and DB – GW schemes confirms the fact that inclusion of bosonic correlations already on the impurity level is also very important and provides the better starting point for extending dynamical mean-field theory.

In Fig. 8, we show the polarization operator corrections $\tilde{\Pi}_{\mathbf{q}\omega}$ at high-symmetry \mathbf{q} points, according to the EDMFT + GW(γ) and DB – GW(γ) approaches. The results of the two approaches DB – GW and EDMFT + GW, that do not take into account the frequency dependent vertex function γ , are similar. The presence of the full local three-point

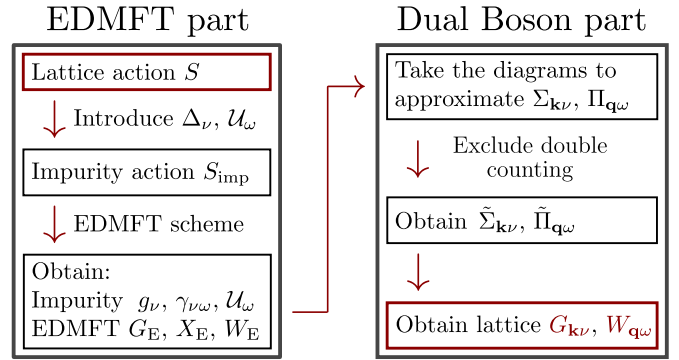


FIG. 6. The recipe to construct an EDMFT++ theory. DMFT + GW is obtained by taking $\mathcal{U}_\omega = U$ instead of determining it self-consistently.

vertex function in the diagrams significantly changes the results [30]. Moreover, the inclusion of the vertex function results in the different behavior of the polarization operator of the DB – GW γ and EDMFT + GW γ approaches. The dual contribution to the polarization operator in this case is larger. Therefore, using the dual way one excludes fewer contributions from the diagrams, than in the case of the EDMFT++ theories. Thus, the main difference in the approaches lies in their description of the collective excitations and comes from the different ways of treating the double-counting problem.

The fermion-boson vertex exhibits less structure as the metallicity of the system is increased and becomes mostly flat as the phase boundary to the CO phase is approached [30]. The influence of nonlocal interaction V on the three-point vertex function $\gamma_{\nu\omega}$ is shown in Fig. 9. The effects of the three-leg vertex are also visible in the nonlocal part of the polarization operator in the difference between DB – GW

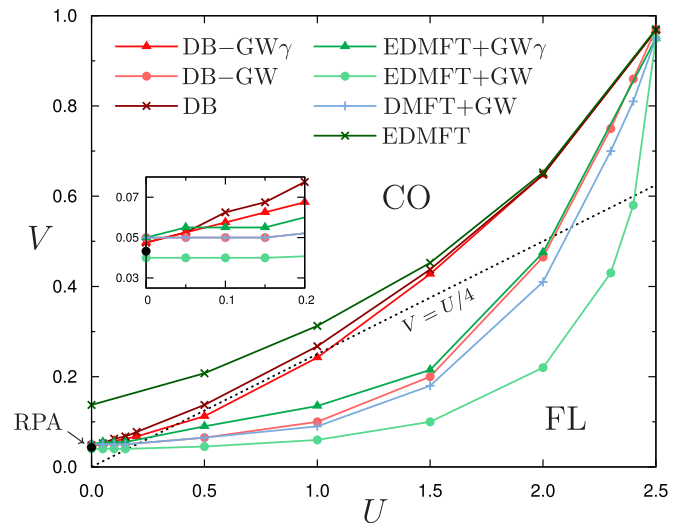


FIG. 7. $U - V$ phase diagram in EDMFT, DB and EDMFT++ theories at inverse temperature $\beta = 50$. The dashed line shows $V = U/4$; the dot at $U = 0$ shows the starting point of RPA data. CO and FL denote charge-ordered and Fermi-liquid metallic phases, respectively. The EDMFT and DB data are taken from [30]; EDMFT + GW data practically coincides with results shown in [15,16] papers.

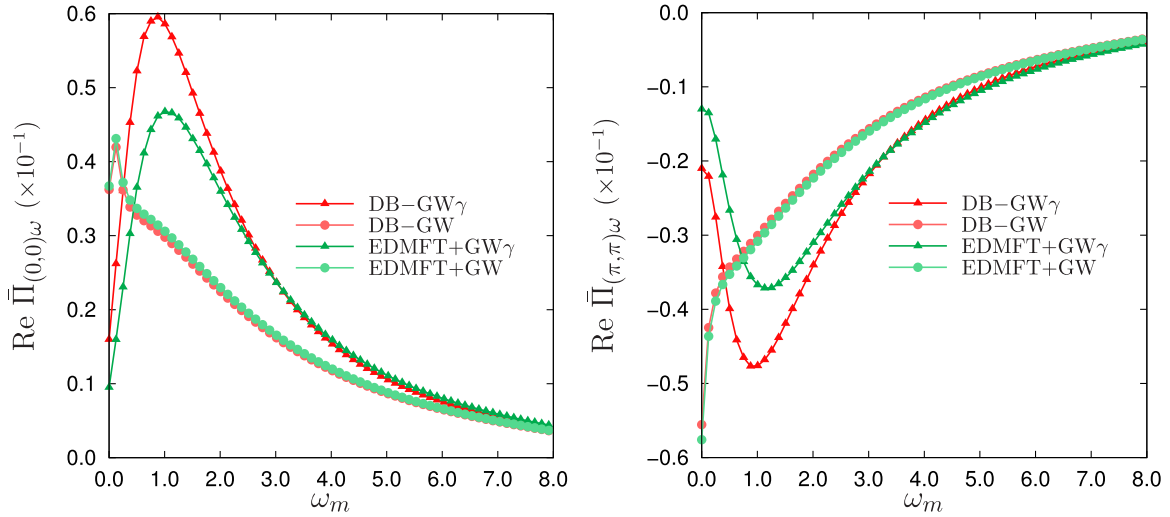


FIG. 8. Frequency dependence of nonlocal $\text{Re } \bar{\Pi}_{\mathbf{q}\omega}$ for momentum $\mathbf{k} = (0,0)$, $\mathbf{k} = (\pi,\pi)$ for on-site interaction $U = 2.3$ and the nearest-neighbor interaction $V = 0.2$.

and DB – GW γ (or between EDMFT + GW and EDMFT + GW γ) approaches (see Fig. 8).

V. CONCLUSIONS

We have presented a recipe to create approximations beyond EDMFT that take into account nonlocal correlation effects while simultaneously avoiding double-counting issues. By properly including nonlocality we see an improvement in the phase boundary between the charge-ordered phase and the Fermi liquid. Even in weakly and moderately interacting systems, the phase boundary is shifted significantly upwards compared to traditional EDMFT + GW. In fact, EDMFT+GW is even improved upon by DMFT + GW, which neglects the effect of nonlocal interactions on the impurity model but does avoid double-counting. This allows us to study the physics in a larger part of parameter space, where EDMFT + GW has undergone a spurious transition. This is important for accurately determining the charge-ordering transition in real materials and in surface systems.

The approaches presented here work without requiring the computationally expensive full two-particle vertex. The frequency dependence of the much simpler fermion-boson vertex already contains most of the relevant physics, and including it via DB – GW γ gives a phase boundary close to the full DB result. Without access to the fermion-boson vertex, deviations are bigger. In both cases, however, the dual way of treating the double-counting problem greatly improves the results.

The ladder Dual Boson approach can be derived from the dual functional, that automatically solves the complicated issue of the conservation laws [31]. For the future, it would be useful to obtain a similar functional description for the approximated theories presented in this work.

ACKNOWLEDGMENTS

The authors would like to thank Alexey Rubtsov for fruitful discussions and Lewin Boehnke and Andrey Katanin for useful

comments. E.A.S., E.G.C.P.v.L., and M.I.K. acknowledge support from ERC Advanced Grant No. 338957 FEMTO/NANO and from NWO via Spinoza Prize, A.I.L. from the DFG Research Unit FOR 1346, A.H. from the DFG via SPP 1459, and computer time at the North-German Supercomputing Alliance (HLRN).

APPENDIX A: DUAL TRANSFORMATIONS

The dual transformations of the nonlocal part of the action S_{rem} can be made in the same way as in previous works on the DB approach. In order to define the three-point vertex in the TRILEX way, here we introduce a different rescaling of the dual bosonic fields. The partition function of our problem is given by

$$Z = \int D[c^*, c] e^{-S}, \quad (\text{A1})$$

where the action S is given by (2). Performing the Hubbard-Stratonovich transformations one can introduce the new *dual* variables f^* , f , ϕ ,

$$\begin{aligned} & e^{\sum_{\mathbf{k}\nu\sigma} c_{\mathbf{k}\nu\sigma}^* [\Delta_{\nu\sigma} - \varepsilon_{\mathbf{k}}] c_{\mathbf{k}\nu\sigma}} \\ &= D_f \int D[f^*, f] e^{-\sum_{\mathbf{k}\nu\sigma} \{f_{\mathbf{k}\nu\sigma}^* [\Delta_{\nu\sigma} - \varepsilon_{\mathbf{k}}]^{-1} f_{\mathbf{k}\nu\sigma} + c_{\nu\sigma}^* f_{\nu\sigma} + f_{\nu\sigma}^* c_{\nu\sigma}\}}, \\ & e^{\frac{1}{2} \sum_{\mathbf{q}\omega} \rho_{\mathbf{q}\omega}^* [\Lambda_{\omega} - V_{\mathbf{q}}] \rho_{\mathbf{q}\omega}} \\ &= D_b \int D[\phi] e^{-\frac{1}{2} \sum_{\mathbf{q}\omega} \{\phi_{\mathbf{q}\omega}^* [\Lambda_{\omega} - V_{\mathbf{q}}]^{-1} \phi_{\mathbf{q}\omega} + \rho_{\omega}^* \phi_{\omega} + \phi_{\omega}^* \rho_{\omega}\}}. \end{aligned} \quad (\text{A2})$$

Terms $D_f = \det[\Delta_{\nu\sigma} - \varepsilon_{\mathbf{k}}]$ and $D_b^{-1} = \sqrt{\det[\Lambda_{\omega} - V_{\mathbf{q}}]}$ can be neglected because they do not contribute to expectation values. Rescaling the fermionic fields $f_{\mathbf{k}\nu\sigma}$ as $f_{\mathbf{k}\nu\sigma} g_{\nu\sigma}^{-1}$, the bosonic fields $\phi_{\mathbf{q}\omega}$ as $\phi_{\mathbf{q}\omega} \alpha_{\omega}^{-1}$, where $\alpha_{\omega} = (1 + \mathcal{U}_{\omega} \chi_{\omega})$, and integrating out the original degrees of freedom c^* and c we arrive at the dual action,

$$\tilde{S} = - \sum_{\mathbf{k}\nu} f_{\mathbf{k}\nu}^* \tilde{G}_0^{-1} f_{\mathbf{k}\nu} - \frac{1}{2} \sum_{\mathbf{q}\omega} \phi_{\mathbf{q}\omega}^* \tilde{W}_0^{-1} \phi_{\mathbf{q}\omega} + \tilde{V}, \quad (\text{A3})$$

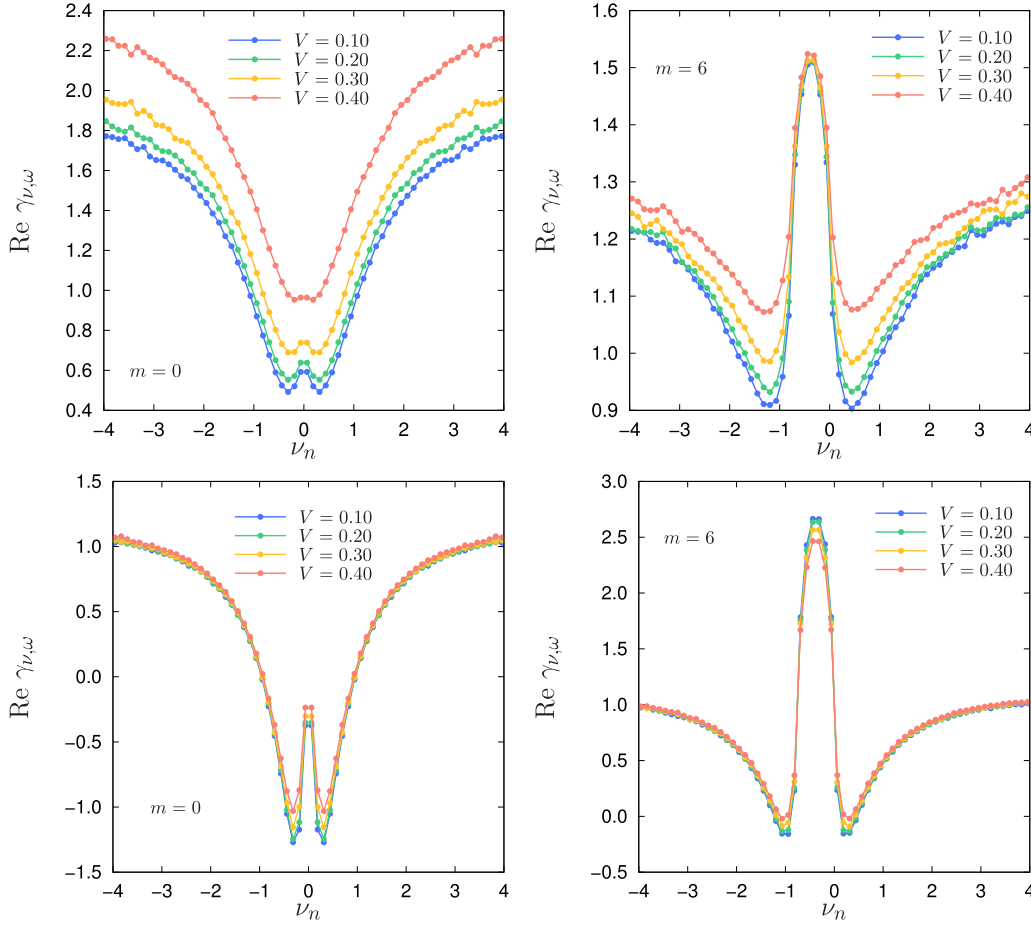


FIG. 9. Local three-point vertex function $\gamma_{\nu\omega}$ for two bosonic frequencies $\omega_m = 2m\pi/\beta$ with $m = 0$ and $m = 6$ for different values of nearest-neighbor interaction V and local interaction $U = 1.5$ (top line) and $U = 2.3$ (bottom line).

with the bare dual propagators,

$$\tilde{G}_0 = [g_v^{-1} + \Delta_v - \varepsilon_{\mathbf{k}}]^{-1} - g_v = G_E - g_v, \quad (\text{A4})$$

$$\tilde{W}_0 = \alpha_\omega [[U_{\mathbf{q}} - \mathcal{U}_\omega]^{-1} - \chi_\omega]^{-1} \alpha_\omega = W_E - \mathcal{W}_\omega, \quad (\text{A5})$$

and the dual interaction term \tilde{V} . The explicit form of the dual interaction can be obtained by expanding the c^* and c dependent part of the partition function in an infinite series and integrating out these degrees of freedom as follows:

$$\begin{aligned} & \int e^{-\sum_{\nu\omega} \{c_\nu^* g_\nu^{-1} f_\nu + f_\nu^* g_\nu^{-1} c_\nu + \rho_\omega^* \alpha_\omega^{-1} \phi_\omega + \phi_\omega^* \alpha_\omega^{-1} \rho_\omega\}}, \\ & e^{-S_{\text{imp}}[c^*, c]} D[c^*, c] \\ &= f_{v_1}^* f_{v_2} \langle c_{v_1} c_{v_2}^* \rangle g_{v_1}^{-1} g_{v_2}^{-1} + \frac{1}{2} \phi_{\omega_1}^* \phi_{\omega_2} \langle \rho_{\omega_1} \rho_{\omega_2}^* \rangle \alpha_{\omega_1}^{-1} \alpha_{\omega_2}^{-1} \\ & \quad - f_{v_1}^* f_{v_2} \phi_{\omega_3}^* \langle c_{v_1} c_{v_2}^* \rho_{\omega_3} \rangle g_{v_1}^{-1} g_{v_2}^{-1} \alpha_{\omega_3}^{-1} \\ & \quad + \frac{1}{4} f_{v_1}^* f_{v_2}^* f_{v_3} f_{v_4} \langle c_{v_1} c_{v_2} c_{v_3}^* c_{v_4}^* \rangle g_{v_1}^{-1} g_{v_2}^{-1} g_{v_3}^{-1} g_{v_4}^{-1} + \dots \\ &= -f_v^* g_v^{-1} f_v - \frac{1}{2} \phi_\omega^* \alpha_\omega^{-1} \chi_\omega \alpha_\omega^{-1} \phi_\omega \\ & \quad - f_{v_1}^* f_{v_2} \phi_{\omega_3}^* \langle c_{v_1} c_{v_2}^* \rho_{\omega_3} \rangle g_{v_1}^{-1} g_{v_2}^{-1} \alpha_{\omega_3}^{-1} \end{aligned}$$

$$\begin{aligned} & + \frac{1}{4} f_{v_1}^* f_{v_2}^* f_{v_3} f_{v_4} \langle c_{v_1} c_{v_2} c_{v_3}^* c_{v_4}^* \rangle g_{v_1}^{-1} g_{v_2}^{-1} g_{v_3}^{-1} g_{v_4}^{-1} + \dots \\ &= e^{-\{f_v^* g_v^{-1} f_v + \frac{1}{2} \phi_\omega^* \alpha_\omega^{-1} \chi_\omega \alpha_\omega^{-1} \phi_\omega + \tilde{V}\}}. \end{aligned} \quad (\text{A6})$$

So the dual interaction has the form of an infinite expansion off the full vertices of the local impurity problem,

$$\begin{aligned} \tilde{V} &= f_{v_1}^* f_{v_2} \phi_{\omega_3}^* \langle c_{v_1} c_{v_2}^* \rho_{\omega_3} \rangle g_{v_1}^{-1} g_{v_2}^{-1} \alpha_{\omega_3}^{-1} \\ & \quad - \frac{1}{4} f_{v_1}^* f_{v_2}^* f_{v_3} f_{v_4} g_{v_1}^{-1} g_{v_2}^{-1} g_{v_3}^{-1} g_{v_4}^{-1} \{ \langle c_{v_1} c_{v_2} c_{v_3}^* c_{v_4}^* \rangle \\ & \quad - \langle c_{v_1} c_{v_4}^* \rangle \langle c_{v_2} c_{v_3}^* \rangle + \langle c_{v_1} c_{v_3}^* \rangle \langle c_{v_2} c_{v_4}^* \rangle \} + \dots \end{aligned} \quad (\text{A7})$$

Here we define the three- and four-point vertex functions as ($\gamma_{\nu\omega}$ is the shorthand notation for the $\gamma_{\nu\omega}^{2,1}$),

$$\gamma_{\nu\omega} = g_v^{-1} g_{v+\omega}^{-1} \alpha_\omega^{-1} \langle c_\nu c_{v+\omega}^* \rho_\omega \rangle, \quad (\text{A8})$$

$$\begin{aligned} \gamma_{\nu\nu'\omega}^{4,0} &= g_v^{-1} g_{v'}^{-1} g_{v'-\omega}^{-1} g_{v+\omega}^{-1} \\ & \quad \times [\langle c_\nu c_{v'} c_{v'-\omega}^* c_{v+\omega}^* \rangle - g_\nu g_{v'} (\delta_\omega - \delta_{v', v+\omega})], \end{aligned} \quad (\text{A9})$$

with the simple connection between them,

$$\gamma_{\nu\omega} = \alpha_\omega^{-1} \sum_{\nu'} [1 - \gamma_{\nu\nu'\omega}^{4,0} g_{\nu'} g_{v'-\omega}]. \quad (\text{A10})$$

In the weakly interacting limit, namely $U \rightarrow 0$, the renormalization factor α_ω goes to unity and the four-point vertex $\gamma^{4,0}$ is zero, as detailed in previous works [29–31] on the DB approach. Then, the three-point vertex can be reduced to its bare form $\gamma_0 = 1$. Frequency dependence of the full local three-point vertex function $\gamma_{v\omega}$ and the influence of nonlocal interaction V is shown in Fig. 9.

Then, the two first terms in \tilde{V} are given by

$$\tilde{V} = \gamma_{v\omega} f_v^* f_{v+\omega} \phi_\omega^* + \frac{1}{4} \gamma_{vv'\omega}^{4,0} f_v^* f_{v'}^* f_{v+\omega} f_{v'-\omega}. \quad (\text{A11})$$

The dual Green's function $\tilde{G}_{\mathbf{k}v} = -\langle f_{\mathbf{k}v} f_{\mathbf{k}v}^* \rangle$ and renormalized dual interaction $\tilde{W}_{\mathbf{q}\omega} = -\langle \phi_{\mathbf{q}\omega} \phi_{\mathbf{q}\omega}^* \rangle$, as well as dual self-energy $\tilde{\Sigma}_{\mathbf{k}v}$ and polarization operator $\tilde{\Pi}_{\mathbf{q}\omega}$, can be obtained diagrammatically [29–31]. These dual quantities have the usual connection,

$$\tilde{G}_{\mathbf{k}v}^{-1} = \tilde{G}_0^{-1} - \tilde{\Sigma}_{\mathbf{k}v}, \quad (\text{A12})$$

$$\tilde{W}_{\mathbf{q}\omega}^{-1} = \tilde{W}_0^{-1} - \tilde{\Pi}_{\mathbf{q}\omega}. \quad (\text{A13})$$

Finally, lattice Green's function $G_{\mathbf{k}v}$ and susceptibility $X_{\mathbf{q}\omega}$ can be expressed in terms of dual propagators via exact relations,

$$G_{\mathbf{k}v} = -[\varepsilon_{\mathbf{k}} - \Delta_v]^{-1} + [\varepsilon_{\mathbf{k}} - \Delta_v]^{-1} g_v^{-1} \tilde{G}_{\mathbf{k}v} g_v^{-1} [\varepsilon_{\mathbf{k}} - \Delta_v]^{-1}, \quad (\text{A14})$$

$$X_{\mathbf{q}\omega} = -[U_{\mathbf{q}} - \mathcal{U}_\omega]^{-1} + [U_{\mathbf{q}} - \mathcal{U}_\omega]^{-1} \alpha_\omega^{-1} \tilde{W}_{\mathbf{q}\omega} \alpha_\omega^{-1} [U_{\mathbf{q}} - \mathcal{U}_\omega]^{-1}. \quad (\text{A15})$$

One can also rewrite the last relation and obtain the relation for the full dual renormalized interaction,

$$\alpha_\omega^{-1} \tilde{W}_{\mathbf{q}\omega} \alpha_\omega^{-1} = [U_{\mathbf{q}} - \mathcal{U}_\omega] + [U_{\mathbf{q}} - \mathcal{U}_\omega] X_{\mathbf{q}\omega} [U_{\mathbf{q}} - \mathcal{U}_\omega], \quad (\text{A16})$$

to show that the dual propagator $\tilde{W}_{\mathbf{q}\omega}$ is evidently a renormalized interaction in the nonlocal part of the action, where the impurity interaction is excluded on the level of the bare interaction. It is worth mentioning, that for the case of $\Lambda_\omega = 0$, which corresponds to the DMFT theory as a basis, the renormalized interaction is exactly that of the usual V -decoupling.

APPENDIX B: COMPARISON OF THE DIFFERENT DECOUPLING SCHEMES WITH THE DB APPROACH

As a consequence of the exact dual transformations presented in Appendix A, the renormalized interaction introduced beyond the DMFT when the bosonic hybridization function Λ_ω is equal to zero (i.e., $U_\omega = U$) should be taken in the form of V -decoupling (A16). Contrary to DMFT, the impurity model in the EDMFT approach contains nonzero bosonic retarded interaction Λ_ω , thus the renormalized interaction in EDMFT++ theories has neither UV -, nor V -decoupling form. In this case the bare nonlocal interaction $U_{\mathbf{q}} - \mathcal{U}_\omega$ for small Λ_ω (i.e., $U_\omega \simeq U$) is closer to $V_{\mathbf{q}}$ than to $U_{\mathbf{q}} = U + V_{\mathbf{q}}$, and therefore in this paper we take $W_{\mathbf{q}}$ in the form of V -decoupling for all EDMFT++ theories.

One more argument to avoid treating the renormalized interaction in the UV -decoupling form is the fact that in this case EDMFT+GW reproduces the results of the GW approach in the region close to the phase boundary. Indeed, the self-energy and polarization operator for the GW approach are given by Eqs. (14) and (15), respectively. The EDMFT + GW approach uses only nonlocal parts of these diagrams beyond the dynamical mean-field solution. They can be written as follows:

$$\tilde{\Sigma}_{\mathbf{k}v}^{\text{E+GW}} = - \sum_{\mathbf{q}\omega} \tilde{G}_{\mathbf{k}+\mathbf{q},v+\omega}^{\text{E+GW}} \tilde{W}_{\mathbf{q}\omega}^{\text{E+GW}}, \quad (\text{B1})$$

$$\tilde{\Pi}_{\mathbf{q}\omega}^{\text{E+GW}} = 2 \sum_{\mathbf{k}v} \tilde{G}_{\mathbf{k}+\mathbf{q},v+\omega}^{\text{E+GW}} \tilde{G}_{\mathbf{k}v}^{\text{E+GW}}, \quad (\text{B2})$$

where $\tilde{G}_{\mathbf{k}v}^{\text{E+GW}} = G_{\mathbf{k}v} - g_v$, $\tilde{W}_{\mathbf{q}\omega}^{\text{E+GW}} = W_{\mathbf{q}\omega} - \mathcal{W}_\omega$ are nonlocal parts of the full lattice Green's function and renormalized interaction, respectively. Then, the full self-energy and polarization operator of the lattice problem can be written as

$$\Sigma_{\mathbf{k}v} = \Sigma_{\text{imp}} + \tilde{\Sigma}_{\mathbf{k}v}^{\text{E+GW}}, \quad (\text{B3})$$

$$\Pi_{\mathbf{q}\omega} = \Pi_{\text{imp}} + \tilde{\Pi}_{\mathbf{q}\omega}^{\text{E+GW}}, \quad (\text{B4})$$

where

$$\Sigma_{\text{imp}} = - \sum_{\omega} g_{v+\omega} \mathcal{W}_\omega \gamma_{v\omega}, \quad (\text{B5})$$

$$\Pi_{\text{imp}} = 2 \sum_v g_{v+\omega} g_v \gamma_{v\omega}, \quad (\text{B6})$$

are the exact self-energy and polarization operator of the impurity problem written in the Hedin form. Then, one can rewrite the full lattice self-energy and polarization operator as

$$\begin{aligned} \Sigma_{\mathbf{k}v} &= - \sum_{\mathbf{q}\omega} G_{\mathbf{k}+\mathbf{q},v+\omega} W_{\mathbf{q}\omega} - \sum_{\omega} g_{v+\omega} \mathcal{W}_\omega (\gamma_{v\omega} - 1) \\ &= \Sigma_{\mathbf{k}v}^{\text{GW}} - \sum_{\omega} g_{v+\omega} \mathcal{W}_\omega (\gamma_{v\omega} - 1), \end{aligned} \quad (\text{B7})$$

$$\begin{aligned} \Pi_{\mathbf{q}\omega} &= 2 \sum_{\mathbf{k}v} G_{\mathbf{k}+\mathbf{q},v+\omega} G_{\mathbf{k}v} + 2 \sum_v g_{v+\omega} g_v (\gamma_{v\omega} - 1) \\ &= \Pi_{\mathbf{q}\omega}^{\text{GW}} + 2 \sum_v g_{v+\omega} g_v (\gamma_{v\omega} - 1). \end{aligned} \quad (\text{B8})$$

Therefore, in the region where the value of the three-point vertex $\gamma_{v\omega}$ is close to the value of the bare three-point vertex $\gamma_0 = 1$, the EDMFT + GW approach reproduces the result of the GW method. Thus, the contribution of the exactly solvable impurity model in this region is lost. It happens, because one cancels the very big local contribution from the GW diagrams in order to avoid the double-counting problem, and then this local contribution suppresses the contribution of the local impurity model. It turns out that the EDMFT + GW approach cancels too much from the diagrams introduced beyond the dynamical mean-field level, and treating of the double-counting problem can be done in a better way.

To see this, one can compare the dual way of exclusion of the double-counting with the UV -decoupling scheme. Since the inner self-consistency for the diagrams beyond the dynamic mean-field level is used, it is hard to compare the

resulting diagrams of these two approaches. Nevertheless, let us consider the polarization operator in the first iteration, when only the bare EDMFT Green's functions enter the diagrams. Studying the first iteration is sufficient since the nonlocal self-energy $\tilde{\Sigma}_{\mathbf{k}\nu}$ is small in our region of interest. Then, one can see, that the polarization operator for EDMFT+GW and DB – GW has the same form,

$$\tilde{\Pi}_{\mathbf{q}\omega}^0 = 2 \sum_{\mathbf{k}\nu} \tilde{G}_0 \tilde{G}_0, \quad (\text{B9})$$

where $\tilde{G}_0 = G_E - g_\nu$. Then, one can obtain for the difference between the renormalized interactions used in EDMFT + GW and DB – GW the following relation:

$$\begin{aligned} [W_{\mathbf{q}\omega} - \mathcal{W}_\omega] - \tilde{W}_{\mathbf{q}\omega} &= \frac{W_E}{1 - \tilde{\Pi}_{\mathbf{q}\omega}^0 W_E} - \frac{\tilde{W}_0}{1 - \tilde{\Pi}_{\mathbf{q}\omega}^0 \tilde{W}_0} - \mathcal{W}_\omega \\ &= \mathcal{W}_\omega [1 - \tilde{\Pi}_{\mathbf{q}\omega}^0 \tilde{W}_0]^{-1} [1 - \tilde{\Pi}_{\mathbf{q}\omega}^0 W_E]^{-1} - \mathcal{W}_\omega \\ &= \mathcal{W}_\omega \tilde{\Pi}_{\mathbf{q}\omega}^0 [\tilde{W}_{\mathbf{q}\omega} + W_{\mathbf{q}\omega} + \tilde{W}_{\mathbf{q}\omega} \tilde{\Pi}_{\mathbf{q}\omega}^0 W_{\mathbf{q}\omega}]. \end{aligned} \quad (\text{B10})$$

Therefore, the self-energy (B1) in the form of UV -decoupling additionally to the nonlocal dual contribution accounts for some diagrams that have local renormalized interaction \mathcal{W}_ω in their structure. In the Dual Boson formalism all local propagators are gathered in the local vertex functions of the impurity problem, including the local renormalized interaction \mathcal{W}_ω , which is a part of the local four-point vertex $\gamma^{4,0}$. For example, the first term in the right-hand side of Eq. (B10) gives the following contribution to the self-energy,



$$(\text{B11})$$

which is a part of the dual diagram for the self-energy shown in Fig. 1(a). The second term in the right-hand side of Eq. (B10), when one takes only the local part of the EDMFT renormalized interaction in Eq. (13), namely $W_{\mathbf{q}\omega} = \frac{W_E}{1 - \tilde{\Pi}_{\mathbf{q}\omega}^0 W_E} \sim \frac{\mathcal{W}_\omega}{1 - \tilde{\Pi}_{\mathbf{q}\omega}^0 \mathcal{W}_\omega}$, is then equal to



$$(\text{B12})$$

which is again a part of the dual diagram for the self-energy shown in Fig. 1(b). This fact leads to two important problems in the EDMFT + GW approach. First of all, these additional self-energy diagrams in case of UV -decoupling presented above are very selective and account only for the local renormalized interaction \mathcal{W}_ω instead of the full local four-point vertex functions $\gamma^{4,0}$, as the DB approach does. This selective choice is not well-controlled and may result in over- or underestimation of interaction effects. Also, the existence of the local propagators as a part of the nonlocal interaction shows that the EDMFT + GW approach in the form of UV -

decoupling is not able to separate local and nonlocal degrees of freedom in a proper way. This leads, in particular, to the double-counting problem in the next-order nonlocal diagrams introduced beyond EDMFT. Indeed, if one does not restrict himself to the simplest GW diagram accounted beyond the dynamical mean-field level and additionally includes the four-point vertex functions $\gamma^{4,0}$ in the diagrams for the self-energy [for example, the diagrams shown in Fig. 1(b)], then, as it was shown in Eqs. (B11)–(B12), the GW diagram (B1) for the self-energy would have contributions with the local \mathcal{W}_ω , that would already be accounted for in these additional diagrams with the local four-point vertices.

Let us study what happens in the region, where the impurity renormalized interaction \mathcal{W}_ω gives the main contribution in the full local four-point vertex $\gamma^{4,0}$. In this region the EDMFT + GW solution should be close to the Dual Boson ladder approximation with the self-energy and polarization operator diagrams shown in Figs. 1(a) and 1(b). Substituting “ $-\mathcal{W}_\omega$ ” for the four-point vertex $\gamma^{4,0}$ in Eq. (A10) and using Eq. (B6) and the relation $\alpha^{-1} = 1 - \Pi_{\text{imp}} \mathcal{U}_\omega$ one can get the trivial solution $\sum_\nu g_{\nu+\omega} g_\nu (\gamma_{\nu\omega} - 1) = 0$. Therefore, as it was shown in Eqs. (B7) and (B8), in this region EDMFT + GW in the UV -decoupling form reproduces the result of the GW approach. In the other regions, where the bare vertex $\gamma_0 = 1$ does not give the main contribution to the full three-point vertex $\gamma_{\nu\omega}$, EDMFT + GW shows a result different from the GW approach, but unfortunately, it is not correct to approximate the full local vertex $\gamma^{4,0}$ by the local \mathcal{W}_ω there. As it was pointed out above, one of the advantages of the DB formalism is that the full impurity vertices, in particular the full four-point vertex $\gamma^{4,0}$, are used in the dual diagrams for the self-energy and polarization operator. This full vertex $\gamma^{4,0}$ is small and consists of the two large contributions: reducible ($\gamma_{\text{red}}^{4,0}$) and irreducible ($-\gamma \mathcal{W}_\omega \gamma$) with respect to renormalized interaction \mathcal{W}_ω . These two contributions compensate each other as shown in Eq. (47). If one accounts for only one large irreducible contribution to the vertex function, it leads to an incorrect description of the collective excitations and problems mentioned above.

Finally, one can rewrite Eq. (B10) as follows:

$$\begin{aligned} \tilde{W}_{\mathbf{q}\omega} &= W_{\mathbf{q}\omega} - \mathcal{W}_\omega [1 + \tilde{\Pi}_{\mathbf{q}\omega}^0 \tilde{W}_{\mathbf{q}\omega} + \tilde{\Pi}_{\mathbf{q}\omega}^0 W_{\mathbf{q}\omega} \\ &\quad + \tilde{\Pi}_{\mathbf{q}\omega}^0 \tilde{W}_{\mathbf{q}\omega} \tilde{\Pi}_{\mathbf{q}\omega}^0 W_{\mathbf{q}\omega}], \end{aligned} \quad (\text{B13})$$

and see that DB excludes not the full local renormalized interaction \mathcal{W}_ω of the impurity model from the full lattice interaction $W_{\mathbf{q}\omega}$, but the local interaction, that is renormalized by nonlocal polarization and nonlocal interactions $W_{\mathbf{q}\omega}$ and $\tilde{W}_{\mathbf{q}\omega}$. Therefore, the DB approach, which is free from the double-counting problem by construction, excludes fewer contributions from the full lattice renormalized interaction than the EDMFT + GW approach, and effects of the impurity model are not suppressed in our calculations.

[1] W. Metzner and D. Vollhardt, *Phys. Rev. Lett.* **62**, 324 (1989).

[2] A. Georges, G. Kotliar, W. Krauth, and M. J. Rozenberg, *Rev. Mod. Phys.* **68**, 13 (1996).

- [3] G. Kotliar, S. Y. Savrasov, K. Haule, V. S. Oudovenko, O. Parcollet, and C. A. Marianetti, *Rev. Mod. Phys.* **78**, 865 (2006).
- [4] P. Werner and M. Casula, *J. Phys. Condens. Matter* **28**, 383001 (2016).
- [5] J. Hubbard, *Proc. R. Soc. London A* **276**, 238 (1963).
- [6] J. Hubbard, *Proc. R. Soc. London A* **281**, 401 (1964).
- [7] N. Mott, *Metal-Insulator Transitions* (Taylor and Francis, Philadelphia, 1974).
- [8] M. Imada, A. Fujimori, and Y. Tokura, *Rev. Mod. Phys.* **70**, 1039 (1998).
- [9] Q. Si and J. L. Smith, *Phys. Rev. Lett.* **77**, 3391 (1996).
- [10] J. L. Smith and Q. Si, *Phys. Rev. B* **61**, 5184 (2000).
- [11] R. Chitra and G. Kotliar, *Phys. Rev. Lett.* **84**, 3678 (2000).
- [12] R. Chitra and G. Kotliar, *Phys. Rev. B* **63**, 115110 (2001).
- [13] P. Sun and G. Kotliar, *Phys. Rev. B* **66**, 085120 (2002).
- [14] S. Biermann, F. Aryasetiawan, and A. Georges, *Phys. Rev. Lett.* **90**, 086402 (2003).
- [15] T. Ayrál, P. Werner, and S. Biermann, *Phys. Rev. Lett.* **109**, 226401 (2012).
- [16] T. Ayrál, S. Biermann, and P. Werner, *Phys. Rev. B* **87**, 125149 (2013).
- [17] L. Huang, T. Ayrál, S. Biermann, and P. Werner, *Phys. Rev. B* **90**, 195114 (2014).
- [18] A. van Roekeghem, T. Ayrál, J. M. Tomczak, M. Casula, N. Xu, H. Ding, M. Ferrero, O. Parcollet, H. Jiang, and S. Biermann, *Phys. Rev. Lett.* **113**, 266403 (2014).
- [19] L. Boehnke, F. Nilsson, F. Aryasetiawan, and P. Werner, [arXiv:1604.02023](https://arxiv.org/abs/1604.02023) [cond-mat.str-el].
- [20] L. Hedin, *Phys. Rev.* **139**, A796 (1965).
- [21] F. Aryasetiawan and O. Gunnarsson, *Rep. Prog. Phys.* **61**, 237 (1998).
- [22] L. Hedin, *J. Phys.: Condens. Matter* **11**, R489 (1999).
- [23] A. Toschi, A. A. Katanin, and K. Held, *Phys. Rev. B* **75**, 045118 (2007).
- [24] G. Rohringer, A. Toschi, H. Hafermann, K. Held, V. I. Anisimov, and A. A. Katanin, *Phys. Rev. B* **88**, 115112 (2013).
- [25] C. Taranto, S. Andergassen, J. Bauer, K. Held, A. Katanin, W. Metzner, G. Rohringer, and A. Toschi, *Phys. Rev. Lett.* **112**, 196402 (2014).
- [26] T. Ayrál and O. Parcollet, *Phys. Rev. B* **92**, 115109 (2015).
- [27] T. Ayrál and O. Parcollet, *Phys. Rev. B* **93**, 235124 (2016).
- [28] A. N. Rubtsov, M. I. Katsnelson, and A. I. Lichtenstein, *Phys. Rev. B* **77**, 033101 (2008).
- [29] A. Rubtsov, M. Katsnelson, and A. Lichtenstein, *Annals of Physics* **327**, 1320 (2012).
- [30] E. G. C. P. van Loon, A. I. Lichtenstein, M. I. Katsnelson, O. Parcollet, and H. Hafermann, *Phys. Rev. B* **90**, 235135 (2014).
- [31] E. A. Stepanov, E. G. C. P. van Loon, A. A. Katanin, A. I. Lichtenstein, M. I. Katsnelson, and A. N. Rubtsov, *Phys. Rev. B* **93**, 045107 (2016).
- [32] E. G. C. P. van Loon, H. Hafermann, A. I. Lichtenstein, A. N. Rubtsov, and M. I. Katsnelson, *Phys. Rev. Lett.* **113**, 246407 (2014).
- [33] E. Gull, A. J. Millis, A. I. Lichtenstein, A. N. Rubtsov, M. Troyer, and P. Werner, *Rev. Mod. Phys.* **83**, 349 (2011).
- [34] P. Werner and A. J. Millis, *Phys. Rev. Lett.* **104**, 146401 (2010).
- [35] L. Pollet, N. V. Prokof'ev, and B. V. Svistunov, *Phys. Rev. B* **83**, 161103 (2011).
- [36] J. Gukelberger, L. Huang, and P. Werner, *Phys. Rev. B* **91**, 235114 (2015).
- [37] B. Altshuler and A. Aronov, *Zh. Eksp. Teor. Fiz.* **77**, 2028 (1979).
- [38] A. Anokhin and M. Katsnelson, *Int. J. Mod. Phys. B* **10**, 2469 (1996).

**IV. EFFECTIVE ISING MODEL FOR CORRELATED SYSTEMS WITH
CHARGE ORDERING**

Collective electronic fluctuations in correlated materials give rise to various important phenomena, such as charge ordering, superconductivity, Mott insulating and magnetic phases, and plasmon and magnon modes^{Note*}. Unfortunately, the description of these correlation effects requires significant effort, since they almost entirely rely on strong local and nonlocal electron-electron interactions. Some collective phenomena, such as magnetism, can be sufficiently described by simple Heisenberg-like models that are formulated in terms of bosonic variables. This fact suggests that other many-body excitations can also be described by simple bosonic models in the spirit of Heisenberg theory. Here we derive an effective bosonic action for charge degrees of freedom for the extended Hubbard model and define a physical regime where the obtained action reduces to a classical Hamiltonian of an effective Ising model.

^{Note*} Major parts of this section have been published as Phys. Rev. B 99, 115124 (2019)

A. Introduction

Studies of highly correlated electron systems are one of the "hot" areas of condensed matter physics. In particular, a tremendous number of papers have been concerned with the problem of collective phenomena in solids, such as charge ordering, superconductivity, Mott insulating and magnetic phases, plasmon, magnon modes and others. Some of these properties, e.g. magnetism, can be described by Heisenberg-like models formulated in terms of bosonic variables only, which drastically simplifies solution of the problem. The existence of a classical "bosonic" description for spin degrees of freedom relies on the existence of a, so called, adiabatic approximation. The latter implies that spin degrees of freedom are much slower and have lower energy than single-particle (electronic) excitations. Therefore, magnetic excitations can be clearly distinguished from electronic fluctuations at the corresponding time and energy scale. Over the past decades, the random phase approximation (RPA) [29–31] was and is still the dominant approximation of collective charge excitations in the modern condensed matter theory. The reason for its success are due to the fulfillment of the charge conservation as well as qualitatively good description of plasmonic modes. However the RPA is limited to weakly correlated systems since plasmons are considered as a infinite summation of electron-hole pairs of bare electron propagators with unrenormalized energy spectrum. For a correct description of plasmons in a correlated system with large electron-electron interactions it is unavoidable to consider diagrammatic vertex corrections to the polarization operator. In practice most of the advanced methods with diagrammatic corrections violate the charge conservation law [12, 32], which is reflected in the plasmonic modes. Nevertheless, recently a new theory that allows a conserving description of plasmons beyond RPA was proposed in [33]. This approach is based

on the Dual Boson (DB) theory [23, 25] and considers the polarization operator in the two-particle ladder form written in terms of local three- and four-point vertex functions. A further extension of this method to the multiorbital case is challenging due to its complicated diagrammatic structure.

Another interesting feature of collective charge excitations in many realistic systems is a tendency to charge ordering (CO), which is widely discussed in the literature starting from the discovery of the Verwey transition in magnetite Fe_3O_4 [34–36]. Nowadays, there is a number of materials, such as the rare-earth compound Yb_4As_3 [37–39], transition metal MX_2 [40–42] and rare-earth R_3X_4 [43–45] chalcogenides ($M = \text{V}, \text{Nb}, \text{Ta}$; $\text{R} = \text{Eu}, \text{Sm}$; $\text{X} = \text{S}, \text{Se}$), Magnéli phase Ti_4O_7 [46–49], vanadium bronzes $\text{Na}_x\text{V}_2\text{O}_5$ and $\text{Li}_x\text{V}_2\text{O}_5$ (see Ref. [39] and [50], and references therein), where CO was observed. Since this phenomenon is based on the presence of strong local and nonlocal electron-electron interactions, the theoretical description of this issue also requires the use of very advanced approaches (see e.g. Refs. [51] and [52]).

Recent theoretical investigations of charge correlation effects caused by the strong nonlocal Coulomb interaction indicate that the description of collective charge excitations in the correlated regime can be drastically simplified. Thus, the study of charge ordering within the DCA [28], Dual Boson [24, 53] and GW+EDMFT [12, 27] approaches showed similar results for the phase boundary between the normal and CO phases. The fact that a much simpler GW+EDMFT theory performs in reasonable agreement with the more advanced DB approach and with almost exact DCA method suggests that collective charge fluctuations can be described via a simple theory, at least in a specific physical regime. Unfortunately, the use of the GW+EDMFT theory for description of charge excitations is not fully

justified, since this approach suffers from the Fierz ambiguity when the charge and spin channels are considered simultaneously [20, 54] and the “HS- UV/V ” decoupling problem [9, 55]. In this regard, the simplified (DB–GW) [24, 53] approximation of the DB theory that does not consider vertex corrections and is free of the above-mentioned problems seems more preferable. However, it provides much worse results than the DB [53] and GW+EDMFT [27] theories. Therefore, the problem of the efficient description of collective charge excitations in correlated materials is still open.

In the case when accurate quantum mechanical calculations are challenging, the initial quantum problem can be replaced by an appropriate classical one. This thermodynamical approach is widely used, for example, for a description of ordering in alloys [56–61]. There, the total energy of the ground state is mapped onto an effective Ising Hamiltonian, with parameters determined from *ab initio* calculations within the framework of the density functional theory [62–64]. However, to our knowledge, no attempts to extend this theory to the description of charge fluctuations in the correlated regime and to derive the pair interaction of the Ising model directly from the quantum problem have been reported yet. Additional impulse for investigation of this important problem is given by theoretical studies of magnetism in correlated electronic systems [65–69], where an effective classical Heisenberg model for the quantum problem was derived. Since magnetism is also a collective electronic property, one may expect that charge degrees of freedom can be treated in a similar way.

Motivated by above discussions, we introduce a new theory that describes charge excitations of the extended Hubbard model in terms of bosonic variables that are related to electronic charge degrees of freedom. The corresponding bosonic action of the model is derived

with the use of the advanced ladder DB approach. Consequently, the charge susceptibility that enters the action has a complicated diagrammatic structure that takes into account frequency dependent vertex corrections. Further, we observe that the dependence of local vertex functions on fermionic frequencies is directly connected to the value of the double occupancy of lattice sites. Moreover, we find that in a wide range of physical parameters, when the double occupancy is large, this dependence is negligible, and the expression for the charge susceptibility can be drastically simplified. Thus, the theory reduces to an improved version of the GW+EDMFT and DB–GW approaches, and the expression for the susceptibility takes a simple RPA-like form constructed from the lattice Green’s functions. Finally, It has been showed that in the case of well-developed collective charge fluctuations the initial quantum problem can be mapped onto an effective classical Ising Hamiltonian written in terms of pair interaction between charge densities.

B. Bosonic action for electronic charge

Let us start with the following action of the extended Hubbard model written in the Matsubara frequency (ν, ω) and momentum (\mathbf{k}, \mathbf{q}) space

$$\mathcal{S} = - \sum_{\mathbf{k}, \nu} c_{\mathbf{k}\nu}^* [i\nu + \mu - \varepsilon_{\mathbf{k}}] c_{\mathbf{k}\nu} + \frac{1}{2} \sum_{\mathbf{q}, \omega} [U + V_{\mathbf{q}}] \rho_{\mathbf{q}\omega}^* \rho_{\mathbf{q}\omega}. \quad (23)$$

Here $c_{\mathbf{k}\nu}^*$ ($c_{\mathbf{k}\nu}$) are Grassmann variables corresponding to the creation (annihilation) of an electron. $\varepsilon_{\mathbf{k}}$ is the Fourier transform of the hopping amplitude t_{ij} , which is considered here in the nearest neighbor approximation on a two-dimensional square lattice. The energy scale is $4t = 1$. U and $V_{\mathbf{q}}$ are local and nonlocal Coulomb interactions, respectively. Charge degrees of freedom are described here

introducing the bosonic variable $\rho_{\mathbf{q}\omega} = n_{\mathbf{q}\omega} - \langle n_{\mathbf{q}\omega} \rangle$ that describes variation of the electronic density $n_{\mathbf{q}\omega} = \sum_{\mathbf{k},\nu,\sigma} c_{\mathbf{k}\nu\sigma}^* c_{\mathbf{k}+\mathbf{q},\nu+\omega,\sigma}$ from the average value. Hereinafter, spin labels $\sigma = \uparrow, \downarrow$ are omitted.

An effective bosonic action for charge degrees of freedom can be derived following transformations, as presented in a recent work [69]. There, the lattice action (23) is divided into the local impurity problem of the extended dynamical mean-field theory (EDMFT) [13–16, 70] and the remaining nonlocal part. In order to decouple the single-electronic and collective charge degrees of freedom, one can perform *dual* transformations of the nonlocal part of the lattice action that lead to a new problem written in the *dual* space [24, 53]. The inverse transformation back to the initial “lattice” space after truncation of the interaction of the *dual* action at the two-particle level results in the following bosonic action for charge variables (for details see Ref. [69] and Appendix IV G)

$$\mathcal{S}_{\text{ch}} = -\frac{1}{2} \sum_{\mathbf{q},\omega} \rho_{\mathbf{q}\omega}^* X_{\mathbf{q}\omega}^{-1} \rho_{\mathbf{q}\omega}. \quad (24)$$

Here, the charge susceptibility $X_{\mathbf{q}\omega}$ in the conserving ladder DB approximation is given by the following relation [69]

$$X_{\mathbf{q}\omega}^{-1} = [X_{\mathbf{q}\omega}^{\text{DMFT}}]^{-1} + \Lambda_{\omega} - V_{\mathbf{q}}, \quad (25)$$

where Λ_{ω} is the local bosonic hybridization function of the impurity problem. $X_{\mathbf{q}\omega}^{\text{DMFT}} = \sum_{\nu\nu'} [X_{\mathbf{q}\omega}^{\text{DMFT}}]_{\nu\nu'}$ is the charge susceptibility in the DMFT form [1, 3] written in terms of lattice Green’s functions $G_{\mathbf{k}\nu}$ and two-particle irreducible (2PI) in the charge channel four-point vertices $\bar{\gamma}_{\nu\nu'\omega}^{2\text{PI}}$ of the local impurity problem (see Appendix IV G)

$$[X_{\mathbf{q}\omega}^{\text{DMFT}}]_{\nu\nu'}^{-1} = [X_{\mathbf{q}\omega}^0]_{\nu\nu'}^{-1} + \bar{\gamma}_{\nu\nu'\omega}^{2\text{PI}}. \quad (26)$$

Here, $[X_{\mathbf{q}\omega}^0]_{\nu\nu'} = \sum_{\mathbf{k}} G_{\mathbf{k}+\mathbf{q},\nu+\omega} G_{\mathbf{k}\nu} \delta_{\nu\nu'}$ is a generalized bare lattice susceptibility, and the inversion should be understood as a matrix operation in the fermionic frequency ν, ν' space. Note that in the ladder DB approximation the lattice Green's function is dressed only in the local impurity self-energy and therefore coincides with the usual EDMFT expression [13–16, 70]. Thus, the relation for the lattice susceptibility can be written as $X_{\mathbf{q}\omega} = \sum_{\nu\nu'} [X_{\mathbf{q}\omega}]_{\nu\nu'}$, where

$$[X_{\mathbf{q}\omega}]_{\nu\nu'}^{-1} = [X_{\mathbf{q}\omega}^0]_{\nu\nu'}^{-1} - U_{\nu\nu'\omega}^{\text{eff}} - V_{\mathbf{q}}, \quad (27)$$

and we introduced an effective bare local Coulomb interaction

$$U_{\nu\nu'\omega}^{\text{eff}} = -\Lambda_{\omega} - \bar{\gamma}_{\nu\nu'\omega}^{2\text{PI}}. \quad (28)$$

Note that the 2PI vertex function $\bar{\gamma}_{\nu\nu'\omega}^{2\text{PI}}$ is defined here in the particle-hole channel.

A recent study of magnetism of correlated electrons [69] shows that if the system exhibits well-developed bosonic fluctuations, the corresponding local vertex functions mostly depend on bosonic frequency ω , while their dependence on fermionic frequencies ν, ν' is negligible. Therefore, one can expect that in a physical regime where charge fluctuations are dominant the local 2PI vertex function in the charge channel can be approximated as $\bar{\gamma}_{\nu\nu'\omega}^{2\text{PI}} \simeq \bar{\gamma}_{\omega}^{2\text{PI}}$, and the charge susceptibility (25) takes the following simple form

$$X_{\mathbf{q}\omega}^{-1} = X_{\mathbf{q}\omega}^0{}^{-1} - U_{\omega}^{\text{eff}} - V_{\mathbf{q}}. \quad (29)$$

Here, $X_{\mathbf{q}\omega}^0 = \sum_{\nu\nu'} [X_{\mathbf{q}\omega}^0]_{\nu\nu'} = \sum_{\mathbf{k}\nu} G_{\mathbf{k}+\mathbf{q},\nu+\omega} G_{\mathbf{k}\nu}$ is the bare lattice susceptibility, and the effective bare local Coulomb interaction (28) transforms to $U_{\omega}^{\text{eff}} = -\Lambda_{\omega} - \bar{\gamma}_{\omega}^{2\text{PI}}$. As it is also shown in Ref. [69] and Appendix IV H, in the considered case of well-developed collective

fluctuations the 2PI vertex function can be approximated as

$$\gamma_{\omega}^{2\text{PI}} \simeq \chi_{\omega}^{-1} - \chi_{\omega}^0{}^{-1} \simeq -U - \Lambda_{\omega}, \quad (30)$$

where χ_{ω} and χ_{ω}^0 are the full and bare local susceptibilities of the impurity problem, respectively. As a consequence, the effective bare local Coulomb interaction reduces to the usual form $U_{\omega}^{\text{eff}} \simeq U$. Therefore, the expression in Eq. [29](#) is nothing more than the RPA susceptibility constructed on top of the EDMFT result for Green's functions. It is worth noting that in the regime of strong charge fluctuations the local self-energy takes the same form as in GW approach [\[21, 71, 72\]](#) (see Ref. [69](#) and Appendix [IV H](#)). Hence, the simplified theory can be reduced to the GW method in the case when the nonlocal contribution to the self-energy is also considered. Thus, we show that it is indeed possible to describe strong charge excitations by a simple bosonic action [\(24\)](#) in terms of charge susceptibility [\(29\)](#) that does not contain vertex corrections.

C. Regime of strong charge fluctuations

Now, let us define the physical regime where the presented above technique is applicable. In Ref. [69](#) collective excitations were studied in the ordered (antiferromagnetic) phase, where the proximity of the local magnetic moment m to its maximum value served as a signature of well-developed spin fluctuations. Here, we are interested in a similar description of a more complicated case when collective charge excitations are present in the system already in the normal phase. Since in the latter case all lattice sites are described by the same local impurity problem, the corresponding signature of strong bosonic fluctuations can no longer be found among local single-particle observables that are identical for every lattice site. It is also worth mentioning that, contrary to the magnetic phase where the order-

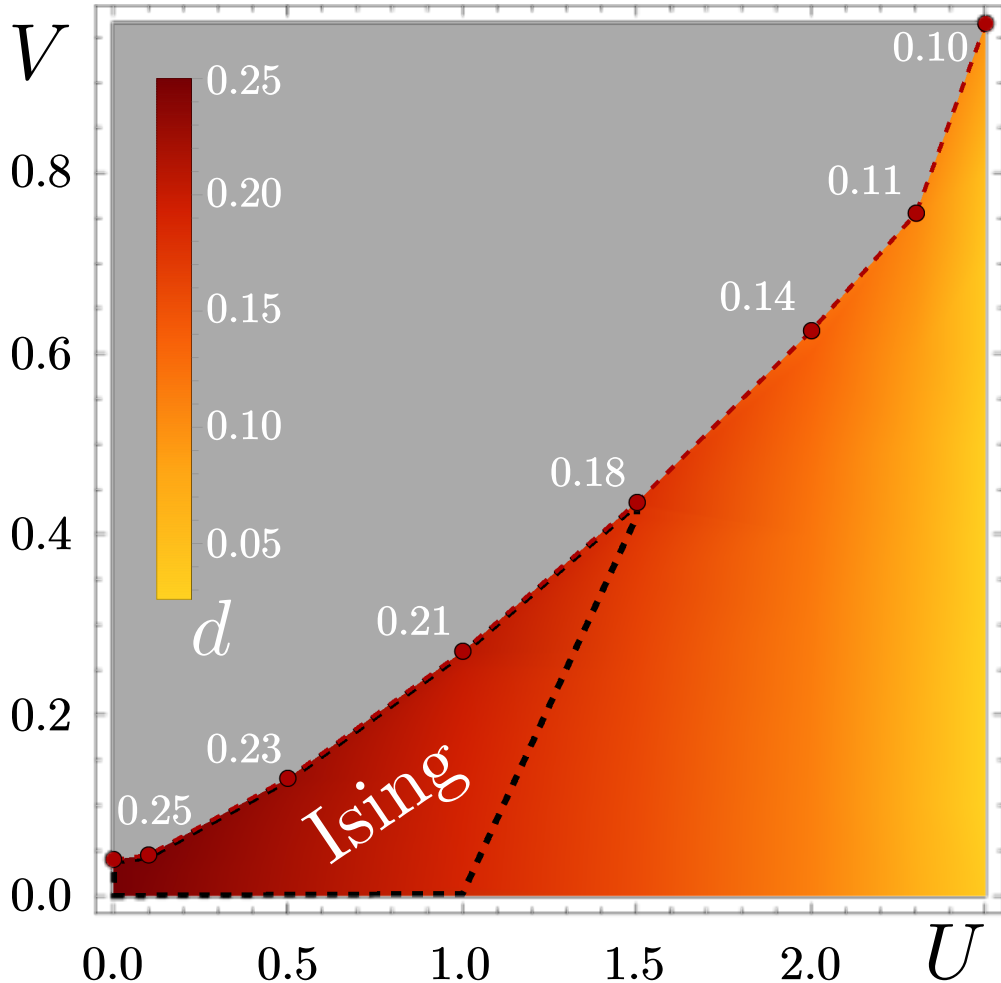


Figure 1. (Color online) Double occupancy of the extended Hubbard model shown on the U - V phase diagram. Calculations are performed in the normal phase where the value of the double occupancy d is depicted by color. The gray part corresponds to the charge ordered phase. Values of the double occupancy at the phase boundary are explicitly mentioned. The area depicted by the black dashed line corresponds to the case of large value of the double occupancy $d \geq 0.18$ and shows the regime where charge excitations can be described by an effective Ising model. Values of Coulomb interactions U and V are given in units of half of the bandwidth ($W/2 = 4t = 1$). Therefore, the effective Ising model can be used for a broad range of values of the Coulomb interaction, which may even exceed half of the bandwidth. The inverse temperature is $\beta = 50$.

ing of single-particle quantities (local magnetizations) is realized, the CO phase on a lattice corresponds to the ordering of doublons (see i.e. Refs. [73] and [74]) that are two-particle observables. For these reasons, the double-occupancy of the lattice site, which is defined as $d = \langle n_{\uparrow} n_{\downarrow} \rangle$ with the maximum value $d_{\max} = 0.25$, could be used as a fingerprint of the existence of strong charge fluctuations in the

system. The corresponding result for the double occupancy of the two-dimensional extended Hubbard model (23) on the square lattice is shown on the U - V phase diagram in Fig. 1 and obtained using the DB approach [75] without the above approximation of the four-point vertex function. The phase boundary (red dashed line) between the normal (colored) and CO (gray) phases is determined from the zeros of the inverse charge susceptibility $X_{\mathbf{q}\omega}^{-1}$ (25) at $\mathbf{q} = (\pi, \pi)$ and $\omega = 0$ point similarly to Refs. [24] and [53]. As expected, large charge fluctuations in the normal phase emerge in the region close to the phase transition to the ordered state. However, one can see that the strength of these fluctuations is not uniformly distributed along the phase boundary, since the value of d decreases with the increase of the local Coulomb interaction.

In order to clarify the connection between the value of the double occupancy and the strength of charge fluctuations, one can study an effective bare local Coulomb interaction $U_{\nu\nu'\omega}^{\text{eff}}$ defined in Eq. 28. Fig. 2 shows the ratio $U_{\nu\nu'\omega}^{\text{eff}}/U$ between the effective and actual local Coulomb interactions as the function of fermionic frequency ν at the $\nu' = \omega = 0$ point. This result is obtained close to the phase boundary between the normal and CO phases shown in Fig. 1 for different values of the local Coulomb interaction U and, as a consequence, of the double occupancy d . The exact values of U , V , and d for these calculations are specified in Table II. Here, one can immediately see that the effective Coulomb interaction at small values of U (large values of d) is almost frequency independent. Decreasing the double occupancy the frequency dependence of U^{eff} becomes crucial and one can no longer approximate the local 2PI vertex function by neglecting its dependence on fermionic frequencies. Remarkably, the effective Coulomb interaction tends to the actual value of the local Coulomb interaction at large frequencies for every value of U ,

which is in perfect agreement with the theory presented above. A similar asymptotic behavior was reported for the 2PI vertex function of the DMFT impurity problem ($\Lambda_\omega = 0$) in Ref. [76]. Thus, one can conclude that the inclusion of the bosonic hybridization function Λ_ω in the local impurity problem changes the ω -dependence of local vertex functions. The presence of Λ_ω in Eq. [25] restores the correct frequency behavior of the lattice susceptibility. Therefore, the inclusion of the Λ_ω in the theory has to be done consistently both in the local impurity problem and the lattice susceptibility ([25]), otherwise it may lead to incorrect frequency behavior of bosonic quantities. Results for $U_{\nu\nu'\omega}^{\text{eff}}/U$ for other values of ν' and ω can be found in Appendix IV G and show a similar connection of the double occupancy to the frequency dependence of the effective Coulomb interaction.

Let us now investigate the dependence of the effective local Coulomb interaction on the bosonic frequency ω . As shown in Fig. [2], the use of the approximation presented above for the 2PI vertex $\bar{\gamma}_{\nu\nu'\omega}^{2\text{PI}} \simeq \bar{\gamma}_\omega^{2\text{PI}}$ in the large double occupancy regime is now justified. Then, the effective Coulomb interaction U_ω^{eff} can be extracted from the simplified expression for the charge susceptibility ([29]), where the left-hand side is substituted from Eq. [25]. Since the leading contribution to the lattice susceptibility in this regime is given by the $\mathbf{q} = (\pi, \pi)$ momentum, the corresponding effective interaction shown in Fig. [3] reads

$$U_\omega^{\text{eff}} = X_{(\pi,\pi),\omega}^{0-1} - \left[X_{(\pi,\pi),\omega}^{\text{DMFT}} \right]^{-1} - \Lambda_\omega. \quad (31)$$

Here, the result is obtained in the normal phase close to the CO for the same values of Coulomb interactions as in Fig. [2]. It is worth mentioning that the above definition of the effective local Coulomb interaction is similar to the one of the two-particle self-consistent theory proposed by Vilk and Tremblay [77]. However, we use a more

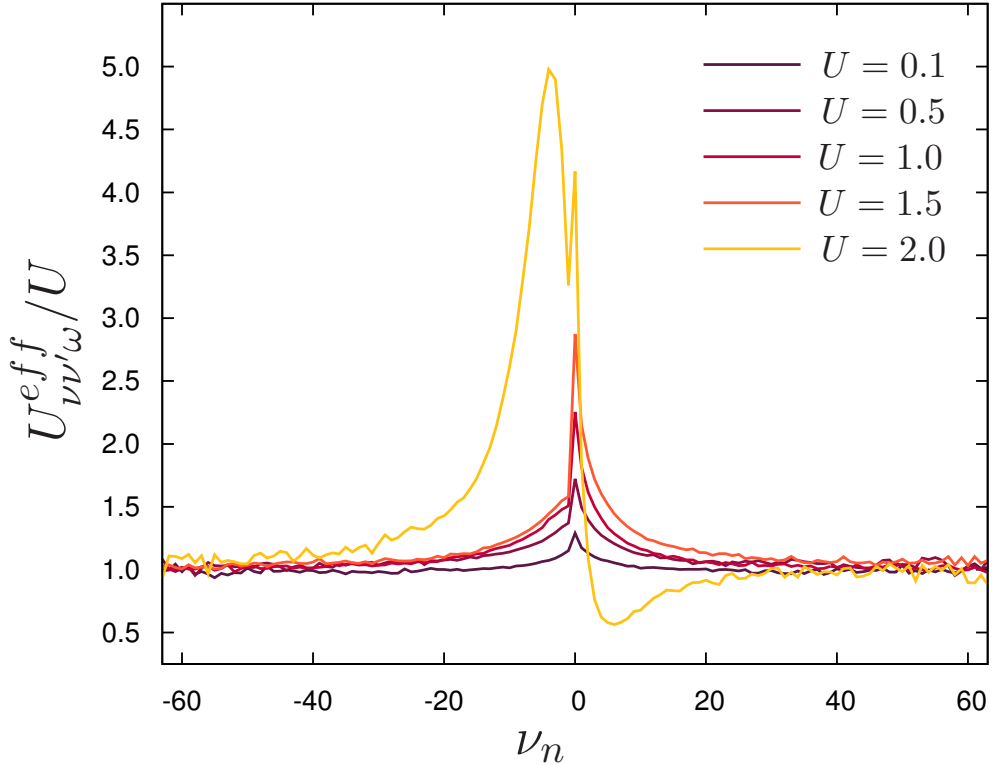


Figure 2. (Color online) Frequency dependence of the effective local Coulomb interaction $U_{\nu\nu'\omega}^{\text{eff}}$ obtained for different values of U at the phase boundary between the normal and CO phases at the $\nu' = \omega = 0$ point for $\beta = 50$. As the double occupancy is decreased, the dependence of the effective interaction on fermionic frequency becomes larger.

advanced expression for the lattice susceptibility $X_{\mathbf{q}\omega}$, contrary to the RPA form with the bare Green's functions considered in their work. Remarkably, in the case when the double occupancy is close to its maximum value, the effective Coulomb interaction U^{eff} does not depend on bosonic frequency either, and again coincides with the actual Coulomb interaction. In the smaller d regime the bosonic frequency dependence appears and cannot be avoided for consideration anymore. Therefore, the large value of the double occupancy is indeed an indicator of a well-developed charge fluctuations. Taking into account results shown in Figs. [2](#) and [3](#), the value of the double occupancy for which the effective local interaction is frequency independent and coincides with the bare local Coulomb interaction U can be estimated as $d \geq 0.18$. As schematically shown in Fig. [1](#),

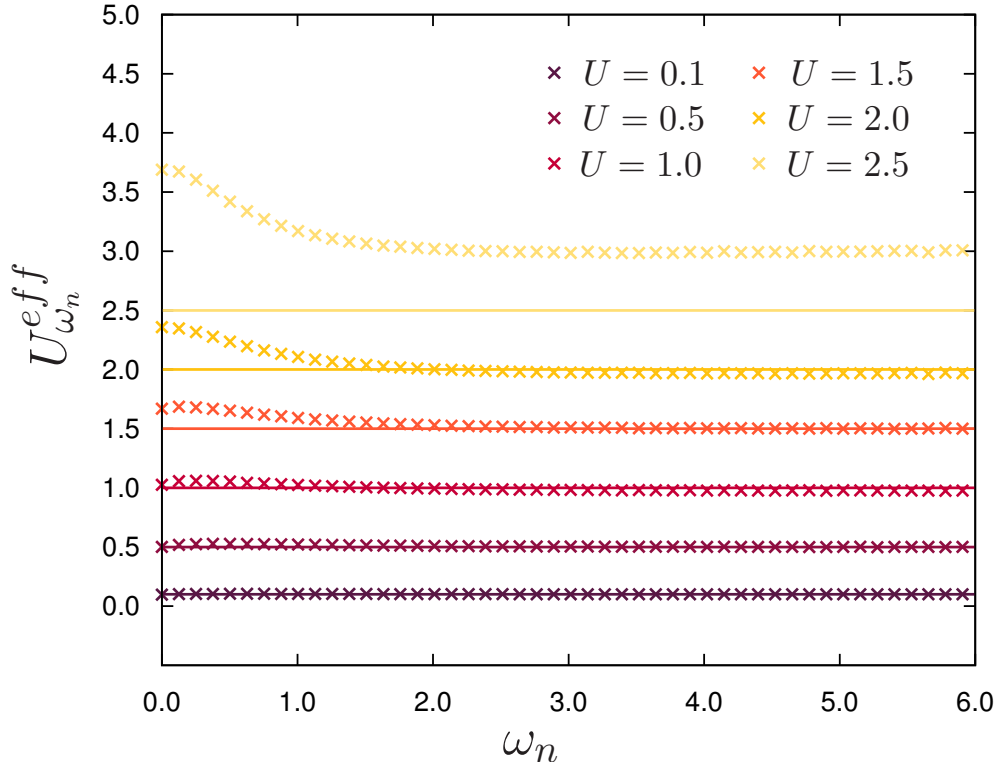


Figure 3. (Color online) Frequency dependence of the effective local Coulomb interaction U_{ω}^{eff} obtained for $\beta = 50$ close to the phase boundary between the normal and charge ordered phases for different values of the actual Coulomb interaction U . When the double occupancy is decreased, the difference between the effective and actual local Coulomb interactions becomes more notable.

the corresponding region depicted by the black dashed line can be distinguished for the relatively broad range of Coulomb interactions. Remarkably, the latter may even exceed half of the bandwidth.

D. Extended Hubbard model upon doping

In order to demonstrate the power of the derived above approach, let us investigate the phase boundary of the extended Hubbard model in the hole doped case. Recently, this issue was addressed in the Ref. [78] with the use of the within the dynamical cluster approximation (DCA). It can be argued the latter method is much more elaborate than the one presented in this work, and provides a quantitatively good result for the phase boundary between the normal and CO phases. Here, the simplified result for the phase boundary

is obtained using the expression (29) for the charge susceptibility, where the effective local interaction U_{ω}^{eff} is replaced by the actual value of the Coulomb interaction U according to the above discussions. Parameters for numerical calculations are taken the same as in the Ref. [78].

E. Effective Ising model

In general, the existence of separate dynamics and a corresponding classical Hamiltonian for charge degrees of freedom is questionable. The possibility to introduce a classical problem for certain collective excitations is usually related to the existence of an adiabatic parameter that distinguishes these excitations from others that belong to different energy and time scales. Thus, in the case of spin fluctuations the adiabatic approximation is intuitive and implies that collective (spin) degrees of freedom are slower and have lower energy than single-particle (electronic) excitations [79]. Unfortunately, the corresponding adiabatic approximation for charge degrees of freedom does not exist. Therefore, it is very challenging to find a specific physical regime where the classical problem for charge degrees of freedom can still be introduced. As was recently obtained for spin fluctuations [69], the possibility of different energy and time scales separation lies in a nontrivial frequency behavior of local vertex functions. If the dependence of the local vertex on fermionic (single-particle) frequencies is negligibly small compared to the bosonic (collective) frequency dependence, the separation of the corresponding bosonic excitation is justified.

Thus, in the regime of large double occupancy ($d \geq 0.18$), which is shown in Fig. 1 by the dashed black line, the quantum action (24) can be mapped onto an effective classical Hamiltonian, similarly to the case of collective spin fluctuations with the well-defined local

moment [69]. Note that in the case of charge degrees of freedom, the classical problem is given by the effective Ising Hamiltonian

$$H_{\text{ch}} = \sum_{\mathbf{q}} J_{\mathbf{q}} \sigma_{\mathbf{q}} \sigma_{-\mathbf{q}} \quad (32)$$

written in terms of classical variables $\sigma = \pm 1$. An effective pair interaction $J_{\mathbf{q}}$ between electronic densities can be defined from the non-local part of the inverse charge susceptibility at the zero bosonic frequency [68, 69]. Additionally, every quantum variable $\rho_{\mathbf{q}\omega}$ in Eq. 24 has to be replaced by a classical value $\rho_{\mathbf{q}\omega} \rightarrow 2\sqrt{d}$ that describes a deviation of the local electronic density from the average (half-filled) value in the large double occupancy regime. In order to distinguish local and nonlocal contributions to the inverse susceptibility (25), one can again use an approximated version of the local 2PI vertex function in the charge channel. Since the latter does not depend on fermionic frequencies in the regime of well-developed charge fluctuations, the full four-point vertex $\bar{\gamma}_{\nu\nu'\omega}$ of the impurity problem can also be approximated by the leading bosonic contribution. According to the Ref. [69] the latter corresponds to the full local charge susceptibility χ_{ω} that connects two three-point vertex functions $\gamma_{\nu\omega}$ (for details see Appendix IV G)

$$\bar{\gamma}_{\nu\nu'\omega} \simeq -\gamma_{\nu\omega} \chi_{\omega} \gamma_{\nu'+\omega, -\omega} = \triangleleft \text{---} \text{---} \text{---} \triangleright. \quad (33)$$

Then, the relation (25) for the charge susceptibility reduces to

$$X_{\mathbf{q}\omega}^{-1} = \chi_{\omega}^{-1} + \Lambda_{\omega} - V_{\mathbf{q}} - \tilde{\Pi}_{\mathbf{q}\omega}^{(2)}, \quad (34)$$

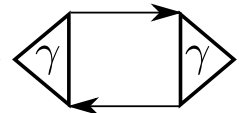
where the second order polarization operator reads

$$\tilde{\Pi}_{\mathbf{q}\omega}^{(2)} = \sum_{\mathbf{k}\nu} \gamma_{\nu+\omega, -\omega} \tilde{G}_{\mathbf{k}+\mathbf{q}, \nu+\omega} \tilde{G}_{\mathbf{k}\nu} \gamma_{\nu, \omega}, \quad (35)$$

Table I. Double occupancy d , correction U' to the effective local Coulomb interaction U^{eff} , and static dielectric function ε obtained close to the phase boundary between the normal and CO phases for the given values of the local U and nonlocal V Coulomb interactions.

U	0.1	0.5	1.0	1.5	2.0	2.5
V	0.045	0.130	0.265	0.420	0.630	0.965
d	0.25	0.23	0.21	0.18	0.14	0.10
U'	-0.48	-0.68	-1.11	-1.81	-2.85	-5.24
ε	1.26	3.78	10.09	6.00	3.35	1.91

and $\tilde{G}_{\mathbf{k}\nu}$ is a nonlocal part of the lattice Green's function. Then, the effective pair interaction takes the following form

$$\frac{J_{\mathbf{q}}}{4d} = V_{\mathbf{q}} + \sum_{\mathbf{k},\nu} \gamma_{\nu,0} \tilde{G}_{\mathbf{k}+\mathbf{q},\nu} \tilde{G}_{\mathbf{k}\nu} \gamma_{\nu,0} = V_{\mathbf{q}} + \text{Diagram} \quad (36)$$


Using an exact relation between the 2PI four-point and full three-point vertices, the latter can also be approximated as

$$\gamma_{\nu\omega} \simeq \chi_{\omega}^{-1} + \Lambda_{\omega} + U_{\nu\nu'\omega}^{\text{eff}} \simeq \chi_{\omega}^0{}^{-1}, \quad (37)$$

as shown in Appendix [IV H](#). Therefore, the result for the pair interaction [\(36\)](#) between electronic densities at first glance reduces to a similar expression for the exchange interaction derived for the magnetic system in Ref. [69](#). However, the “correction”

$$U' = \chi_{\omega=0}^{-1} + \Lambda_{\omega=0} \quad (38)$$

to the effective bare Coulomb interaction U^{eff} in expression [\(37\)](#) is larger than the local Coulomb interaction U as shown in Table [II](#). This is not surprising, because the relatively large value of the inversed local charge susceptibility, which is defined as $\chi_{\omega} =$

– $\langle n_\omega^* n_\omega \rangle$, when two electrons occupy the same lattice site is expected. Therefore, the term U' cannot be neglected, contrary to the case of spin fluctuations at half-filling when the inversed local magnetic susceptibility $\chi_{\omega=0}^{-1}$ is negligibly small [69]. Since the effective bare Coulomb interaction U^{eff} in the regime of large double occupancy coincides with the actual value of U , one can obtain a static approximation for the three-point vertex (see Appendix IV H)

$$\gamma_{\nu,0} \simeq \chi_{\omega=0}^{0-1} \simeq -\frac{U}{\varepsilon - 1} = -\tilde{U}, \quad (39)$$

where $\varepsilon = U/\mathcal{W}_0$ is a static dielectric function defined via the renormalized local interaction \mathcal{W}_ω . Therefore, the final expression for the pair interaction of the effective classical Ising model reads

$$\frac{J_{\mathbf{q}}}{4d} = V_{\mathbf{q}} + \sum_{\mathbf{k},\nu} \tilde{U} \tilde{G}_{\mathbf{k}+\mathbf{q},\nu} \tilde{G}_{\mathbf{k}\nu} \tilde{U}. \quad (40)$$

The effective Ising model is then can be used for modeling finite-temperature thermodynamic properties of the system, such as the electronic density, charge susceptibility, ground-state energy, and configurational structure of material [56–61]. All these observables make more sense in the broken symmetry (CO) phase, which is beyond the scope of the current study. However, the Ising model also provides the analytical result for the transition temperature between the normal and CO phases

$$T_c = 2J/\ln(1 + \sqrt{2}), \quad (41)$$

where $J = J_{\mathbf{q}=(\pi,\pi)}$ is the nearest-neighbor pair interaction. The result for the transition temperature can be compared to the one of the Ref. [78]. To this aim, the effective exchange interaction J is calculated using the expression (40) for the model parameters specified

in this work.

F. Conclusion

In this work the bosonic action (24) for charge degrees of freedom of the extended Hubbard model (23) has been derived. It was found that local four-point vertex function of the impurity model is independent on fermionic frequencies in the regime of well-developed charge fluctuations. Remarkably, the latter can be efficiently determined looking at the deviation of the double occupancy from its maximum value. Thus, strong charge fluctuations are revealed in the case of large double occupancy ($d \geq 0.18$), which corresponds to a broad range of values of Coulomb interaction. As a consequence, it was found that in this regime the dynamics of charge fluctuations can be described via a simplified RPA-like charge susceptibility (29) constructed from the EDMFT Green's functions. Moreover the effective local Coulomb interaction in this case coincides with the actual value of the bare Coulomb interaction. Further, it was shown that in the regime of well-developed charge fluctuations, the initial quantum problem can be mapped onto an effective classical Ising model written in terms of a pair interaction between local electronic densities. Importantly, the expression for the pair interaction contains only single-particle quantities, which can be efficiently used in realistic multiband calculations. We further speculate that similar approximations are valid for systems that reveal strong charge fluctuations beyond the half-filling (see e.g. Ref. 80 and references therein). We believe therefore that results obtained in this work will help to describe collective charge excitations and ordering in a very broad class of realistic materials with strong local and nonlocal electron-electron interactions.

G. Appendix A: Bosonic action for the extended Hubbard model

Here we explicitly derive a bosonic problem for charge degrees of freedom of the extended Hubbard model. For this reason, one can divide the lattice action (23) into the local impurity \mathcal{S}_{imp} and nonlocal \mathcal{S}_{rem} parts following the standard procedure of the DB theory [23, 24]

$$\mathcal{S}_{\text{imp}} = - \sum_{\nu, \sigma} c_{\nu\sigma}^* [i\nu + \mu - \Delta_\nu] c_{\nu\sigma} \quad (42)$$

$$+ U \sum_{\omega} n_{\omega\uparrow}^* n_{\omega\downarrow} + \frac{1}{2} \sum_{\omega} \Lambda_\omega \rho_\omega^* \rho_\omega,$$

$$\mathcal{S}_{\text{rem}} = - \sum_{\mathbf{k}, \nu, \sigma} c_{\mathbf{k}\nu\sigma}^* [\Delta_\nu - \varepsilon_{\mathbf{k}}] c_{\mathbf{k}\nu\sigma} \quad (43)$$

$$+ \frac{1}{2} \sum_{\mathbf{q}, \omega} [V_{\mathbf{q}} - \Lambda_\omega] \rho_{\mathbf{q}\omega}^* \rho_{\mathbf{q}\omega} + \sum_{\mathbf{q}, \omega} j_{\mathbf{q}\omega}^* \rho_{\mathbf{q}\omega},$$

where we introduced fermionic Δ_ν and bosonic Λ_ω hybridization functions, and sources $j_{\mathbf{q}\omega}$ for bosonic variables. The partition function of our problem is given by the following relation

$$\mathcal{Z} = \int D[c^*, c] e^{-\mathcal{S}}, \quad (44)$$

where the action \mathcal{S} is given by the Eq. 23. Using the Hubbard–Stratonovich transformation of the reminder term \mathcal{S}_{rem} , one can in-

roduce *dual* fermionic f^* , f , and bosonic variables ϕ as follows

$$e^{\sum_{\mathbf{k},\nu,\sigma} c_{\mathbf{k}\nu\sigma}^* [\Delta_\nu - \varepsilon_{\mathbf{k}}] c_{\mathbf{k}\nu\sigma}} = \quad (45)$$

$$D_f \int D[f] e^{-\sum_{\mathbf{k},\nu,\sigma} (f_{\mathbf{k}\nu\sigma}^* [\Delta_\nu - \varepsilon_{\mathbf{k}}]^{-1} f_{\mathbf{k}\nu\sigma} + c_{\mathbf{k}\nu\sigma}^* f_{\mathbf{k}\nu\sigma} + f_{\mathbf{k}\nu\sigma}^* c_{\mathbf{k}\nu\sigma})},$$

$$e^{\frac{1}{2} \sum_{\mathbf{q},\omega} \rho_{\mathbf{q}\omega}^* [\Lambda_\omega - V_{\mathbf{q}}] \rho_{\mathbf{q}\omega}} = \quad (46)$$

$$D_\phi \int D[\phi] e^{-\left(\frac{1}{2} \sum_{\mathbf{q},\omega} \phi_{\mathbf{q}\omega}^* [\Lambda_\omega - V_{\mathbf{q}}]^{-1} \phi_{\mathbf{q}\omega} + \phi_{\mathbf{q}\omega}^* \rho_{\mathbf{q}\omega}\right)},$$

where terms $D_f = \det[\Delta_\nu - \varepsilon_{\mathbf{k}}]$ and $D_\phi^{-1} = \sqrt{\det[\Lambda_\omega - V_{\mathbf{q}}]}$ can be neglected when calculating expectation values. Rescaling fermionic and bosonic fields on corresponding Green's functions of the impurity problem as $f_{\mathbf{k}\nu}^{(*)} \rightarrow f_{\mathbf{k}\nu}^{(*)} g_\nu^{-1}$ and $\phi_{\mathbf{q}\omega} \rightarrow \phi_{\mathbf{q}\omega} \chi_\omega^{-1}$, and shifting bosonic variables, the nonlocal part of the action transforms to

$$\begin{aligned} \mathcal{S}_{\text{DB}} = & - \sum_{\mathbf{k},\nu,\sigma} f_{\mathbf{k}\nu\sigma}^* g_{\nu\sigma}^{-1} [\varepsilon_{\mathbf{k}} - \Delta_\nu]^{-1} g_{\nu\sigma}^{-1} f_{\mathbf{k}\nu\sigma} \quad (47) \\ & + \sum_{\mathbf{k},\nu,\sigma} [c_{\mathbf{k}\nu\sigma}^* g_{\nu\sigma}^{-1} f_{\mathbf{k}\nu\sigma} + f_{\mathbf{k}\nu\sigma}^* g_{\nu\sigma}^{-1} c_{\mathbf{k}\nu\sigma}] + \sum_{\mathbf{q},\omega} \phi_{\mathbf{q}\omega} \chi_\omega^{-1} \rho_{\mathbf{q}\omega} \\ & - \frac{1}{2} \sum_{\mathbf{q},\omega} (\phi_{\mathbf{q}\omega}^* - j_{\mathbf{q}\omega}^* \chi_\omega) \chi_\omega^{-1} [V_{\mathbf{q}} - \Lambda_\omega]^{-1} \chi_\omega^{-1} (\phi_{\mathbf{q}\omega} - \chi_\omega j_{\mathbf{q}\omega}). \end{aligned}$$

Integrating out initial degrees of freedom with respect to the impurity action (42), one gets (23)

$$\begin{aligned} \int D[c] e^{-\sum_i \mathcal{S}_{\text{imp}}^{(i)} - \sum_{\mathbf{k},\nu,\sigma} [c_{\mathbf{k}\nu\sigma}^* g_{\nu\sigma}^{-1} f_{\mathbf{k}\nu\sigma} + f_{\mathbf{k}\nu\sigma}^* g_{\nu\sigma}^{-1} c_{\mathbf{k}\nu\sigma}] - \sum_{\mathbf{q},\omega} \phi_{\mathbf{q}\omega}^* \chi_\omega^{-1} \rho_{\mathbf{q}\omega}} = \\ \mathcal{Z}_{\text{imp}} \times e^{-\sum_{\mathbf{k},\nu,\sigma} f_{\mathbf{k}\nu\sigma}^* g_{\nu\sigma}^{-1} f_{\mathbf{k}\nu\sigma} - \frac{1}{2} \sum_{\mathbf{q},\omega} \phi_{\mathbf{q}\omega}^* \chi_\omega^{-1} \phi_{\mathbf{q}\omega} - \tilde{W}[f,\phi]}, \quad (48) \end{aligned}$$

where \mathcal{Z}_{imp} is a partition function of the impurity problem. Here, the interaction $\tilde{W}[f,\phi]$ is presented as an infinite series of full vertex functions of the local impurity problem (42) (23, 25). The lowest

order interaction terms are

$$\begin{aligned} \tilde{W}[f, \phi] = & \sum_{\mathbf{k}, \mathbf{k}', \mathbf{q}} \sum_{\nu, \nu', \omega} \sum_{\sigma(\prime)} \left(\phi_{\mathbf{q}\omega}^* \gamma_{\nu\omega} f_{\mathbf{k}\nu\sigma}^* f_{\mathbf{k}+\mathbf{q}, \nu+\omega, \sigma} \right. \\ & \left. - \frac{1}{4} \bar{\gamma}_{\nu\nu'\omega} f_{\mathbf{k}\nu\sigma}^* f_{\mathbf{k}+\mathbf{q}, \nu+\omega, \sigma'} f_{\mathbf{k}'+\mathbf{q}, \nu'+\omega, \sigma''}^* f_{\mathbf{k}'\nu'\sigma'''} \right), \end{aligned} \quad (49)$$

where the full three- and four-point vertex functions are defined as

$$\begin{aligned} \gamma_{\nu\omega} &= \langle c_{\nu\sigma} c_{\nu+\omega, \sigma}^* \rho_{\omega} \rangle_{\text{imp}} \chi_{\omega}^{-1} g_{\nu\sigma}^{-1} g_{\nu+\omega, \sigma}^{-1}, \\ \bar{\gamma}_{\nu\nu'\omega} &= \langle c_{\nu\sigma} c_{\nu+\omega, \sigma'}^* c_{\nu'+\omega, \sigma''} c_{\nu'\sigma'''}^* \rangle_{\text{c imp}} g_{\nu\sigma}^{-1} g_{\nu+\omega, \sigma'}^{-1} g_{\nu'+\omega, \sigma''}^{-1} g_{\nu'\sigma'''}^{-1}. \end{aligned} \quad (50)$$

Note that the four-point vertex $\bar{\gamma}_{\nu\nu'\omega}$ is defined here in the particle-hole channel.

Therefore, the initial lattice problem transforms to the following *dual* action

$$\begin{aligned} \tilde{\mathcal{S}} = & - \sum_{\mathbf{k}, \nu, \sigma} f_{\mathbf{k}\nu\sigma}^* g_{\nu\sigma}^{-1} [\varepsilon_{\mathbf{k}} - \Delta_{\nu}]^{-1} g_{\nu\sigma}^{-1} f_{\mathbf{k}\nu\sigma} \\ & + \sum_{\mathbf{k}, \nu} f_{\mathbf{k}\nu\sigma}^* g_{\nu\sigma}^{-1} f_{\mathbf{k}\nu\sigma} + \frac{1}{2} \sum_{\mathbf{q}, \omega} \phi_{\mathbf{q}\omega}^* \chi_{\omega}^{-1} \phi_{\mathbf{q}\omega} + \tilde{W}[f, \phi] \\ & - \frac{1}{2} \sum_{\mathbf{q}, \omega} (\phi_{\mathbf{q}\omega}^* - j_{\mathbf{q}\omega}^* \chi_{\omega}) \chi_{\omega}^{-1} [V_{\mathbf{q}} - \Lambda_{\omega}]^{-1} \chi_{\omega}^{-1} (\phi_{\mathbf{q}\omega} - \chi_{\omega} j_{\mathbf{q}\omega}). \end{aligned} \quad (51)$$

In order to come back to the original bosonic variables, one can perform the third Hubbard-Stratonovich transformation as

$$\begin{aligned} e^{\frac{1}{2} \sum_{\mathbf{q}, \omega} (\phi_{\mathbf{q}\omega}^* - j_{\mathbf{q}\omega}^* \chi_{\omega}) \chi_{\omega}^{-1} [V_{\mathbf{q}} - \Lambda_{\omega}]^{-1} \chi_{\omega}^{-1} (\phi_{\mathbf{q}\omega} - \chi_{\omega} j_{\mathbf{q}\omega})} = \\ D_{\bar{\rho}} \int D[\bar{\rho}] e^{-\sum_{\mathbf{q}, \omega} (\frac{1}{2} T \bar{\rho}_{\mathbf{q}\omega} [V_{\mathbf{q}} - \Lambda_{\omega}] \bar{\rho}_{\mathbf{q}\omega} - \phi_{\mathbf{q}\omega} \chi_{\omega}^{-1} \bar{\rho}_{-\mathbf{q}, -\omega} + j_{\mathbf{q}\omega} \bar{\rho}_{-\mathbf{q}, -\omega})}. \end{aligned} \quad (52)$$

Comparing this expression to the Eq. [43](#), one can see that sources $j_{\mathbf{q}\omega}^*$ introduced for the initial degrees of freedom $\rho_{\mathbf{q}\omega}$ are also the sources

for new bosonic fields $\bar{\rho}_{\mathbf{q}\omega}$. Therefore, fields $\bar{\rho}_{\mathbf{q}\omega}$ indeed represent initial degrees of freedom and have the same physical meaning as original *composite* bosonic variables $\rho_{\mathbf{q}\omega} = \sum_{\mathbf{k}\nu\sigma} c_{\mathbf{k}\nu\sigma}^* c_{\mathbf{k}+\mathbf{q},\nu+\omega,\sigma} - \langle n_{\mathbf{q}\omega} \rangle$ of the lattice problem (23). Nevertheless, $\bar{\rho}_{\mathbf{q}\omega}$ can now be treated as *elementary* bosonic fields that have a well-defined propagator, since they are introduced as a decoupling fields of dual degrees of freedom $\phi_{\mathbf{q}\omega}$ and therefore, independent on fermionic variables $c_{\mathbf{k}\nu\sigma}^*$ ($c_{\mathbf{k}\nu\sigma}$). Taking sources to zero and replacing $\bar{\rho}_{\mathbf{q}\omega}$ by $\rho_{\mathbf{q}\omega}$, dual bosonic fields can be integrated out as [69]

$$\int D[\phi] e^{-\frac{1}{2} \sum_{\mathbf{q},\omega} \phi_{\mathbf{q}\omega}^* \chi_{\omega}^{-1} \phi_{\mathbf{q}\omega} - \phi_{\mathbf{q}\omega}^* \chi_{\omega}^{-1} \rho_{\mathbf{q}\omega} - \tilde{W}[f,\phi]} = \quad (53)$$

$$\mathcal{Z}_{\phi} \times e^{\frac{1}{2} \sum_{\mathbf{q},\omega} \rho_{\mathbf{q}\omega}^* \chi_{\omega}^{-1} \rho_{\mathbf{q}\omega} - W[f,\rho]},$$

where \mathcal{Z}_{ϕ} is a partition function of the Gaussian part of the bosonic action. Here, we restrict ourselves to the lowest order interaction terms of $\tilde{W}[f,\phi]$ shown in Eq. 49. Then, the integration of dual bosonic fields in Eq. 53 simplifies and $W[f,\rho]$ keeps an efficient dual form of $\tilde{W}[f,\phi]$ (49) with replacement of bosonic variables $\phi \rightarrow \rho$

$$W[f,\rho] = \sum_{\mathbf{k},\mathbf{k}',\mathbf{q}} \sum_{\nu,\nu',\omega} \sum_{\sigma^{(l)}} (\rho_{\mathbf{q}\omega}^* \gamma_{\nu\omega} f_{\mathbf{k}\nu\sigma}^* f_{\mathbf{k}+\mathbf{q},\nu+\omega,\sigma} \quad (54)$$

$$- [\bar{\gamma}_{\nu\nu'\omega} + \gamma_{\nu\omega} \chi_{\omega} \gamma_{\nu'+\omega,-\omega}] f_{\mathbf{k}\nu\sigma}^* f_{\mathbf{k}+\mathbf{q},\nu+\omega,\sigma} f_{\mathbf{k}'+\mathbf{q},\nu'+\omega,\sigma'}^* f_{\mathbf{k}'\nu'\sigma'}) .$$

As can be seen in Ref. [69], the four-point vertex becomes irreducible with respect to the full local bosonic propagator χ_{ω} , while the three-point vertex $\gamma_{\nu\omega}$ remains invariant. Therefore, the problem transforms to the following action of an effective s - d model

$$\mathcal{S}_{s-d} = - \sum_{\mathbf{k},\nu,\sigma} f_{\mathbf{k}\nu\sigma}^* \tilde{G}_0^{-1} f_{\mathbf{k}\nu\sigma} - \frac{1}{2} \sum_{\mathbf{q},\omega} \rho_{\mathbf{q}\omega}^* X_{\text{E}}^{-1} \rho_{\mathbf{q}\omega} + W[f,\rho], \quad (55)$$

where

$$X_E = [\chi_\omega^{-1} + \Lambda_\omega - V_{\mathbf{q}}]^{-1} \quad (56)$$

is the EDMFT susceptibility and \tilde{G}_0 is a nonlocal part of the EDMFT Green's function. When the main contribution to the four-point vertex is given by the reducible contribution with respect to the full local bosonic propagator, i.e.

$$\bar{\gamma}_{\nu\nu'\omega} \simeq -\gamma_{\nu\omega} \chi_\omega \gamma_{\nu'+\omega,-\omega} = \triangleleft \text{---} \text{---} \text{---} \triangleright, \quad (57)$$

the interaction part of the action (55) takes the most simple form that contains only the three-point vertex function

$$W'[f, \rho] \simeq \sum_{\mathbf{k}, \mathbf{q}} \sum_{\nu, \omega, \sigma} \rho_{\mathbf{q}\omega}^* \gamma_{\nu\omega} f_{\mathbf{k}\nu\sigma}^* f_{\mathbf{k}+\mathbf{q}, \nu+\omega, \sigma}. \quad (58)$$

According to derivations presented in Ref. [69], one can integrate out *dual* fermionic degrees of freedom using the ladder approximation and obtain an effective problem written in terms of bosonic degrees of freedom only

$$\mathcal{S} = -\frac{1}{2} \sum_{\mathbf{q}, \omega} \rho_{\mathbf{q}\omega}^* X_{\mathbf{q}\omega}^{-1} \rho_{\mathbf{q}\omega}, \quad (59)$$

where the expression for the lattice susceptibility reads

$$[X_{\mathbf{q}\omega}^{\text{ladd}}]^{-1} = [X_{\mathbf{q}\omega}^{\text{DMFT}}]^{-1} + \Lambda_\omega - V_{\mathbf{q}}. \quad (60)$$

Here,

$$\hat{X}_{\mathbf{q}\omega}^{\text{DMFT}} = \text{Tr} \left\{ \hat{X}_{\mathbf{q}\omega}^0 \left[I + \hat{\gamma}_\omega^{2\text{PI}} \hat{X}_{\mathbf{q}\omega}^0 \right]^{-1} \right\} \quad (61)$$

is the DMFT-like [1, 3] susceptibility written in terms of lattice Green's functions, and 2PI vertex functions of impurity model de-

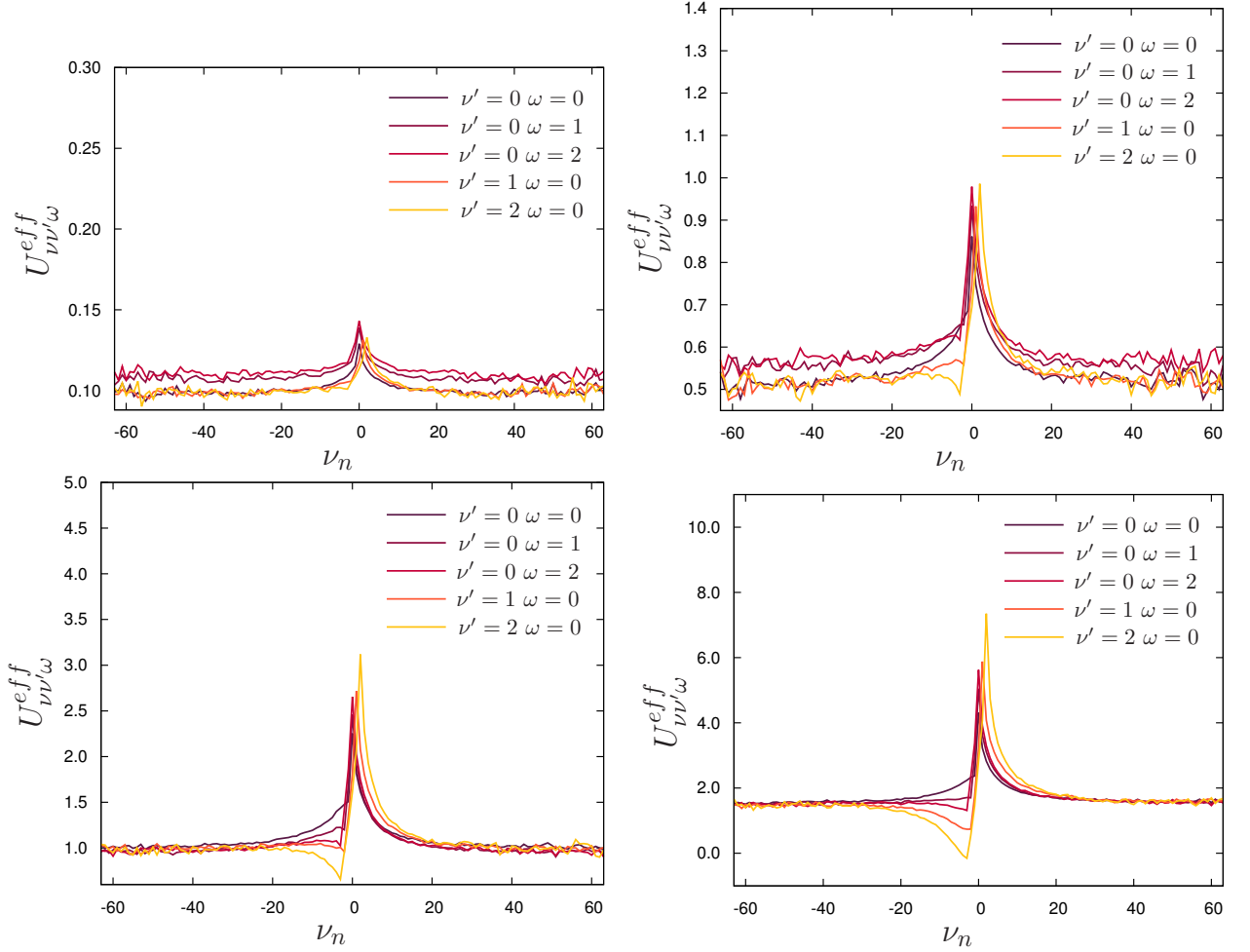


Figure 4. Frequency dependence of the effective local Coulomb interaction $U_{\nu\nu'\omega}^{eff}$ obtained for different values of the actual Coulomb interaction $U = 0.1; 0.5; 1.0; 1.5$ (from left to right) in the normal phase close to the charge ordering for different values of fermionic ν' and bosonic ω frequencies for $\beta = 50$. The dependence of the effective interaction on fermionic frequency becomes larger at larger Coulomb interaction.

fined as

$$\hat{\gamma}_{\omega}^{2PI} = \hat{\gamma}_{\omega} \left[I - \hat{\chi}_{\omega}^0 \hat{\gamma}_{\omega} \right]^{-1}. \quad (62)$$

Here, multiplication and inversion should be understood as a standard matrix operations in the space of fermionic frequencies ν, ν' . I is the identity matrix in the same space, and the trace is taken over the external fermionic indices. For simplicity, we omit fermionic indices wherever they are not crucial for understanding. Matrix elements

of the bare lattice $\hat{X}_{\mathbf{q}\omega}^0$ and local impurity $\hat{\chi}_\omega^0$ charge susceptibilities are defined as

$$X_{\mathbf{q}\omega; \nu\nu'}^0 = \sum_{\mathbf{k}, \sigma} G_{\mathbf{k}+\mathbf{q}, \nu+\omega, \sigma} G_{\mathbf{k}\nu\sigma} \delta_{\nu\nu'} \quad (63)$$

$$\chi_{\omega; \nu\nu'}^0 = \sum_{\sigma} g_{\nu+\omega, \sigma} g_{\nu\sigma} \delta_{\nu\nu'}. \quad (64)$$

Matrix elements $\bar{\gamma}_{\nu\nu'\omega}$ of the four-point vertex function $\hat{\gamma}_\omega$ are defined in (50).

Therefore, the charge susceptibility (60) in the ladder approximation can be rewritten as

$$X_{\mathbf{q}\omega}^{\text{ladd}} = \text{Tr} \left\{ \hat{X}_{\mathbf{q}\omega}^0 \left[I - \left(I V_{\mathbf{q}} + \hat{U}_\omega^{\text{eff}} \right) \hat{X}_{\mathbf{q}\omega}^0 \right]^{-1} \right\}, \quad (65)$$

where we introduced an effective bare local interaction

$$U_{\nu\nu'\omega}^{\text{eff}} = -\Lambda_\omega - \bar{\gamma}_{\nu\nu'\omega}^{2\text{PI}} \quad (66)$$

shown in Fig. 4 for different values of fermionic ν' and bosonic ω frequencies.

Another simplified expression for the charge susceptibility can be obtained after expanding the simplified form of interaction $W[f, \rho]$ given by Eq. 58 up to the second order with respect to bosonic fields ρ in the expression for the partition function of the action (55). This results in

$$\left[X_{\mathbf{q}\omega}^{(2)} \right]^{-1} = -V_{\mathbf{q}} + \Lambda_\omega + \chi_\omega^{-1} - \tilde{\Pi}_{\mathbf{q}\omega}^{(2)}, \quad (67)$$

where

$$\tilde{\Pi}_{\mathbf{q}\omega}^{(2)} = \sum_{\mathbf{k}, \nu, \sigma} \gamma_{\nu+\omega, -\omega} \tilde{G}_{\mathbf{k}+\mathbf{q}, \nu+\omega\sigma} \tilde{G}_{\mathbf{k}\nu\sigma} \gamma_{\nu, \omega} \quad (68)$$

is the second order polarization operator and $\tilde{G}_{\mathbf{k}\nu}$ is a nonlocal part of the lattice (EDMFT) Green's function. As discussed in the main text, this expression can be transformed to a pair interaction of the classical Ising model.

H. Appendix B: Vertex approximation

According to discussions presented in the main text, the expression for the 2PI four-point vertex function can be approximated as $\bar{\gamma}_{\nu\nu'\omega}^{2\text{PI}} \simeq \bar{\gamma}_{\omega}^{2\text{PI}}$ when its dependence on fermionic frequencies is negligible. Then, using the exact relation for the local impurity susceptibility

$$\chi_{\omega} = \text{Tr} \left\{ \hat{\chi}_{\omega}^0 - \hat{\chi}_{\omega}^0 \hat{\gamma}_{\omega} \hat{\chi}_{\omega}^0 \right\} = \text{Tr} \left\{ \hat{\chi}_{\omega}^0 \left[I + \hat{\gamma}_{\omega}^{2\text{PI}} \hat{\chi}_{\omega}^0 \right]^{-1} \right\} \quad (69)$$

and assuming that the 2PI vertex does not depend on fermionic frequencies, one gets

$$\bar{\gamma}_{\nu\nu'\omega}^{2\text{PI}} \simeq \bar{\gamma}_{\omega}^{2\text{PI}} = \chi_{\omega}^{-1} - \chi_{\omega}^0{}^{-1}. \quad (70)$$

As shown in Ref. [69], in the case of well-developed collective fluctuations the four-point function is described by the bosonic frequency and three-point vertex function that enters the exact Hedin equation [21] for the self-energy and polarization operator of the impurity problem is close to unity. As a consequence, the local self-energy and polarization operator take the same form as in GW approach [21, 71, 72]. Thus, the polarization operator of the impurity problem can be approximated as $\Pi_{\omega} \simeq \chi_{\omega}^0$ neglecting the vertex function. Using the exact relation for the local charge susceptibility

of the impurity problem, one gets the following relation

$$\chi_\omega^{-1} = \Pi_\omega^{-1} - (U + \Lambda_\omega) \simeq \chi_\omega^0{}^{-1} - (U + \Lambda_\omega). \quad (71)$$

Therefore, in the regime of strong charge fluctuations the 2PI vertex function can be approximated as

$$\bar{\gamma}_{\nu\nu'\omega}^{2\text{PI}} \simeq -U - \Lambda_\omega. \quad (72)$$

The three-point vertex can also be approximated using the exact relation between three- and four-point vertex functions, and the simplified form of the 2PI vertex [69]

$$\gamma_{\nu\omega} \simeq \gamma_\omega = \chi_\omega^{-1} - \bar{\gamma}_\omega^{2\text{PI}} = \chi_\omega^{-1} + \Lambda_\omega + U_\omega^{\text{eff}}, \quad (73)$$

where $U_\omega^{\text{eff}} = -\Lambda_\omega - \bar{\gamma}_\omega^{2\text{PI}}$. Taking into account that in the regime of well-developed charge fluctuations the effective interaction coincides with the actual value of the bare local Coulomb interaction $U_\omega^{\text{eff}} \simeq U$, one can further write

$$\gamma_\omega \simeq \chi_\omega^{-1} + \Lambda_\omega + U = \Pi_\omega^{-1} = \frac{U\mathcal{W}_\omega}{\mathcal{W}_\omega - U} = \frac{U}{1 - \varepsilon_\omega}, \quad (74)$$

where we introduced the renormalized local Coulomb interaction $\mathcal{W}_\omega = U/(1 - \Pi_\omega U)$ that is connected to the bare Coulomb interaction via the dielectric function $\varepsilon_\omega = U/\mathcal{W}_\omega$.

V. PLASMONS IN DOPED MOTT INSULATORS

A. Introduction

The progress in the study of the electronic structure in strongly correlated systems has gone very far. The development of the dynamical mean-field theory (DMFT) [1, 3] was an essential step forward for correlated systems since it covers the interpolation between atomic and band limits. In DMFT just the local correlations are taken into account through the self-energy which is purely local and frequency-dependent. Phenomena like the formation of Hubbard bands which, arises from the spectral weight transfer, the band renormalization and the associated mass enhancement, and the Mott transition [1, 7] are described by DMFT. The success of DMFT gave rise to various extension including non-local correlations. For example extensions of DMFT are quantum cluster approaches [81] as well as the diagrammatic extensions such as the D Γ A [17], dual fermion [22], and one-particle irreducible approach [18]. In contrast to that realistic description of collective excitations in strongly correlated systems has not progressed as much. For example plasmons can be described within the random phase approximation (RPA) [82–84] by the Lindhardt function. RPA, where the bare Greens functions are used within the bubble diagram renormalization has been applied to many physical problems like the Landau-Fermi-liquid theory of He³ and also to ordinary metals [83]. If one uses the RPA approximation for the electron liquid, it is known to capture the essential physics in the high-density regime. RPA leads to the screening of the long-range part of the Coulomb interaction and effectively reducing it. Also the well known GW and GW+EDMFT approximations do not capture the essential effects due to their simple perturbative

structure. Recently plasmons for a strongly correlated model system have been calculated with the Dual Boson approach [33] with very interesting effects like spectral weight transfer and renormalized dispersion. The DB approach can be seen as a diagrammatic extension around EDMFT. The momentum dependence of the polarization operator is restored through a ladder summation of diagrams containing three-point and four-point vertex corrections, which are crucial for a conserving theory. Within DB one needs at least the ladder approximation to restore a conserving theory.

Plasmonics seems to be the only viable way of realization of nanophotonics, that means control of light at scales much smaller than the wavelength. [85–87] On the other hand, plasmonics is a key component for implementation of most metamaterials, and all the interesting phenomena like negative refraction, superlensing, and cloaking that they enable [86, 88, 89]. Plasmonic materials which have tunable plasmons and low loss in the visible–ultraviolet range are of interest. In principle such plasmons occur in metals but have high plasmonic loss in the optical range. Since correlated plasmons are found to be tunable with low loss in the visible–ultraviolet range plasmonics research in insulating and strongly-correlated materials is of high interest [90]. In addition properties of graphene still continue to attract intense research and the interest has also expanded to stable graphene derivatives. Since graphene physics and plasmonics, two rapidly developing fields match, this motivates us to explore plasmons and in a newly available Mott Insulator materials C_2F and C_2H with interesting properties. In this context, C_2F and C_2H emerge as alternative, unique two-dimensional plasmonic materials that contain a wide range of specific properties (see Ref. [91] and references therein). To describe plasmons in a material with strong nonlocal Coulomb interaction like C_2F and C_2H we have to

understand screening of Coulomb interaction induced by many-body effects.

For the theory of interacting electron liquids exact sum rules are good way to gain insight and to test the validity of certain approximations. In the theory of two-dimensional and three-dimensional Landau-Fermi liquids the f-sum rule was widely used. Especially in the high-density regime, the relevant excitations are correctly captured by the RPA resummation and give rise to Landau quasiparticles and a collective plasmon mode.

Here we study the plasmon spectrum with the DB and RPA approximation for doped C₂F and C₂H at arbitrary wave vector q and frequency ω .

B. Calculation

For our purpose we introduce the extended Hubbard model which is the canonical example of a strongly correlated system which capture non-local correlation effects. In momentum space, its action is given by

$$S = - \sum_{\mathbf{k}\nu\sigma} c_{\mathbf{k}\nu\sigma}^* [i\nu + \mu - \varepsilon_{\mathbf{k}}] c_{\mathbf{k}\nu\sigma} + \frac{1}{2} \sum_{\mathbf{q}\omega} U_{\mathbf{q}} \rho_{\mathbf{q}\omega}^* \rho_{\mathbf{q}\omega}. \quad (75)$$

Since we are interested just in charge fluctuations, the spin labels will be suppressed in the following. Here Grassmann variables $c_{\mathbf{q}\nu}^*$ ($c_{\mathbf{q}\nu}$) corresponding to creation (annihilation) of an electron with momentum \mathbf{k} and fermionic Matsubara frequency ν . The charge fluctuations are given by the complex bosonic variable $\rho_{\omega} = n_{\omega} - \langle n \rangle \delta_{\omega}$, where $n_{\omega} = \sum_{\nu\sigma} c_{\nu}^* c_{\nu+\omega}$ counts the number of electrons and ω is a bosonic Matsubara frequency. Additionally μ is the chemical potential and $\varepsilon_{\mathbf{k}}$ is the Fourier transform of the hopping matrix element t . In our case we choose five next nearest neighbors, where the matrix elements are taken from a Wannier parametrization of the first-principles LDA+SO Hamiltonian [91].

The long-range Coulomb interaction $U_{\mathbf{q}} = U + V_{\mathbf{q}}$ is constructed by first fitting the Coulomb interaction $U_{\mathbf{R}}$ in the real space with parameters from table II. Afterwards the summation is performed over 720 basis vectors of the lattice taking care of divergent terms and tails. The used Coulomb matrix elements were calculated using the constrained random-phase approximation technique (cRPA) [92, 93]. For calculation details see [91].

For our calculations, we choose the inverse temperature as $\beta = 5$, while varying the chemical potential μ from 1.7 to 2.0, where $\mu = 2.0$ corresponding the half-filled case. Our lattice size is chosen as 144×144 . In each case, we start from a standard, self-consistent

Table II. The local and nonlocal partially screened Coulomb interactions (in eV) and the hopping parameters (in meV) for C₂F and C₂H.

	C ₂ H	C ₂ F
Interaction		
U_{00}	4.69	5.16
U_{01}	2.19	2.46
U_{02}	1.11	1.66
U_{03}	0.85	1.46
Hopping		
t_{01}	39	-246
t_{02}	-115	6
t_{03}	-99	-21
t_{04}	28	-12
t_{05}	12	-10

EDMFT calculation. For this purpose a hybridization expansion continuous-time quantum Monte Carlo solver [94, 95] with improved estimators [96] is used to compute the imaginary-time correlation functions of the impurity model. After the last impurity solver step, we additionally calculate the full impurity vertex $\gamma_{\nu,\nu',\omega}$ in the charge channel where ν and ω are fermionic and bosonic Matsubara frequencies respectively. In the DB theory all non-local contributions are constructed through dual fermionic (bosonic) self-energies $\tilde{\Sigma}_\nu$ ($\tilde{\Pi}_\nu$). In our case the dual fermionic self-energy is zero and the polarization operator in DB formalism [23] is represented in the form

$$\Pi_{\omega}^{-1}(\mathbf{q}) = [\chi_{\omega} + \chi_{\omega} \tilde{\Pi}_{\nu}(\mathbf{q}) \chi_{\omega}]^{-1} - U_{\omega}, \quad (76)$$

where χ_{ω} denotes the impurity charge susceptibility and U_{ω} is the retarded interaction, which describes the mean-field screening of the local interaction. The dual bosonic self-energy is given by

$$\tilde{\Pi}_{\omega}(\mathbf{q}) = \sum_{\nu} \lambda_{\nu+\omega, -\omega} \tilde{X}_{\nu\omega}^0(\mathbf{q}) \Lambda_{\nu\omega}(\mathbf{q}) \quad (77)$$

and

$$\tilde{\chi}_{\omega}^0(\mathbf{q}) = \frac{T}{N} \sum_{\mathbf{k}\nu} \tilde{G}_{\nu+\omega}^0(\mathbf{k} + \mathbf{q}) \tilde{G}_{\nu}^0(\mathbf{k}) \quad (78)$$

where $\tilde{X}_{\nu\omega}^0(\mathbf{q})$ is the non-local part of the bubble diagram [78](#) and $\lambda_{\nu\omega}$ denotes the triangular electron-boson impurity vertex.

In the DB ladder approximation the vertex corrections are taken into account by

$$\Lambda_{\nu\omega}(\mathbf{q}) = \lambda_{\nu\omega} + \sum_{\nu'} \Gamma_{\nu\nu'\omega}(\mathbf{q}) \tilde{X}_{\nu'\omega}^0(\mathbf{q}) \lambda_{\nu'\omega}, \quad (79)$$

where $\Gamma_{\nu\nu'\omega}(\mathbf{q})$ is the lattice vertex function in the particle-hole channel, which is obtained by the Bethe-Salpeter equation [23](#). The ladder approximation in the DB approach, which is obtained by the Bethe-Salpeter equation describes the repeated particle-hole scattering processes that cause the long-wavelength collective excitations. In comparison the RPA charge susceptibility reads as

$$\chi_{\omega}^{RPA}(\mathbf{q}) = \frac{\chi_{\mathbf{q}}^0}{1 - U\chi_{\mathbf{q}}^0}, \quad (80)$$

where $\chi_{\mathbf{q}}^0$ is defined in [78] without the tilde.

C. Analysis of the Results

In Fig. [5] we show the local density of states (DOS) for different chemical potentials for C_2H and C_2F describes by an extended Hubbard model within the DB and RPA approximation. Indeed we see for RPA that the DOS exhibits a single quasiparticle peak at the Fermi energy. In contrast the DOS in the DB approximation is completely different and one can see two separated Hubbard bands.

Now we move to the discussion of the collective excitations. In Fig. [6] we plot the real part of the lattice susceptibility $-\frac{1}{\pi}\chi_{\omega}(\mathbf{q})$ as a function of momenta and real energies obtained by an optimized implementation of a stochastic analytical continuation procedure proposed by Andrey S. Mishchenko [97, 98]. One can compare the obtained spectrum with experimental data from the angular resolved electron energy loss spectroscopy (EELS) [82, 99]. We find in the doped case, that the overall behavior of the DB results is qualitatively similar to RPA. In the undoped case RPA gives still a metallic solution, whereby in the DB case it is a Mott insulator. In the vicinity of the Γ point one can see a single plasmon branch for all chemical potentials. The small difference in the plasmon spectrum between RPA and DB is that in the DB approximation the spectrum is rather well-defined whereas in the RPA case its more broadened. Throughout the Brillouin zone we see a continuum of particle-hole excitations which are vanishing at the Γ point. The maximum energy of the branch for C_2H can be found between the Γ and the M point

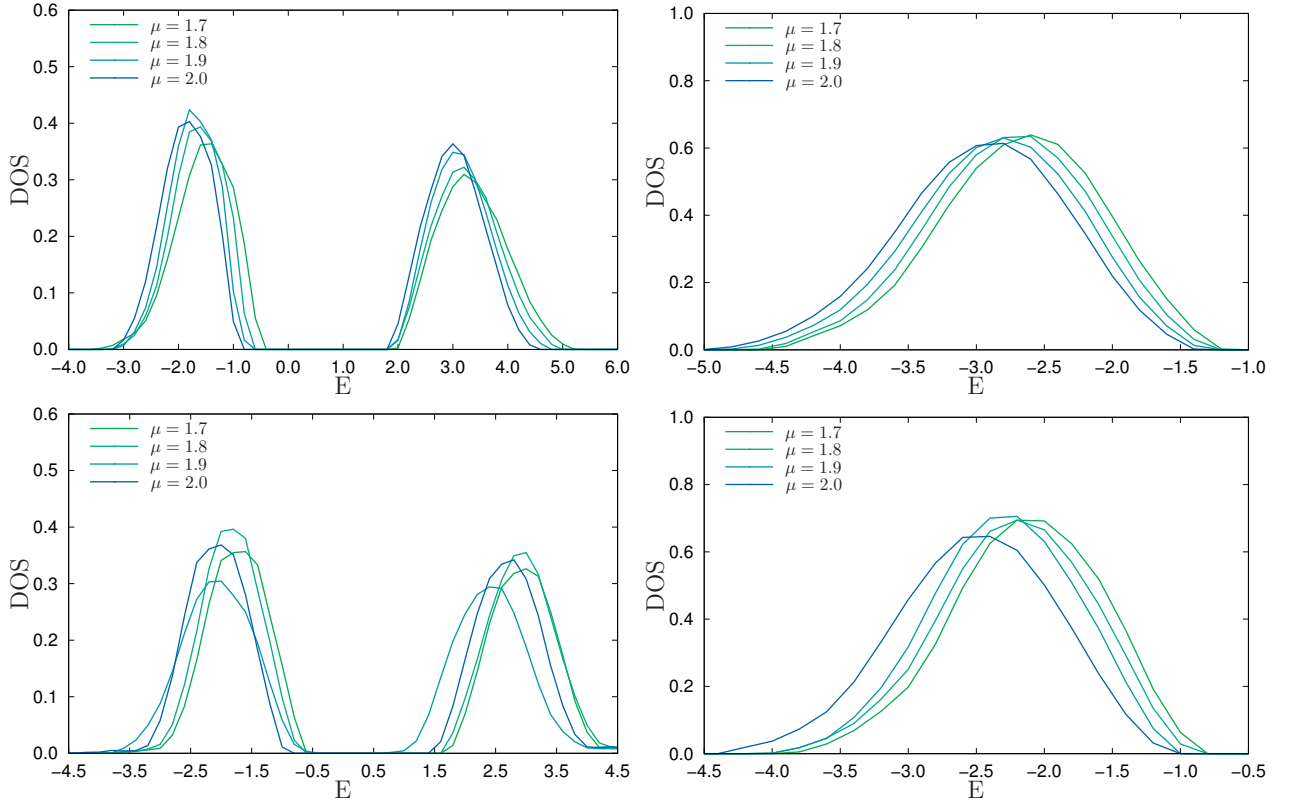


Figure 5. Finite temperature local density of states of the two-dimensional extended Hubbard model calculated within DB and RPA approximation for different values of the chemical potential. On the right side one can see the DOS calculated within DB for C_2F (top) and C_2H (bottom) with its characteristic double peak structure. On the left side one can see the DOS calculated within RPA for C_2F (top) and C_2H (bottom) with its characteristic single quasiparticle peak. Analytical continuation was obtained via Maxent.

as well as K and Γ . In Fig. [7](#) one can see two branches. The lower branch can be seen in Fig. [6](#). On the one hand the lower branch stems mainly from particle-hole excitations for which the electron is excited from the Hubbard band to the quasiparticle peak. On the other hand the upper branch stems from excitations between the Hubbard bands. These kind of splitting was also observed in EDMFT+GW calculations with short-range interaction described by the extended Hubbard model [\[11\]](#), [\[12\]](#).

Systematic experimental studies should give a clear evidence of plasmon mode in doped Mott Insulators, which can be observed in angle resolved photoemission spectroscopy ARPES experiments.

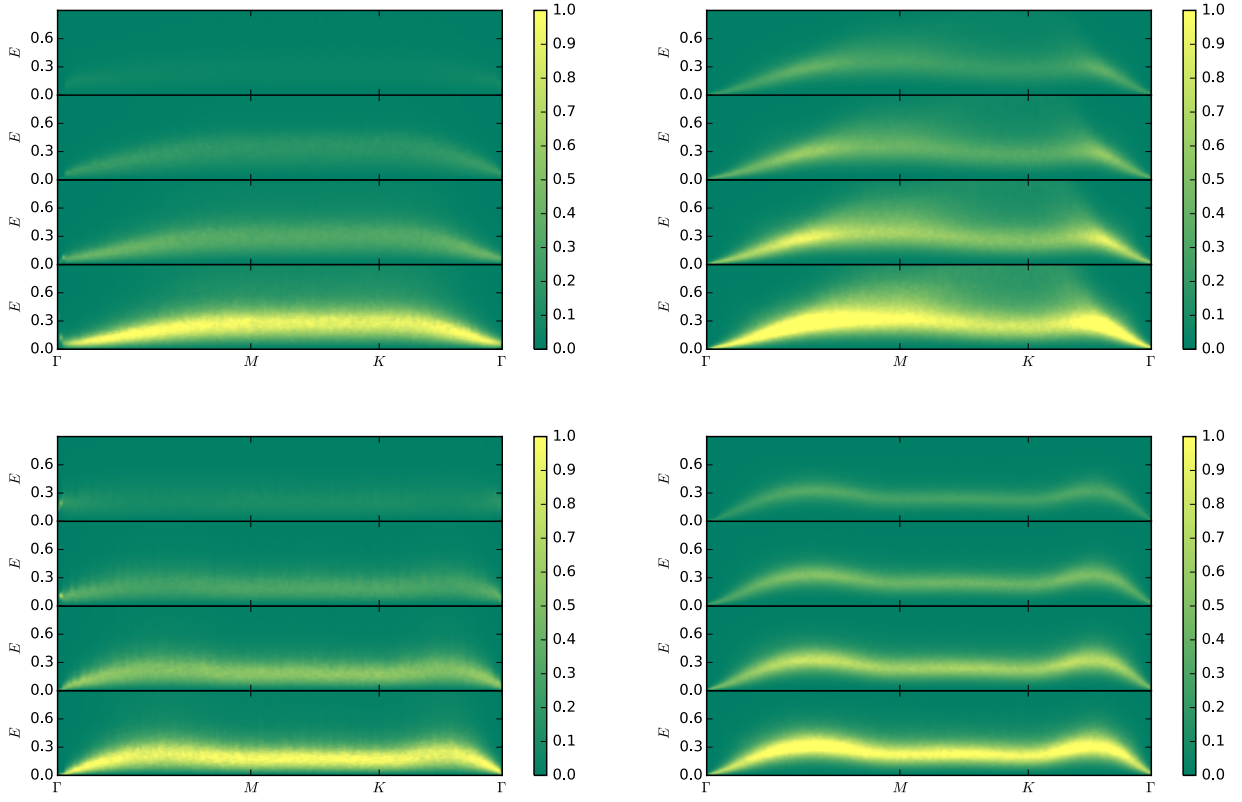


Figure 6. Real part of the inverse susceptibility function of the 2D Hubbard model with for different values of the chemical potential.

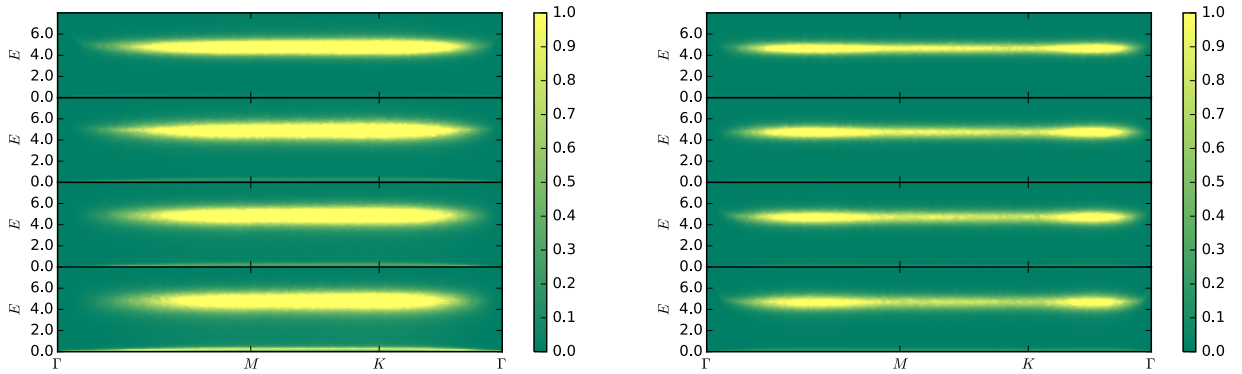


Figure 7. Real part of the inverse susceptibility function of the 2D Hubbard model with for different values of the chemical potential.

D. Conclusions

We have presented the plasmon spectrum at high doping for C_2F and C_2H which are located at the Mott Insulator Phase. We showed that the RPA approximation can describe plasmons in the strongly doped Mott insulators well.

VI. PROBING OF VALLEY POLARIZATION IN GRAPHENE VIA OPTICAL SECOND-HARMONIC GENERATION

Graphene which is a monolayer of carbon atoms arranged in a honeycomb lattice became several years ago one of the most promising material with very interesting effects for applications [100–102]. In the short history of Graphene there is already a considerable amount of new fundamental physics. Through its unusual electronic spectrum Graphene gives rise to the emergence of relativistic condensed matter physics, where relativistic phenomena can be mimicked and observed on the table (see e.g. [103]). The electronic band structure of Graphene allows for a description of the electronic properties in terms of an effective field theory which is equivalent to quantum electrodynamics (QED) in $2 + 1$ dimensions. The most significant phenomena which were observed in Graphene are the Klein paradox [104] and the Zitterbewegung [104]. The electronic spectrum of Graphene results from the charge carriers which are massless Dirac fermions [105, 106]. Graphene also fascinates with its high crystal quality responsible for the ability of charge carriers to bypass thousands of interatomic distances without scattering [105, 107, 108].

The valley degree of freedom of charge carriers for Graphene and other semiconductor systems with Valleys gives rise to promising applications [109, 110]. So far different proposals have been made how to probe valley generation in Graphene [111–115]. Nevertheless the lack of efficient and robust methods to create valley polarization in

Graphene is still a challenge. In this work, we use a single-particle approximation to describe valley polarization in Graphene through breaking inversion symmetry which leads to second harmonic generation. This could be used for investigating ultrafast valleytronics in Graphene.

**Probing of valley polarization in graphene via optical
second-harmonic generation**

Reprinted with permissions from

T. O. Wehling, A. Huber, A. I. Lichtenstein, M. I. Katsnelson
Phys. Rev. B **91**, 041404(R) (2015).

©2015 by the American Physical Society

The reference numbering used in this reprinted article is only valid
within this specific article.

Probing of valley polarization in graphene via optical second-harmonic generation

T. O. Wehling,^{1,2,*} A. Huber,³ A. I. Lichtenstein,³ and M. I. Katsnelson⁴

¹*Institut für Theoretische Physik, Universität Bremen, Otto-Hahn-Allee 1, 28359 Bremen, Germany*

²*Bremen Center for Computational Materials Science, Universität Bremen, Am Fallturm 1a, 28359 Bremen, Germany*

³*I. Institut für Theoretische Physik, Universität Hamburg, Jungiusstraße 9, D-20355 Hamburg, Germany*

⁴*Radboud University of Nijmegen, Institute for Molecules and Materials, Heijendaalseweg 135, 6525 AJ Nijmegen, The Netherlands*

(Received 25 July 2014; revised manuscript received 27 October 2014; published 9 January 2015)

Valley polarization in graphene breaks inversion symmetry and therefore leads to second-harmonic generation. We present a complete theory of this effect within a single-particle approximation. It is shown that this may be a sensitive tool to measure the valley polarization created, e.g., by polarized light and, thus, can be used for the development of ultrafast valleytronics in graphene.

DOI: [10.1103/PhysRevB.91.041404](https://doi.org/10.1103/PhysRevB.91.041404)

PACS number(s): 78.67.Wj, 42.65.Ky

The unique electronic properties of graphene [1–3] open ways for many interesting and unusual applications. In particular, a concept of *valleytronics* was suggested [4], that is, a manipulation of valley degree of freedom (conical points K and K'), in analogy with the well-known field of spintronics [5]. Up to now, many different ways for the creation of the valley polarization in graphene have been proposed (see, e.g., Refs. [6–8]). At the same time, *detection* of the valley polarization is a tricky issue. The first suggestion, the use of a superconducting current through graphene [9], does not look suitable for practical applications, e.g., due to a requirement of low temperatures. It was mentioned in Ref. [7] that the breaking of inversion symmetry by the valley polarization can be probed via second-harmonic generation (SHG), a well-known nonlinear optical effect [10]. Together with their suggestion to use linearly polarized light to create the valley polarization (recently, it was experimentally realized for another two-dimensional crystal, MoS₂ [11,12], with circularly polarized light) it would open a way to ultrafast valleytronics where all manipulations with the valley degree of freedom are performed via short laser pulses, as illustrated in Fig. 1. In spintronics, this is now one of the most prospective lines of development [13].

There is, however, a problem. SHG is related to the term in the current density \vec{j} proportional to the square of the electric field \vec{E} :

$$j_\alpha = \chi_{\alpha\beta\gamma} E_\beta E_\gamma. \quad (1)$$

For a system with inversion center $\hat{\chi} = 0$. This does not mean, however, that SHG is impossible since the photon wave vector \vec{q} plays the role of a factor violating inversion symmetry, and there is a contribution to the current

$$j_\alpha = \phi_{\alpha\beta\gamma\delta} E_\beta E_\gamma q_\delta. \quad (2)$$

For the case of graphene and other two-dimensional electron systems it was calculated in Ref. [14]. In comparison with Eq. (1) it contains a relativistic smallness parameter $v_F/c \approx 1/300$ where v_F is the Fermi velocity and c is the velocity of light. At the same time, the current in Eq. (1) is expected to be proportional to the valley polarization. The order of magnitude

of the valley polarization which can be really probed via SHG depends on explicit values of the tensor $\hat{\chi}$, which will be calculated in this work.

Valley polarization can refer either to different occupations or to different current densities due to electrons from the K and K' valleys [4]. In the following, we consider different occupations in the K and K' valleys, which corresponds to different chemical potentials $\mu \pm \delta\mu$, as illustrated in Fig. 1. Possibilities to generate this kind of valley polarization include quantum pumping [8], nonuniform valley current densities [4] as well as valley Hall effects [15].

We start with a derivation of the effective Hamiltonian of electron-photon interaction for the case of graphene (c.f., e.g., Refs. [3,16]), as the case of nonlinear optics requires special care. Let us consider a general Hamiltonian of band electrons in electromagnetic field described by the vector potential $\mathbf{A}(\mathbf{r}, t)$:

$$H = \sum_{ij, LL', \sigma} t_{ij}^{L'L} \exp\left(i \frac{e}{c} \int_{\mathbf{R}_{jL'}}^{\mathbf{R}_{iL}} d\mathbf{r} \mathbf{A}(\mathbf{r}, t)\right) c_{iL\sigma}^\dagger c_{jL'\sigma}, \quad (3)$$

where \mathbf{R}_{iL} is the atomic position and $L = (n, l, m, \gamma)$ is a combined index of quantum numbers of atom γ (in the equations we assume $\hbar = 1$). The atomic positions can be separated into two parts

$$\mathbf{R}_{iL} = \mathbf{R}_i + \rho_L, \quad (4)$$

where the former indexes the unit cell i and the latter the atom L within the cell in the case of a multiatomic unit cell (like the honeycomb lattice of graphene). We assume, as usual, that the interaction with the electromagnetic field is taken into account via Peierls substitution

$$c_{iL\sigma}^\dagger \rightarrow c_{iL\sigma}^\dagger \exp\left(i \frac{e}{c} \int^{\mathbf{R}_{iL}} d\mathbf{r} \mathbf{A}(\mathbf{r}, t)\right) \quad (5)$$

for the electron creation operators $c_{iL\sigma}^\dagger$ and similarly for the electron annihilation operators $c_{iL\sigma}$. $t_{ij}^{L'L}$ are the parameters of the band-structure Hamiltonian.

Since we are interested in terms up to second order in the vector potential we expand the hopping and treat the additional terms proportional to the vector potential as perturbation. The

*wehling@itp.uni-bremen.de

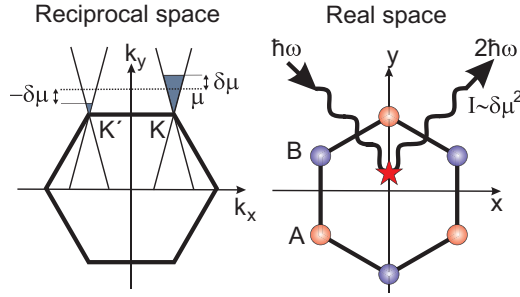


FIG. 1. (Color online) Illustration of second-harmonic generation in graphene. SHG requires breaking of inversion symmetry which can be achieved through valley polarization as illustrated in the left panel. Valley polarization is modeled in terms of different chemical potentials $\mu \pm \delta\mu$ in valleys K and K' . With the choice of the coordinate system illustrated in the right panel, valley polarization breaks the $x \rightarrow -x$ mirror symmetry. The second-harmonic intensity I is proportional to $\delta\mu^2$.

Hamiltonian then becomes

$$\begin{aligned}
 H &\equiv H^{(0)} + H^{(1)} + H^{(2)} + O(A^3) \\
 &= \sum_{ij,LL',\sigma} t_{ij}^{L'L} c_{iL'\sigma}^\dagger c_{jL\sigma} + i \frac{e}{c} A_\alpha(t) \\
 &\quad \times \sum_{ij,LL',\sigma} t_{ij}^{L'L} (R_{iL'\alpha} - R_{jL\alpha}) c_{iL'\sigma}^\dagger c_{jL\sigma} \\
 &\quad + \frac{1}{2} \left(i \frac{e}{c} \right)^2 A_\alpha(t) A_\beta(t) \sum_{ij,LL',\sigma} t_{ij}^{L'L} (R_{iL'\alpha} \\
 &\quad - R_{jL\alpha})(R_{iL'\beta} - R_{jL\beta}) c_{iL'\sigma}^\dagger c_{jL\sigma} + O(A^3), \quad (6)
 \end{aligned}$$

where the second equation is defined in powers of the vector potential and we further assumed that the vector potential slowly varies in \mathbf{r} . With a basis transformation to Bloch waves $c_{\mathbf{k}L\sigma} = \frac{1}{\sqrt{N}} \sum_j \exp(i\mathbf{k}\mathbf{R}_j) c_{jL\sigma}$ the bare part of the Hamiltonian is diagonalized according to $H^{(0)} = \sum_{\mathbf{k},LL',\sigma} H_{\mathbf{k},LL'}^0 c_{\mathbf{k}L\sigma}^\dagger c_{\mathbf{k}L'\sigma}$ with

$$H_{\mathbf{k},LL'}^0 = \sum_{ij} t_{ij}^{L'L} \exp[-i\mathbf{k}(\mathbf{R}_i - \mathbf{R}_j)]. \quad (7)$$

Now one can distinguish between two currents which are defined using the Hamiltonian (6) by

$$j_\alpha^{(1)} \equiv \left. \frac{\delta H}{\delta A_\alpha(\mathbf{r},t)} \right|_{\mathbf{A}=0} = e \sum_{LL',\mathbf{k},\sigma} v_{\mathbf{k}\alpha}^{LL'} c_{\mathbf{k}L'\sigma}^\dagger c_{\mathbf{k}L\sigma}, \quad (8)$$

$$j_{\alpha\beta}^{(2)} \equiv \left. \frac{\delta^2 H}{\delta A_\alpha(\mathbf{r},t) \delta A_\beta(\mathbf{r},t)} \right|_{\mathbf{A}=0} = e^2 \sum_{LL',\mathbf{k},\sigma} v_{\mathbf{k}\alpha\beta}^{LL'} c_{\mathbf{k}L'\sigma}^\dagger c_{\mathbf{k}L\sigma}, \quad (9)$$

where

$$\begin{aligned}
 v_{\mathbf{k}\alpha}^{LL'} &\equiv i \sum_{i-j} t_{ij}^{L'L} (R_{iL'\alpha} - R_{jL\alpha}) \\
 &\quad \times \exp[-i\mathbf{k}(\mathbf{R}_i - \mathbf{R}_j)]
 \end{aligned} \quad (10)$$

and

$$\begin{aligned}
 v_{\mathbf{k}\alpha\beta}^{LL'} &\equiv (i)^2 \sum_{i-j} t_{ij}^{L'L} (R_{iL'\alpha} - R_{jL\alpha})(R_{iL'\beta} - R_{jL\beta}) \\
 &\quad \times \exp[-i\mathbf{k}(\mathbf{R}_i - \mathbf{R}_j)]. \quad (11)
 \end{aligned}$$

With Fourier transform of the band Hamiltonian (6) we can reexpress the generalized velocities resulting from Eq. (10) according to

$$v_{\mathbf{k}\alpha}^{LL'} = [\partial_{k_\alpha} - i(\rho_{L'}^\alpha - \rho_L^\alpha)] H_{\mathbf{k},LL'}^{(0)} \quad (12)$$

and Eq. (11) leads to

$$\begin{aligned}
 v_{\mathbf{k}\alpha\beta}^{LL'} &= [\partial_{k_\alpha} \partial_{k_\beta} + i(\rho_{L'}^\alpha - \rho_L^\alpha) \partial_{k_\beta} + i(\rho_{L'}^\beta - \rho_L^\beta) \partial_{k_\alpha} \\
 &\quad - (\rho_{L'}^\alpha - \rho_L^\alpha)(\rho_{L'}^\beta - \rho_L^\beta)] H_{\mathbf{k},LL'}^{(0)}. \quad (13)
 \end{aligned}$$

We will use these general expressions for the particular case of graphene, in a single-band approximation (π bands only) taking into account only the nearest-neighbor (t) and the next-nearest-neighbor (t') hopping parameters [17]; the latter can be important since it breaks the electron-hole symmetry of the Hamiltonian which as we will see is essential for SHG.

There are two contributions to the electric current quadratic in the vector potential $\mathbf{A}(\mathbf{r},t)$. Note that we now switch to the response of an electric field by using the identity

$$\frac{1}{c} A_\alpha(\mathbf{r},t) = -i \frac{E_\alpha(\mathbf{r},t)}{\omega}. \quad (14)$$

The contributions to the nonlinear optical conductivity (1) via Feynman diagrams are drawn in Fig. 2.

The corresponding algebraic equation for the triangle diagram is given by

$$\begin{aligned}
 \chi_{\alpha\beta\gamma}^{\text{triangle}}(i\omega, i\omega, 2i\omega) \\
 &= -i \frac{e^3}{\omega^2} \frac{1}{\beta} \sum_{\nu} \sum_{\mathbf{k}} \sum_{L_1, \dots, L_6} v_{\mathbf{k}\alpha}^{L_6 L_1} G_{L_1 L_2}(\mathbf{k}, i\nu) \\
 &\quad \times v_{\mathbf{k}\beta}^{L_2 L_3} G_{L_3 L_4}(\mathbf{k}, i\nu + i\omega) v_{\mathbf{k}\gamma}^{L_4 L_5} G_{L_5 L_6}(\mathbf{k}, i\nu - i\omega), \quad (15)
 \end{aligned}$$

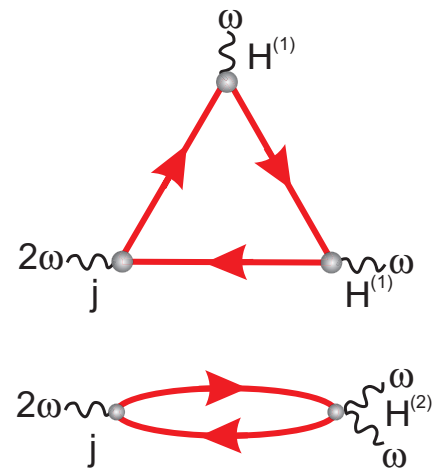


FIG. 2. (Color online) Two second-order contributions to the nonlinear susceptibility. Top: triangle diagram. Bottom: nonlinear bubble diagram. Solid lines are electron Green's functions and wavy tails indicate photons involved in the processes.

and for the nonlinear bubble diagram

$$\begin{aligned} \chi_{\alpha\beta\gamma}^{\text{bubble}}(i\omega, i\omega, 2i\omega) \\ = -i \frac{e^3}{\omega^2} \frac{1}{\beta} \sum_{\nu} \sum_{\mathbf{k}} \sum_{L_1, \dots, L_4} \\ \times v_{\mathbf{k}\alpha\beta}^{L_4 L_1} G_{L_1 L_2}(\mathbf{k}, i\nu - i\omega) v_{\mathbf{k}\gamma}^{L_2 L_3} G_{L_3 L_4}(\mathbf{k}, i\nu + i\omega). \end{aligned} \quad (16)$$

Here L_1, \dots, L_6 are pseudospin indices, $\beta = 1/T$ is the inverse temperature (we use the units $\hbar = k_B = 1$), and

$$\widehat{G}(i\nu) = \frac{1}{i\nu + \mu - \widehat{H}} \quad (17)$$

is the Green's function with μ being the chemical potential counted from the neutrality (conical) point. Thus, the nonlinear susceptibility is given by

$$\chi_{\alpha\beta\gamma} = \chi_{\alpha\beta\gamma}^{\text{bubble}} + \chi_{\alpha\beta\gamma}^{\text{triangle}}. \quad (18)$$

Note that the minus sign from the fermion loop should be taken into account in both diagrams. The factor $\frac{1}{\omega^2}$ appears due to Eq. (14). We pass, as usual [18] to imaginary (Matsubara) frequencies; at the end of the calculations the analytical continuation to the real axis $i\omega \rightarrow \omega + i\delta$ is performed.

If we take into account electron-electron interactions the nonlinear conductivity will be renormalized by three-leg and six-leg electron vertices; the corresponding expressions can be found in Ref. [19].

It is obvious by inversion symmetry that for the non-valley-polarized case $\hat{\chi} = 0$. We mimic the valley polarization by splitting the Brillouin zone into two symmetrically chosen parts, one containing the point K and the other part containing the point K' , and assuming different chemical potentials for these two parts. We then expand all the quantities dependent on the chemical potential as

$$f(\mu + \delta\mu) - f(\mu - \delta\mu) \approx 2 \frac{\partial f(\mu)}{\partial \mu} \delta\mu. \quad (19)$$

We evaluated the derivative $\partial\chi/\partial\delta\mu$ analytically using Eqs. (15) and (16) and then performed a numerical summation over Matsubara frequencies and wave vectors involving half of the Brillouin zone. We choose $\beta = 40/\text{eV}$, which corresponds to a temperature of 290 K. In this case, sampling of the Brillouin with 121×121 k points and summation of 200 (1000) fermionic Matsubara frequencies are required to reach convergence for the triangle (nonlinear bubble) diagram at bosonic Matsubara frequencies $\Omega_n = 2\pi n/\beta$ in the range of $n = 1, \dots, 20$.

A symmetry analysis shows that there are only two independent components of the tensor $\hat{\chi}$, $\chi_{xxx} = -\chi_{xyy} = -\chi_{yyx} = -\chi_{yxy}$ and $\chi_{yyy} = -\chi_{yxx} = -\chi_{xxy} = -\chi_{xyx}$ [10]. With the choice of coordinates made here, the K and K' points of the Brillouin zone are on the positive/negative x axis (see Fig. 1). Thus valley polarization breaks inversion symmetry with respect to the x direction, $x \rightarrow -x$, but the $y \rightarrow -y$ symmetry is preserved. Thus, we have $\chi_{yyy} = 0$ and we will show the results only for χ_{xxx} .

The computational results for the case of finite chemical potential $\mu = 0.2t$ are shown in Fig. 3. For the case $\mu = 0, t' = 0$ one finds $d\chi_{xxx}/d\mu = 0$, due to electron-hole symmetry. Nearest-neighbor hopping t' breaks this symmetry and leads

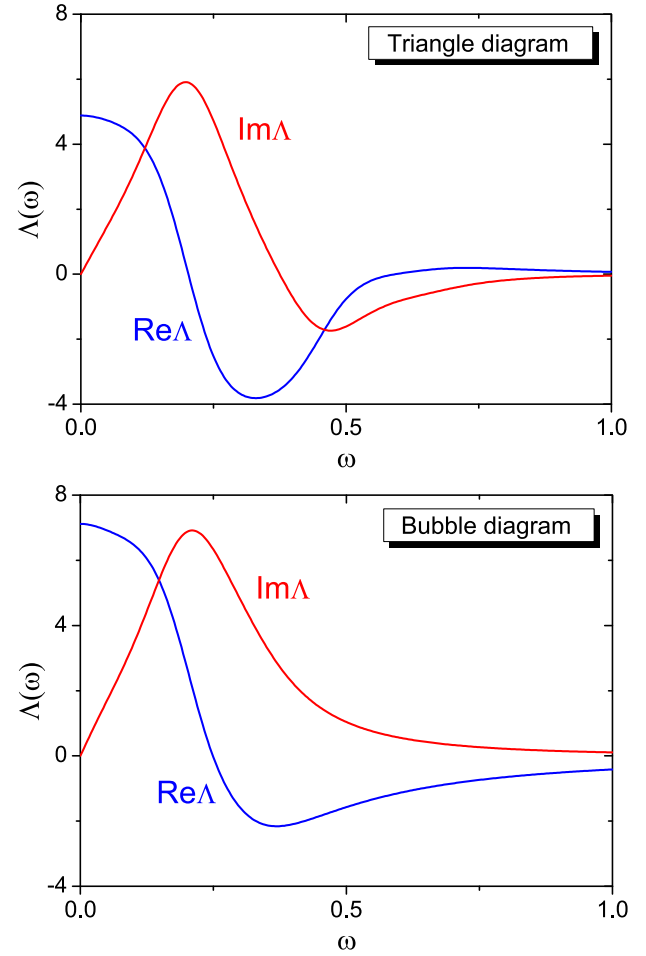


FIG. 3. (Color online) Computational results for $\Lambda = -(\hbar\omega)^2 \frac{\partial \chi_{xxx}}{\partial \mu}$ (in the units of $e^3 a/\hbar$, a is the lattice constant) as a function of real frequency ω (in the units of t/\hbar). The total answer is the sum of the triangle and bubble contributions.

to nonzero $d\chi_{xxx}/d\mu$ even at $\mu = 0$ and according to Ref. [17] we have $t' \approx 0.1t$. Our calculations show, however, that for $\mu = 0.2t$ the effects of finite t' are negligible leading only to a few-percent corrections.

One can see from Fig. 3 that a dimensionless quantity Λ characterizing the valley-polarization induced SHG is pretty large, of the order of ten, despite the smallness of the ratios t'/t and μ/t . It is consistent with the computational results [20–22] on SHG in chiral nanotubes which turned out to be strongly enhanced in comparison with conventional materials without inversion symmetry. A comparison with the results of Ref. [14] shows that the valley-polarization induced SHG will be dominant if $|\delta\mu|/t > 0.01v_F/c \approx 3 \times 10^{-5}$. Note, that one additional smallness in order of magnitude originates from the factor $3/8\pi \approx 0.1$ in Ref. [14] and another one from the fact that $\Lambda \approx 10$.

Typical nonlinear crystals have second-order nonlinear susceptibilities on the order of $\tilde{\chi} = 0.1$ to 100 pm/V [10]. It is interesting to see which amount of valley polarization is required to reach this order in graphene. From the current density $j = \chi E^2$ we obtain the oscillating in-plane charge density $|\sigma| = |j|/c$ and the associated

electric field $E_{2\omega} = \sigma/\epsilon_0 = \chi E^2/\epsilon_0 c = \tilde{\chi} E^2$. With photon energies on the order of $\hbar\omega = 1.5 \text{ eV} \approx 0.5t$ and $\Lambda \approx 10$ we find thus $\tilde{\chi}/\delta\mu = -\Lambda(e^3 a/\hbar)/[\epsilon_0 c(\hbar\omega)^2] \approx 1(\text{\AA}/\text{V})/\text{eV} = 100 \text{ (pm/V)/eV}$. Thus $\delta\mu \gtrsim 1 \text{ meV}$ is required to reach $\tilde{\chi} = 0.1 \text{ pm/V}$.

This means that SHG is, indeed, a very efficient tool to probe the valley polarization in graphene. Our results show that “triangle” and “bubble” contributions to the second-harmonic generation are, in general, comparable. Also, one can see that they have quite a similar frequency dependence. An alternative way to probe the valley polarization is the photogalvanic effect, that is, generation of dc current under laser pulses. This process is described by the quantity $\chi_{\alpha\beta\gamma}(\omega, \omega, 0)$ which is of the same order of magnitude as $\chi_{\alpha\beta\gamma}(\omega, \omega, 2\omega)$ calculated here. It would be very interesting to probe both of these effects experimentally in graphene with valley polarization.

In monolayer MoS₂, valley polarization is controllable by (linear) optics [11,12]. Symmetry-wise MoS₂ corresponds to graphene with broken sublattice symmetry (i.e., D_{3h}), where Mo atoms occupy sublattice *A* and the S atoms reside on sublattice *B*. Thus, there is no $y \rightarrow -y$ mirror symmetry and $\chi_{yyy} \neq 0$ even in the absence of valley polarization. The initial $x \rightarrow -x$ mirror symmetry of MoS₂ ensures, however, that nonzero χ_{xxx} requires additional symmetry break as provided, e.g., by valley polarization. Thus, the concept of nonlinear optics and photogalvanic effects to detect valley polarization is partly transferable to MoS₂. It works with light

which is linearly polarized in the x direction but not in the y direction.

Lattice matched graphene-hBN (hexagonal boron nitride) heterostructures have proven to allow for nonlocal transport phenomena based on the valley degree of freedom over micron scale distances [15]. It appears thus highly promising to combine the advantages of MoS₂ (optical generation of valley polarization [11,12]) with those of graphene (transport properties). Finally, for graphene (not lattice matched to hBN) very close to the neutrality point a flavor Hall effect has been observed which could be of spin or valley origin [23]. Measuring SHG could solve this puzzle, since only valley but not spin polarization would lead to an SHG signal.

Note added. Recently, a related work, Ref. [24], reporting similar results has been published. While Ref. [24] focuses on lower energies (the authors of that work use Dirac spectrum with trigonal warping corrections, instead of the full tight-binding spectrum as in the present work), the conclusions drawn here and in Ref. [24] are in agreement.

The authors acknowledge financial support from European Union Seventh Framework Program under grant agreement Graphene Flagship and the Deutsche Forschungsgemeinschaft (DFG) through SPP 1459. M.I.K. also acknowledges financial support from the European Research Council Advanced Grant program (Contract No. 338957).

-
- [1] A. K. Geim and K. S. Novoselov, *Nat. Mater.* **6**, 183 (2007).
 [2] A. H. Castro Neto, F. Guinea, N. M. R. Peres, K. S. Novoselov, and A. K. Geim, *Rev. Mod. Phys.* **80**, 315 (2008).
 [3] M. I. Katsnelson, *Graphene: Carbon in Two Dimensions* (Cambridge University Press, Cambridge, 2012).
 [4] A. Rycerz, J. Tworzydło, and C. W. J. Beenakker, *Nat. Phys.* **3**, 172 (2007).
 [5] I. Žutić, J. Fabian, and S. Das Sarma, *Rev. Mod. Phys.* **76**, 323 (2004).
 [6] I. Martin, Y. M. Blanter, and A. F. Morpurgo, *Phys. Rev. Lett.* **100**, 036804 (2008).
 [7] L. E. Golub, S. A. Tarasenko, M. V. Entin, and L. I. Magarill, *Phys. Rev. B* **84**, 195408 (2011).
 [8] Y. Jiang, T. Low, K. Chang, M. I. Katsnelson, and F. Guinea, *Phys. Rev. Lett.* **110**, 046601 (2013).
 [9] A. R. Akhmerov and C. W. J. Beenakker, *Phys. Rev. Lett.* **98**, 157003 (2007).
 [10] R. W. Boyd, *Nonlinear Optics* (Academic, New York, 1992).
 [11] H. Zeng, J. Dai, W. Yao, D. Xiao, and X. Cui, *Nat. Nanotechnol.* **7**, 490 (2012).
 [12] K. F. Mak, K. He, J. Shan, and T. F. Heinz, *Nat. Nanotechnol.* **7**, 494 (2012).
 [13] A. Kirilyuk, A. V. Kimel, and T. Rasing, *Rev. Mod. Phys.* **82**, 2731 (2010).
 [14] S. A. Mikhailov, *Phys. Rev. B* **84**, 045432 (2011).
 [15] R. V. Gorbachev, J. C. W. Song, G. L. Yu, A. V. Kretinin, F. Withers, Y. Cao, A. Mishchenko, I. V. Grigorieva, K. S. Novoselov, L. S. Levitov, and A. K. Geim, *Science* **346**, 448 (2014).
 [16] T. Stauber, N. M. R. Peres, and A. K. Geim, *Phys. Rev. B* **78**, 085432 (2008).
 [17] A. Kretinin, G. L. Yu, R. Jalil, Y. Cao, F. Withers, A. Mishchenko, M. I. Katsnelson, K. S. Novoselov, A. K. Geim, and F. Guinea, *Phys. Rev. B* **88**, 165427 (2013).
 [18] G. Mahan, *Many-Particle Physics* (Plenum, New York, 2000).
 [19] M. I. Katsnelson and A. I. Lichtenstein, *J. Phys.: Condens. Matter* **22**, 382201 (2010).
 [20] G. Y. Guo, K. C. Chu, D.-S. Wang, and C.-G. Duan, *Phys. Rev. B* **69**, 205416 (2004).
 [21] J. Zhou, H. Weng, G. Wu, and J. Dong, *Appl. Phys. Lett.* **89**, 013102 (2006).
 [22] T. G. Pedersen and K. Pedersen, *Phys. Rev. B* **79**, 035422 (2009).
 [23] D. A. Abanin, S. V. Morozov, L. A. Ponomarenko, R. V. Gorbachev, A. S. Mayorov, M. I. Katsnelson, K. Watanabe, T. Taniguchi, K. S. Novoselov, L. S. Levitov, and A. K. Geim, *Science* **332**, 328 (2011).
 [24] L. E. Golub and S. A. Tarasenko, *Phys. Rev. B* **90**, 201402(R) (2014).

VII. GENERAL CONCLUSIONS AND PERSPECTIVES

The work presented in this thesis has contributed to the development of an approximation improving over EDMFT, which takes local correlations from EDMFT and includes in a proper way non-local correlations. It is based on the exact path-integral transformation from numerically exact local solutions to pure non-local dual variables. This technic serves a way to include non-local correlation to EDMFT already at the propagator level in the diagrams and is by construction free of double-counting problems. This way of including non-locality gives an improvement in the phase boundary between the charge-ordered and the Fermi liquid phase compared to the EDMFT+GW in the V-decoupling schema. It is also shown, that previous approaches, such as EDMFT+GW and TRILEX, can be easily derived from the exact dual transformations. Moreover, the dual way of exclusion of the double-counting can be straightforwardly extended to all EDMFT++ approaches. Therefore, for the same computational complexity as the standard EDMFT+GW approach. The non-trivial "dual boson" way of including local vertices in the first-principle EDMFT+GW approach opens a new direction in the description of collective excitations in solids.

Additionally we derived the bosonic action for charge degrees of freedom of the extended Hubbard model. In the region where the charge fluctuations are prominent, the local four-point vertex of the underlying impurity model does not depend on the fermionic frequencies. In the region where the charge fluctuations are well-developed one can decisively determine by looking at the deviation of the double occupancy from its maximum. As our study shows, the latter

corresponds to a large value of the double occupancy and can be distinguished for a broad range of values of Coulomb interaction. Remarkably, the local Coulomb interaction may even exceed half of the band-width. Thus, in the case of well-developed charge fluctuations, the derived quantum bosonic problem can be mapped onto an effective classical Ising model formulated in terms of a pair interaction between local electronic densities. Importantly, this pair interaction can be obtained calculating a convolution of two non-local Green's functions without vertex corrections. To our knowledge, the derived simple formalism was never presented in the literature before and is believed to be applicable to a very broad class of alloys and ordered systems.

Finally, we showed that second harmonic generation is, indeed, a very efficient tool to probe the valley polarization in Graphene. The "bubble" and the "triangular" diagrams which were calculated have a comparable magnitude. The third diagram of third order with three curly lines and a bubble, which is a constant, gives no contribution. The frequency dependence of both diagrams has similar behavior.

APPENDIX

A: LIST OF PUBLICATIONS AND AUTHORS CONTRIBUTIONS

Publications discussed in this thesis

1. From local to non-local correlations: the Dual Boson perspective
E. A. Stepanov, A. Huber, E. G. C. P. van Loon, A. I. Lichtenstein, M. I. Katsnelson
Phys. Rev. B94, 205110 (2016)
Reprinted on Page 20
This author participated in the development of the algorithms, implemented it, performed parts of the calculations and contributed to analysis and the preparation of the manuscript.
2. Effective Ising model for correlated systems with charge ordering
E. A. Stepanov, A. Huber, A. I. Lichtenstein, M. I. Katsnelson
Phys. Rev. B 99, 115124 (2019)
This author participated in the development of the algorithms, implemented it, performed parts of the calculations and contributed to analysis and the preparation of the manuscript.
3. Probing of valley polarization in graphene via optical second-harmonic generation

T. O. Wehling, A. Huber, A. I. Lichtenstein, M. I. Katsnelson
Phys. Rev. B91, 041404(R) (2015)

Reprinted on Page 82

This author participated in the development of the algorithms, implemented it, performed parts of the calculations and contributed to analysis and the preparation of the manuscript.

BIBLIOGRAPHY

- [1] A. Georges, G. Kotliar, W. Krauth, and M. J. Rozenberg, *Rev. Mod. Phys.* **68**, 13 (1996).
- [2] P. A. Lee, N. Nagaosa, and X.-G. Wen, *Rev. Mod. Phys.* **78**, 17 (2006).
- [3] W. Metzner and D. Vollhardt, *Phys. Rev. Lett.* **62**, 324 (1989).
- [4] Proceedings of the Royal Society of London A: Mathematical, Physical and Engineering Sciences **276**, 238 (1963), <http://rspa.royalsocietypublishing.org/content/276/1365/238.full.pdf>.
- [5] Proceedings of the Royal Society of London A: Mathematical, Physical and Engineering Sciences **281**, 401 (1964), <http://rspa.royalsocietypublishing.org/content/281/1386/401.full.pdf>.
- [6] N. F. Mott and L. Friedman, *Philosophical Magazine* **30**, 389 (1974), <http://dx.doi.org/10.1080/14786439808206565>.
- [7] M. Imada, A. Fujimori, and Y. Tokura, *Rev. Mod. Phys.* **70**, 1039 (1998).
- [8] P. Hansmann, T. Ayrál, L. Vaugier, P. Werner, and S. Biermann, *Phys. Rev. Lett.* **110**, 166401 (2013).
- [9] P. Sun and G. Kotliar, *Phys. Rev. B* **66**, 085120 (2002).
- [10] K.-S. Chen, Z. Y. Meng, S.-X. Yang, T. Pruschke, J. Moreno, and M. Jarrell, *Phys. Rev. B* **88**, 245110 (2013).
- [11] T. Ayrál, P. Werner, and S. Biermann, *Phys. Rev. Lett.* **109**, 226401 (2012).
- [12] T. Ayrál, S. Biermann, and P. Werner, *Phys. Rev. B* **87**,

-
- 125149 (2013).
- [13] Q. Si and J. L. Smith, *Phys. Rev. Lett.* **77**, 3391 (1996).
 - [14] J. L. Smith and Q. Si, *Phys. Rev. B* **61**, 5184 (2000).
 - [15] R. Chitra and G. Kotliar, *Phys. Rev. Lett.* **84**, 3678 (2000).
 - [16] R. Chitra and G. Kotliar, *Phys. Rev. B* **63**, 115110 (2001).
 - [17] A. Toschi, A. A. Katanin, and K. Held, *Phys. Rev. B* **75**, 045118 (2007).
 - [18] G. Rohringer, A. Toschi, H. Hafermann, K. Held, V. I. Anisimov, and A. A. Katanin, *Phys. Rev. B* **88**, 115112 (2013).
 - [19] C. Taranto, S. Andergassen, J. Bauer, K. Held, A. Katanin, W. Metzner, G. Rohringer, and A. Toschi, *Phys. Rev. Lett.* **112**, 196402 (2014).
 - [20] T. Ayrál and O. Parcollet, *Phys. Rev. B* **92**, 115109 (2015).
 - [21] L. Hedin, *Phys. Rev.* **139**, A796 (1965).
 - [22] A. N. Rubtsov, M. I. Katsnelson, and A. I. Lichtenstein, *Phys. Rev. B* **77**, 033101 (2008).
 - [23] A. N. Rubtsov, M. I. Katsnelson, and A. I. Lichtenstein, *Annals of Physics* **327**, 1320 (2012).
 - [24] E. G. C. P. van Loon, A. I. Lichtenstein, M. I. Katsnelson, O. Parcollet, and H. Hafermann, *Phys. Rev. B* **90**, 235135 (2014).
 - [25] E. A. Stepanov, E. G. C. P. van Loon, A. A. Katanin, A. I. Lichtenstein, M. I. Katsnelson, and A. N. Rubtsov, *Phys. Rev. B* **93**, 045107 (2016).
 - [26] P. Sun and G. Kotliar, *Phys. Rev. Lett.* **92**, 196402 (2004).
 - [27] T. Ayrál, S. Biermann, P. Werner, and L. Boehnke, *Phys. Rev. B* **95**, 245130 (2017).
 - [28] H. Terletska, T. Chen, and E. Gull, *Phys. Rev. B* **95**, 115149 (2017).
 - [29] D. Pines and P. Nozieres, *The Theory of Quantum Liquids:*

- Normal Fermi liquids. Theory of quantum liquids* (W.A. Benjamin, Philadelphia, 1966).
- [30] P. M. Platzman and P. A. Wolff, *Waves and interactions in solid state plasmas*, Vol. 13 (Academic Press, New York, 1973).
- [31] S. V. Vonsovsky and M. I. Katsnelson, *Quantum solid-state physics* (Springer Verlag, Berlin, 1989).
- [32] H. Hafermann, E. G. C. P. van Loon, M. I. Katsnelson, A. I. Lichtenstein, and O. Parcollet, [Phys. Rev. B **90**, 235105 \(2014\)](#).
- [33] E. G. C. P. van Loon, H. Hafermann, A. I. Lichtenstein, A. N. Rubtsov, and M. I. Katsnelson, [Phys. Rev. Lett. **113**, 246407 \(2014\)](#).
- [34] E. J. W. Verwey and P. W. Haayman, [Physica **8**, 979 \(1941\)](#).
- [35] E. J. W. Verwey, P. W. Haayman, and F. C. Romeijn, [The Journal of Chemical Physics **15**, 181 \(1947\)](#).
- [36] N. F. Mott, *Metal-insulator transitions* (London: Taylor & Francis, 1974).
- [37] U. Staub, M. Shi, C. Schulze-Briesche, B. D. Patterson, F. Fauth, E. Dooryhee, L. Soderholm, J. O. Cross, D. Mannix, and A. Ochiai, [Phys. Rev. B **71**, 075115 \(2005\)](#).
- [38] P. Fulde, B. Schmidt, and P. Thalmeier, [EPL \(Europhysics Letters\) **31**, 323 \(1995\)](#).
- [39] T. Goto and B. Lüthi, [Advances in Physics **52**, 67 \(2003\)](#).
- [40] C. J. Arguello, S. P. Chockalingam, E. P. Rosenthal, L. Zhao, C. Gutiérrez, J. H. Kang, W. C. Chung, R. M. Fernandes, S. Jia, A. J. Millis, R. J. Cava, and A. N. Pasupathy, [Phys. Rev. B **89**, 235115 \(2014\)](#).
- [41] T. Ritschel, J. Trinckauf, K. Koepernik, B. Büchner, M. v. Zimmermann, H. Berger, Y. I. Joe, P. Abbamonte, and J. Geck,

- Nature physics **11**, 328 (2015).
- [42] M. M. Ugeda, A. J. Bradley, Y. Zhang, S. Onishi, Y. Chen, W. Ruan, C. Ojeda-Aristizabal, H. Ryu, M. T. Edmonds, H.-Z. Tsai, *et al.*, Nature Physics **12**, 92 (2016).
- [43] T. Furuno, K. Ando, S. Kunii, A. Ochiai, H. Suzuki, M. Fujioka, T. Suzuki, W. Sasaki, and T. Kasuya, [Journal of Magnetism and Magnetic Materials](#) **76-77**, 117 (1988).
- [44] V. Y. Irkhin and M. I. Katsnelson, [Physics Letters A](#) **150**, 47 (1990).
- [45] P. Wachter, [Philosophical Magazine B](#) **42**, 497 (1980).
- [46] C. Schlenker and M. Marezio, [Philosophical Magazine B](#) **42**, 453 (1980).
- [47] B. K. Chakraverty, [Philosophical Magazine B](#) **42**, 473 (1980).
- [48] V. Eyert, U. Schwingenschlögl, and U. Eckern, [Chemical Physics Letters](#) **390**, 151 (2004).
- [49] I. Leonov, A. N. Yaresko, V. N. Antonov, U. Schwingenschlögl, V. Eyert, and V. I. Anisimov, [Journal of Physics: Condensed Matter](#) **18**, 10955 (2006).
- [50] J. Dumas, C. Schlenker, and R. Buder, [Philosophical Magazine B](#) **42**, 485 (1980).
- [51] A. Galler, P. Thunström, P. Gunacker, J. M. Tomczak, and K. Held, [Phys. Rev. B](#) **95**, 115107 (2017).
- [52] E. G. C. P. van Loon, M. Rösner, G. Schönhoff, M. I. Katsnelson, and T. O. Wehling, [npj Quantum Materials](#) **3**, 32 (2018).
- [53] E. A. Stepanov, A. Huber, E. G. C. P. van Loon, A. I. Lichtenstein, and M. I. Katsnelson, [Phys. Rev. B](#) **94**, 205110 (2016).
- [54] T. Ayrál and O. Parcollet, [Phys. Rev. B](#) **93**, 235124 (2016).
- [55] S. Biermann, F. Aryasetiawan, and A. Georges, [Phys. Rev. Lett.](#) **90**, 086402 (2003).

- [56] A. V. Ruban, S. Shallcross, S. I. Simak, and H. L. Skriver, [Phys. Rev. B **70**, 125115 \(2004\)](#).
- [57] S. Shallcross, A. E. Kissavos, V. Meded, and A. V. Ruban, [Phys. Rev. B **72**, 104437 \(2005\)](#).
- [58] P. A. Korzhavyi, A. V. Ruban, J. Odqvist, J.-O. Nilsson, and B. Johansson, [Phys. Rev. B **79**, 054202 \(2009\)](#).
- [59] M. Ekholm, H. Zapolsky, A. V. Ruban, I. Vernyhora, D. Ledue, and I. A. Abrikosov, [Phys. Rev. Lett. **105**, 167208 \(2010\)](#).
- [60] B. Alling, A. V. Ruban, A. Karimi, L. Hultman, and I. A. Abrikosov, [Phys. Rev. B **83**, 104203 \(2011\)](#).
- [61] A. V. Ruban and I. A. Abrikosov, [Reports on Progress in Physics **71**, 046501 \(2008\)](#).
- [62] J. W. D. Connolly and A. R. Williams, [Phys. Rev. B **27**, 5169 \(1983\)](#).
- [63] M. Hennion, [Journal of Physics F: Metal Physics **13**, 2351 \(1983\)](#).
- [64] F. Ducastelle and F. Ducastelle, *Order and phase stability in alloys* (North-Holland Amsterdam, 1991).
- [65] A. I. Liechtenstein, M. I. Katsnelson, and V. A. Gubanov, [Journal of Physics F: Metal Physics **14**, L125 \(1984\)](#).
- [66] A. I. Liechtenstein, M. I. Katsnelson, and V. A. Gubanov, [Solid State Communications **54**, 327 \(1985\)](#).
- [67] A. I. Liechtenstein, M. I. Katsnelson, V. P. Antropov, and V. A. Gubanov, [Journal of Magnetism and Magnetic Materials **67**, 65 \(1987\)](#).
- [68] M. I. Katsnelson and A. I. Lichtenstein, [Phys. Rev. B **61**, 8906 \(2000\)](#).
- [69] E. A. Stepanov, S. Brener, F. Krien, M. Harland, A. I. Lichtenstein, and M. I. Katsnelson, [Phys. Rev. Lett. **121**, 037204 \(2018\)](#).

- [70] A. M. Sengupta and A. Georges, [Phys. Rev. B **52**, 10295 \(1995\)](#).
- [71] F. Aryasetiawan and O. Gunnarsson, [Reports on Progress in Physics **61**, 237 \(1998\)](#).
- [72] L. Hedin, [Journal of Physics: Condensed Matter **11**, R489 \(1999\)](#).
- [73] S. V. Vonsovsky and M. I. Katsnelson, [Journal of Physics C: Solid State Physics **12**, 2043 \(1979\)](#).
- [74] A. K. Zhuravlev, M. I. Katsnelson, and A. V. Trefilov, [Phys. Rev. B **56**, 12939 \(1997\)](#).
- [75] E. G. C. P. van Loon, F. Krien, H. Hafermann, E. A. Stepanov, A. I. Lichtenstein, and M. I. Katsnelson, [Phys. Rev. B **93**, 155162 \(2016\)](#).
- [76] G. Rohringer, A. Valli, and A. Toschi, [Phys. Rev. B **86**, 125114 \(2012\)](#).
- [77] Y. M. Vilk and A.-M. S. Tremblay, [J. Phys. I France **7**, 1309 \(1997\)](#).
- [78] H. Terletska, T. Chen, J. Paki, and E. Gull, [Phys. Rev. B **97**, 115117 \(2018\)](#).
- [79] V. P. Antropov, M. I. Katsnelson, M. van Schilfgaarde, and B. N. Harmon, [Phys. Rev. Lett. **75**, 729 \(1995\)](#).
- [80] D. Nicoletti, E. Casandruc, D. Fu, P. Giraldo-Gallo, I. R. Fisher, and A. Cavalleri, [Proceedings of the National Academy of Sciences **114**, 9020 \(2017\)](#).
- [81] T. Maier, M. Jarrell, T. Pruschke, and M. H. Hettler, [Rev. Mod. Phys. **77**, 1027 \(2005\)](#).
- [82] S. V. Vonsovsky and M. I. Katsnelson, Springer Verlag, Berlin (1989).
- [83] G. Giuliani and G. Vignale, *Quantum theory of the electron liquid* (Cambridge university press, 2005).

- [84] P. Nozières and D. Pines, *Theory of quantum liquids* (Hachette UK, 1999).
- [85] W. L. Barnes, A. Dereux, and T. W. Ebbesen, [Nature **424**, 824 \(2003\)](#).
- [86] J. T. Robinson, J. S. Burgess, C. E. Junkermeier, S. C. Badescu, T. L. Reinecke, F. K. Perkins, M. K. Zalalutdniov, J. W. Baldwin, J. C. Culbertson, P. E. Sheehan, and E. S. Snow, [Nano Letters **10**, 3001 \(2010\)](#), pMID: 20698613.
- [87] A. Karalis, E. Lidorikis, M. Ibanescu, J. D. Joannopoulos, and M. Soljačić, [Phys. Rev. Lett. **95**, 063901 \(2005\)](#).
- [88] J. B. Pendry, [Phys. Rev. Lett. **85**, 3966 \(2000\)](#).
- [89] D. R. Smith, J. B. Pendry, and M. C. K. Wiltshire, [Science **305**, 788 \(2004\)](#), <http://science.sciencemag.org/content/305/5685/788.full.pdf>.
- [90] T. C. Asmara, D. Wan, Y. Zhao, M. A. Majidi, C. T. Nelson, M. C. Scott, Y. Cai, B. Yan, D. Schmidt, M. Yang, T. Zhu, P. E. Trevisanutto, M. R. Motapothula, Y. P. Feng, M. B. H. Breese, M. Sherburne, M. Asta, A. Minor, T. Venkatesan, and A. Rusydi, [Nature Communications **8**, 15271 EP \(2017\)](#).
- [91] V. V. Mazurenko, A. N. Rudenko, S. A. Nikolaev, D. S. Medvedeva, A. I. Lichtenstein, and M. I. Katsnelson, [Phys. Rev. B **94**, 214411 \(2016\)](#).
- [92] F. Aryasetiawan, K. Karlsson, O. Jepsen, and U. Schönberger, [Phys. Rev. B **74**, 125106 \(2006\)](#).
- [93] T. Miyake and F. Aryasetiawan, [Phys. Rev. B **77**, 085122 \(2008\)](#).
- [94] P. Werner, A. Comanac, L. de' Medici, M. Troyer, and A. J. Millis, [Phys. Rev. Lett. **97**, 076405 \(2006\)](#).
- [95] H. Hafermann, P. Werner, and E. Gull, [Computer Physics Communications **184**, 1280 \(2013\)](#).

- [96] H. Hafermann, [Phys. Rev. B **89**, 235128 \(2014\)](#).
- [97] I. Krivenko and M. Harland, [eprint arXiv:1808.00603 \(2018\)](#), [1808.00603](#).
- [98] A. S. Mishchenko, N. V. Prokof'ev, A. Sakamoto, and B. V. Svistunov, [Phys. Rev. B **62**, 6317 \(2000\)](#).
- [99] P. M. Platzman and P. A. Wolff, Academic Press, New York **Vol. 13** (1973).
- [100] A. K. Geim and K. S. Novoselov, [Nature Materials **6**, 183 EP \(2007\)](#).
- [101] M. I. Katsnelson, V. Y. Irkhin, L. Chioncel, A. I. Lichtenstein, and R. A. de Groot, [Rev. Mod. Phys. **80**, 315 \(2008\)](#).
- [102] M. I. Katsnelson, *Graphene: Carbon in Two Dimensions* (Cambridge University Press, 2012).
- [103] G. W. Semenoff, [Phys. Rev. Lett. **53**, 2449 \(1984\)](#).
- [104] M. I. Katsnelson, K. S. Novoselov, and A. K. Geim, [Nature Physics **2**, 620 EP \(2006\)](#), article.
- [105] K. S. Novoselov, A. K. Geim, S. V. Morozov, D. Jiang, M. I. Katsnelson, I. V. Grigorieva, S. V. Dubonos, and A. A. Firsov, [Nature **438**, 197 EP \(2005\)](#).
- [106] Y. Zhang, Y.-W. Tan, H. L. Stormer, and P. Kim, [Nature **438**, 201 EP \(2005\)](#).
- [107] K. S. Novoselov, A. K. Geim, S. V. Morozov, D. Jiang, Y. Zhang, S. V. Dubonos, I. V. Grigorieva, and A. A. Firsov, [Science **306**, 666 \(2004\)](#), <http://science.sciencemag.org/content/306/5696/666.full.pdf>.
- [108] K. S. Novoselov, D. Jiang, F. Schedin, T. J. Booth, V. V. Khotkevich, S. V. Morozov, and A. K. Geim, [Proceedings of the National Academy of Sciences **102**, 10451 \(2005\)](#), <http://www.pnas.org/content/102/30/10451.full.pdf>.
- [109] E. A. Laird, F. Pei, and L. P. Kouwenhoven, [Nature Nanotech-](#)

-
- nology **8**, 565 EP (2013).
- [110] N. Rohling and G. Burkard, [New Journal of Physics **14**, 083008 \(2012\)](#).
- [111] Y. Jiang, T. Low, K. Chang, M. I. Katsnelson, and F. Guinea, [Phys. Rev. Lett. **110**, 046601 \(2013\)](#).
- [112] L. E. Golub, S. A. Tarasenko, M. V. Entin, and L. I. Magarill, [Phys. Rev. B **84**, 195408 \(2011\)](#).
- [113] I. Martin, Y. M. Blanter, and A. F. Morpurgo, [Phys. Rev. Lett. **100**, 036804 \(2008\)](#).
- [114] M. M. Grujić, M. i. c. v. Tadić, and F. m. c. M. Peeters, [Phys. Rev. Lett. **113**, 046601 \(2014\)](#).
- [115] T. Oka and H. Aoki, [Phys. Rev. B **79**, 081406 \(2009\)](#).

Eidesstattliche Erklärung

Hiermit versichere ich an Eides statt, die vorliegende Dissertationsschrift selbst verfasst und keine anderen als die angegebenen Hilfsmittel und Quellen benutzt zu haben.

Die eingereichte schriftliche Fassung entspricht der auf dem elektronischen Speichermedium.

Die Dissertation wurde in der vorgelegten oder einer ähnlichen Form nicht schon einmal in einem früheren Promotionsverfahren angenommen oder als ungenügend beurteilt.

Datum

Unterschrift

